THE ROLE OF BIOMATERIAL PROPERTIES IN PERI-IMPLANT NEOVASCULARIZATION

A Dissertation
Presented to
The Academic Faculty

By

Andrew Lawrence Raines

In Partial Fulfillment
of the Requirements for the Degree
Doctor of Philosophy in the
Department of Biomedical Engineering

Georgia Institute of Technology
August, 2011

THE ROLE OF BIOMATERIAL PROPERTIES IN PERI-IMPLANT NEOVASCULARIZATION

Approved by:

Dr. Barbara D. Boyan, Advisor
Department of Biomedical Engineering
Georgia Institute of Technology

Dr. Robert E. Guldberg
School of Mechanical Engineering
Georgia Institute of Technology

Dr. Zvi Schwartz
Department of Biomedical Engineering
Georgia Institute of Technology

Dr. David J. Mooney
School of Engineering and Applied Sciences
Harvard University

Dr. W. Robert Taylor
School of Medicine
Emory University

Date Approved: April 27, 2011

ACKNOWLEDGEMENTS

I would first like to thank my advisor, Dr. Barbara D. Boyan for her role in the completion of this thesis. I began working in the Boyan laboratory in 2004 when I was an undergraduate student. It was Dr. Boyan's course that really sparked my interest in research and Dr. Boyan was kind enough to take in a young undergraduate with no research experience. When I completed my undergraduate degree and decided to attend graduate school, Dr. Boyan convinced me to stay at Georgia Tech and continue the project that my undergraduate mentor, Alice Zhao had been working on. Throughout my time as a graduate student, Dr. Boyan has pushed me to understand the science and always demanded more from me. She has also been a strong influence outside of research by listening to what I want to do with my career and providing sound advice. She has been very passionate about my research and instrumental to me being able to get to this point and for that I am deeply thankful. I would also like to thank my co-advisor, Dr. Zvi Schwartz. Dr. Schwartz has been very involved from the beginning in the design of my experiments and the direction in which my research has gone. He has been in the PRL at 5:30 am with me numerous times, performing animal surgeries that have been critical in my research. He also has made me think about what the data means and has always expected me to do more. Both Dr. Boyan and Dr. Schwartz have set excellent examples for me with their hard work and dedication and that will help me greatly throughout my career. I would also like to thank my thesis committee members. Dr. Robert Guldberg has been a great collaborator and I have learned much about how to properly conduct animal research from taking his course. Drs. W. Robert Taylor and David J. Mooney have provided their time and insight and I am very appreciative to them for that.

I would also like to thank the past and present members of the Boyan laboratory. Without the help I have received from all of them throughout the years, this would not have been possible. I would like to especially thank the Boyan laboratory staff: Leang Chhun, John Dooley, Crystal Branan, and Sri Vemula have been extremely helpful in culturing cells throughout my Ph.D. Reyhaan Chaudhri and Sharon Hyzy have been very supportive in their roles as laboratory manager during the last several years. Dr. Rene Olivares-Navarrete, Dr. Yun Wang, and Dr. Hai Yao have been an excellent source for knowledge and assistance on various topics. All of the Boyan laboratory graduate students have made my time here more enjoyable: Reyhaan Chaudhri, Bryan Bell, Ramsey Kinney, Alice Zhao, Tracy Denison, Chris Lee, Jiaxuan Chen, Khairat El-Baradie, Jennifer Hurst-Kennedy, Jamie Lazin, Maya Fisher, Ming Zhong, Tanya Farooque, Chris Hermann, Rolando Gittens, Jennie Park, Kathryn Smith, Maryam Doroudi, Brandy Rogers, Shirae Leslie, Meredith Myers, Qingfen Pan, Erin Hewitt, James Wade. Ms. Brentis Henderson has been enormously helpful in tracking down Dr. Boyan throughout the years. I would also like to thank the undergraduate students who have worked for me over the years: James Lee and Nehal Patel were very helpful in providing an extra set of hands for numerous experiments and assays.

I would also like to thank my parents for their support during these past 5 years. They may have asked how much longer until I was finished several times, but they always knew I would get here. Finally, I would like to acknowledge my fiance, Crystal Branan. I met her while I was a student and she was a laboratory technician and the last few years with her have been amazing. Without her love and support, I would certainly not be here today and for that I am extremely grateful.

TABLE OF CONTENTS

LIST OF TABLES

LIST OF FIGURES

SUMMARY

An understanding of the interactions between orthopaedic and dental implant surfaces with the surrounding host tissue is critical in the design of next generation implants to improve osseointegration and clinical success rates. Critical to the process of osseointegration is the rapid establishment of a patent neovasculature in the peri-implant space to allow for the delivery of oxygen, nutrients, and progenitor cells. The central aim of this thesis is to understand how biomaterials regulate cellular and host tissue response to elicit a pro-angiogenic microenvironment at the implant/tissue interface. To address this question, the studies performed in this thesis aim to 1) determine whether biomaterial surface properties can modulate the production and secretion of pro-angiogenic growth factors by cells, 2) determine the role of integrin and VEGF-A signaling in the angiogenic response of cells to implant surface features, and 3) to determine whether neovascularization in response to an implanted biomaterial can be modulated *in vivo*. The results demonstrate that biomaterial surface microtopography and surface energy can increase the production of pro-angiogenic growth factors by osteoblasts and that these growth factors stimulate the differentiation of endothelial cells in a paracrine manner and the results suggest that signaling through specific integrin receptors affects the production of angiogenic growth factors by osteoblast-like cells. Further, using a novel *in vivo* model, the results demonstrate that a combination of a rough surface microtopography and high surface energy can improve bone-to-implant contact and neovascularization. The results of these studies also suggest that VEGF-A produced by osteoblast-like cells has both an autocrine and paracrine effect. VEGF-A silenced cells exhibited reduced production of both pro-angiogenic and osteogenic growth factors in response to surface microtopgraphy and surface energy, and

conditioned media from VEGF-A silenced osteoblast-like cell cultures failed to stimulate endothelial cell differentiation in an *in vitro* model. Finally, the results show that by combining angiogenic and osteogenic biomaterials, new bone formation and neovascularization can be enhanced. Taken together, this research helps to provide a better understanding of the role of material properties in cell and host tissue response and will aid in the improvement of the design of new implants.

CHAPTER 1. Introduction

Musculoskeletal disease is one of the leading causes of long-term pain and disability and affects hundreds of millions of people worldwide [1]. In the United States alone, the estimated costs of all musculoskeletal disease in terms of medical bills and lost wages is $849 billion annually [2]. With an increasingly aging population this number is expected to grow significantly over the next several decades [3]. Implants in the fields of orthopaedics and dentistry aim to relieve pain and restore the function of joints and damaged or diseased tissue. The goal of any implant in orthopaedics or dentistry is osseointegration of the implant with the surrounding host tissue. In young patients or in sites of healthy bone, the success rates of orthopaedic and dental implants can be as high as 95% [4, 5]. However, in sites of poor bone quality, either due to disease or other factors such as smoking, the overall clinical success of implants drops significantly [6, 7], highlighting the need for better designed implants to promote osseointegration and ultimately improve implant success. Critical to the process of implant osseointegration is the establishment of a patent vascular supply at the implant/tissue interface to allow for the delivery of oxygen, nutrients, and progenitor cells to the injury site.

The studies presented in this thesis aim to 1) determine whether biomaterial surface properties can modulate the production and secretion of pro-angiogenic growth factors by cells, 2) determine the role of integrin and VEGF-A signaling in the angiogenic response of cells to implant surface features, and 3) to determine whether neovascularization in response to an implanted biomaterial can be modulated *in vivo*. The remainder of this chapter will discuss the relevant background material that serves as a basis for the aims of this thesis. These topics include a discussion of general bone

biology and the process of neovascularization. Next, there will be a discussion of the properties and use of titanium (Ti) as a biomaterial and host cellular and tissue response to titanium implants. There will also be a section concerning bone graft substitutes and their use in orthopaedic applications. Finally, the overall objective of this thesis will be outlined with regard to the highlighted clinical and scientific needs.

1.1 Bone Biology

1.1.1 Bone Structure

Bone is one of the hardest tissues in the human body. It is a dynamic tissue that provides structural support and protection to internal organs as well as metabolic and physiological functions for the body. Bone is also the strongest tissue in the human body with tensile strengths of up to 130 MPa and compressive strengths of up to 190 MPa [8]. Despite its strong mechanical properties, the density of human bone ranges from 0.30 g/cm^3 to 1.85 g/cm^3, making bone a highly efficient structure [9]. From a metabolic and physiological perspective, bone serves as a source for calcium and phosphorus in the body, which, when released during bone resorption, helps to maintain overall mineral ion homeostasis. In general, bone can be classified into two types within the body, cortical bone and trabecular bone.

Cortical bone, also known as compact bone, comprises the outer layer of all bones and the diaphysis of long bones [10]. The modulus of cortical bone is approximately 17,000 MPa [11]. Cortical bone is composed of distinct units, termed osteons, which consist of vascular channels circumferentially surrounded by lamellar bone. The vascular channels located in osteons are called haversian canals and typically consist of cells, blood vessels and sometimes nerves. The blood vessels within haversian canals are capillary-like and are derived from the epiphyseal metaphyseal arteries [12].

Trabecular, or cancellous bone, is primarily found in the metaphysis and epiphysis of long bones and in the vertebrae [10]. Trabecular bone is composed of a three-dimensional lattice network of bone spicules aligned along areas of stress. The highly porous structure of trabecular bone results in a much lower density than that of cortical bone and a corresponding lower modulus, with values typically ranging between 10 and 2,000 MPa, depending on the location of the bone [11, 13]. Trabecular bone has a much larger surface area than does cortical bone and is subject to a much greater rate of bone turnover.

Bone is a composite material, consisting of both organic and inorganic phases. The inorganic component of bone is calcium hydroxyapatite [$Ca_{10}(PO_4)_6(OH)_2$] which occurs in the matrix as crystals approximately 20-80 nm in length and 2-5 nm in thickness [14]. The organic component of bone is principally type I collagen, which comprises about 90% of the organic matrix [15]. The remainder of the organic matrix contains proteins such as osteocalcin, osteopontin, bone sialoprotein, osteonectin and bone proteoglycans [15]. The hierarchical organization of bone from individual collagen fibers and hydroxyapatite crystals to lamellar structures and osteons to the macroscopic bone is outlined in Figure 1-1.

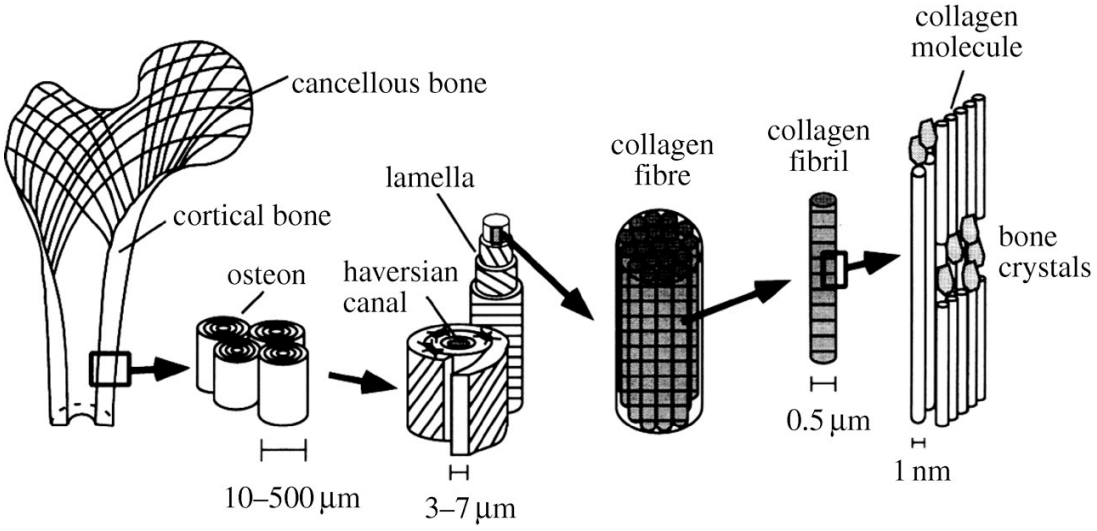

Figure 1-1. Schematic illustrating the hierarchical structure of bone from the whole bone to individual collagen molecules and hydroxyapatite crystals [16]

1.1.2 Bone Remodeling

As mentioned above, bone is a dynamic tissue that is constantly remodeled throughout life through bone resorption and new bone formation. Bone is resorbed by cells called osteoclasts. Mature osteoclasts are large, multinucleated cells derived from haematopoietic precursors that also give rise to monocytes and macrophages [17]. Osteoclasts are identified by their ability to produce tartrate-resistant acid phosphatase (TRAP) and by their ruffled border which results from infoldings of the cell membrane at the bone surface interface. At sites of bone remodeling, osteoclasts attach to the bone surface, lower the pH of the local environment through the generation of hydrogen ions, and produce and release matrix metalloproteases and proteolytic enzymes to dissolve the hydroxyapatite crystals and remove the organic components of the bone matrix [18].

New bone is laid down at sites of bone resorption by bone forming cells called osteoblasts. Unlike osteoclasts, osteoblasts are derived from mesenchymal progenitor cells [19]. The primary distinctive features of osteoblasts are the ability to produce type I collagen, their responsiveness to parathyroid hormone, and their production of osteocalcin in response to the systesmic osteotropic hormone 1α,25-dihydroxyvitamin D_3. Osteoblasts are recruited to sites of bone resorption by osteoclasts, where they secrete new bone matrix called osteoid. Osteoid is later mineralized as osteoblasts continue to mature. Osteoblasts that have become embedded within a mineralized matrix are called osteocytes. Osteocytes are the most numerous type of bone cell and are terminally differentiated cells that play an important role in communication with each other and bone cells on the surface through the bone canaliculi.

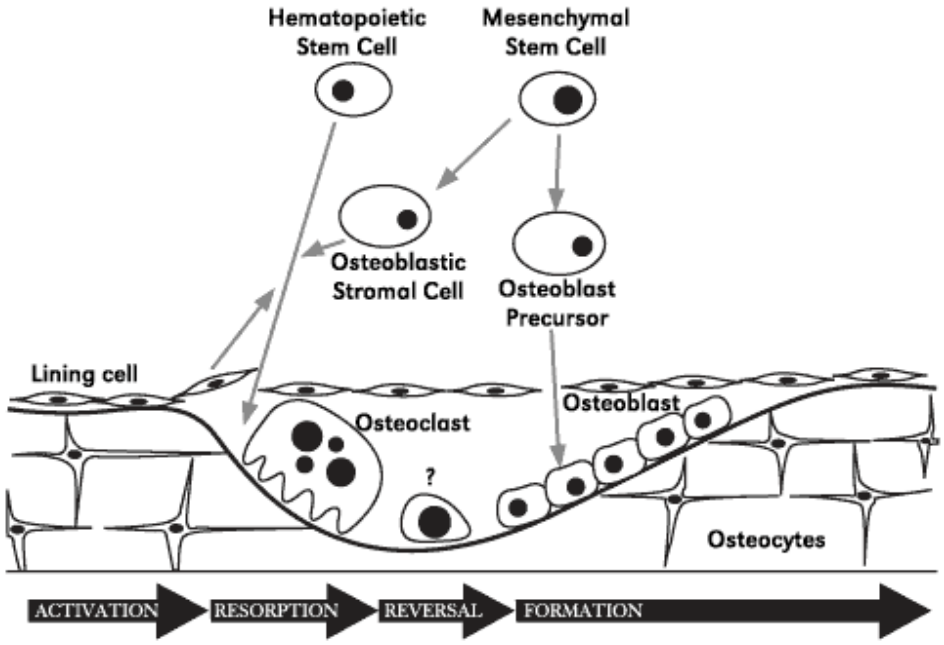

Figure 1-2. Schematic illustrating the basic process of bone resorption and new bone formation [20].

1.1.3 Osteoblast Differentiation and Maturation

Osteoblasts and osteocytes are derived from multipotent, mesenchymal progenitor stem cells (MSCs) that can give rise to cells of multiple different lineages, including bone, cartilage, fat, and muscle [21]. The differentiation of MSCs into the various lineages is controlled tightly by several transcription factors, hormones, and growth factors. Runx2 has been identified as the major transcription factor responsible for controlling osteoblast differentiation [22]. Upregulation of Runx2, along with downregulation of PPARγ and Sox9 pushes MSCs towards an osteoblast lineage. Runx2 belongs to the Runt family of transcription factors and is expressed in MSCs at the onset of skeletal development and throughout osteoblast differentiation. Runx regulatory elements are found within the major osteoblastic genes, including collagen I, osteopontin, bone sialoprotein, and osteocalcin [23]. Numerous other transcription factors have been identified that also play a role in the differentiation of progenitor cells

into fully mature osteoblasts. One of these transcription factors, osterix, is expressed specifically by osteoblasts and is important for osteoblast differentiation. Osterix is expressed downstream from Runx2, and can form a complex with nuclear factor of activated T cells (NFAT) to promote collagen I promoter activity and Wnt signaling [24]. Signaling through the canonical Wnt pathway has been found to be an important signaling pathway in controlling bone formation and bone mass [25, 26]. Inactivation of β-catenin, a downstream member of the canonical Wnt pathway, inhibits osteoblast differentiation from mesenchymal progenitor cell populations [27].

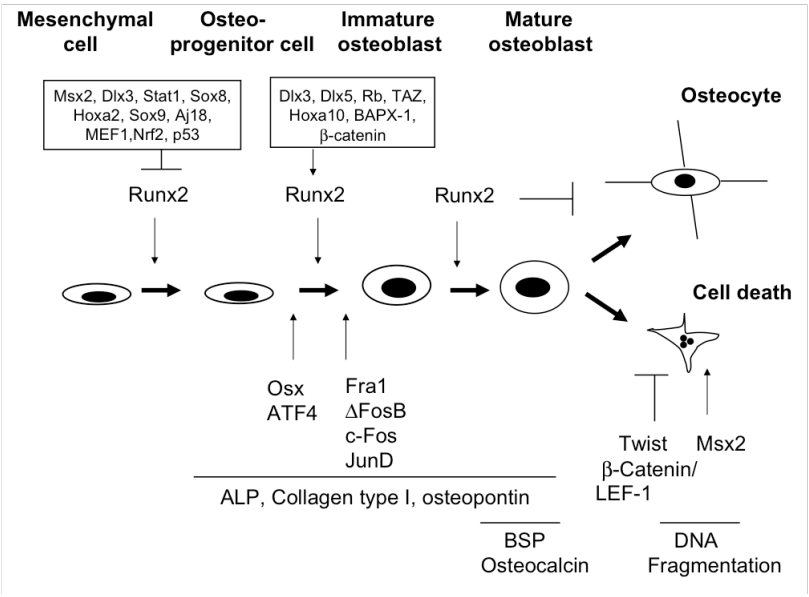

Figure 1-3. Schematic illustrating the differentiation from mesenchymal progenitor cells to osteo-progenitors to fully mature osteoblasts and osteocytes [21]

The differentiation of MSCs down the osteoblastic lineage is also subject to control by systemic hormones and growth factors. Parathyroid hormone (PTH) promotes osteoblast differentiation through the phosphorylation and activation of Runx2 [28]. PTH further inhibits Runx2 degradation and promotes osterix while inhibiting PPARγ expression [29]. The systemic osteotropic hormone, $1\alpha,25(OH)_2D_3$ also upregulates Runx2 expression and downregulates PPARγ, resulting in

osteoblastogenesis [30]. Growth factor signaling has also been found to play a role in osteoblast differentiation in MSCs. Bone morphogenetic protein 2 (BMP-2) promotes both Runx2 and osterix expression in MSCs [31, 32]. Transforming growth factor β and fibroblast growth factor 2 (FGF-2) also promote bone formation by increasing Runx2 phosphorylation and activity [33, 34].

Mesenchymal progenitor cells that differentiate down the osteoblast lineage undergo maturation from osteo-progenitor cells to immature osteoblasts and finally to mature osteoblasts and osteocytes. The maturation process of osteoblasts is generally marked by three stages: proliferation, matrix secretion, and mineralization [35]. Cells express numerous genes and proteins during each of these stages that can be identified to determine osteoblast maturation. During the proliferative stage of osteoblast maturation, cells express cell cycle and cell growth related genes, including c-myc, c-fos, and AP-1 [36]. During this time, cells also express genes related to osteoblast extracellular matrix development. These genes include type I collagen, fibronectin, and TGFβ [37]. Following proliferation, the expression of alkaline phosphatase, an enzyme associated with bone cell phenotype, is increased significantly. Alkaline phosphatase levels remain high in osteoblast like cell cultures until the onset of matrix mineralization. During matrix mineralization, cells upregulate expression of osteocalcin, osteopontin, osteonectin, and other mineralization associated proteins. There is also an increase in calcium associated with mineral deposition in the extracellular matrix. Understanding the temporal sequence of gene expression associated with bone formation allows for the ability to determine osteoblast maturation in cell cultures *in vitro*.

1.1.4 Bone & Blood

The importance of blood vessels in the formation of bone was documented as early as the 1700s [38, 39]. The vascular system transports oxygen, nutrients, systemic hormones, growth factors, and cells throughout the body. Bone formation during development occurs through two distinct mechanisms: intramembranous ossification and endochondral ossification [40]. Both of these ossification processes occur in close proximity to vascular ingrowth. During intramembranous ossification, new capillary invasion into the mesenchymal zone occurs prior to the differentiation of mesenchymal progenitor cells into mature osteoblasts and deposition of mineralized bone spicules [41]. During endochondral ossification, vascular invasion into the hypertrophic zone of the growth plate is necessary for the longitudinal growth of long bones [42]. Hypertrophic chondrocytes are known to secrete several pro-angiogenic growth factors and the coupling of chondrogenesis and osteogenesis during bone growth is highly dependent on the rate of vascularization of the growth plate [43]. The tight interplay between vascularization and bone formation is highlighted by the fact that disruption of this process results in a reduction in bone formation and increase in growth plate thickness [44].

In addition to its importance during development and growth of the skeleton, the presence of a blood supply is also important during bone fracture repair and osseointegration. Bone is a unique tissue in that it has the ability to repair itself without the development of a fibrous scar. Following injury to bone, there is a rapid invasion of capillary blood vessels to the injured site from the surrounding vasculature. This capillary invasion allows for the delivery of mesenchymal cells to the damaged region [45]. The fracture site is stabilized with the formation of a fracture callus, which is remodeled to restore the normal vascular supply and bone structure. In some cases, fractures fail to repair, resulting in non-unions. There are several reasons for the failure

of fractures to heal, including anti-inflammatory drugs, steroids, calcium deficiencies, and the absence of a functional vascular network at the fracture site [46]. The understanding that angiogenesis is an important part of bone formation and repair has led to greater research into combining angiogenic therapies with osteogenic therapies to promote bone formation in tissue engineering.

1.2 Neovascularization

A vascular network is one of the first organ systems to develop during embryogenesis. Within the developing embryo, the vascular network develops from a process called vasculogenesis. In vasculogenesis, mesodermal cells differentiate into hemangioblasts, which are the precursor cells of both haematopoietic and endothelial cells. Hemangioblasts further differentiate into angioblasts that aggregate together to form blood islands. Elongation of these blood islands into cord-like structures forms the primary blood vascular plexus that consists of capillaries formed by endothelial cells [47]. After the development of the primary vascular network and in the adult organism, new blood vessel formation occurs primarily through a process called angiogenesis.

1.2.1 Angiogenesis

Angiogenesis refers to the sprouting and subsequent stabilization of new blood vessels from the pre-existing vasculature [48]. Angiogenesis occurs both physiologically during vascular growth and remodeling (i.e. during long bone growth) as well as pathologically as during diabetes and tumor growth. The process of angiogenesis can generally be broken down into four stages that will be described in further detail: (1) activation of endothelial cells in response to an angiogenic stimulus, (2) degradation of the basement membrane of the surrounding vasculature, (3) migration of endothelial cells in the direction of the angiogenic stimulus, forming the initial capillary sprout, and (4) stabilization and maturation of the newly formed vessel.

1.2.1.1 Endothelial cell activation

Initiation of angiogenesis begins with the activation of endothelial cells in response to an angiogenic stimulus. One of the primary stimuli for the expansion of the vascular bed is hypoxia [48]. Oxygenation of cells within the body occurs via the diffusion of oxygen from the surrounding vasculature. When cells are located beyond the diffusion limit of oxygen in the tissue, the cells become hypoxic, resulting in activation of the hypoxia inducible factor (HIF) pathway [49]. Under conditions of normal oxygen tension, HIF-1α subunits are hydroxylated and marked for degradation by the proteosome by the von Hippel-Lindau (VHL) tumor suppressor protein [50]. However, when oxygen concentrations drop below approximately 5%, HIF-1α accumulates in the cytoplasm and translocates to the nucleus, where it interacts with the constitutively expressed HIF-1β subunit to activate gene transcription. Several genes associated with angiogenesis are either directly or indirectly affected in response to hypoxia, including vascular endothelial growth factor and its receptors, fibroblast growth factors, angiopoietins, and matrix metalloproteinases [51-56]. Secretion of these growth factors by hypoxic cells leads to the activation of endothelial cells.

1.2.1.2 Basement membrane degradation

Several growth factors are known to be mitogenic for endothelial cells including TGFβ, FGF-2, HGF, IL-8 and the angiopoietins [47]. However, the most widely recognized growth factor as being essential for the initiation of angiogenesis is vascular endothelial growth factor (VEGF) A. Endothelial cells express the VEGF receptors VEGFR1 (Flt1) and VEGFR2 (Flk1/KDR). Activation of the VEGF receptors on endothelial cells stimulates their growth and prevents apoptosis [57, 58]. VEGF-A has also been found to stimulate the production of matrix metalloproteinases (MMPs) in endothelial cells [59]. MMPs secreted by endothelial cells in response to VEGF include

MMP-1, -2, and -9 [60]. These MMPs degrade the basement membrane consisting of collagen IV, laminin, and other components allowing for the migration of endothelial cells in the direction of the angiogenic stimulus.

1.2.1.3 Endothelial cell migration

As mendtioned above, VEGF-A acts to promote endothelial cell growth. In response to an angiogenic stimulus, the endothelial cells that are in the leading position are referred to as tip cells [47]. These tip cells sprout filopodia in the direction of the VEGF gradient within the tissue and ultimately guide the direction of the growing capillary within the tissue [61].

1.2.1.4 Vessel maturation

After the development of a capillary sprout in response to an angiogenic stimulus, the newly formed vessel is stabilized by the recruitment of mural cells. The maturation of blood vessels is regulated by many different growth factors and signaling systems. Platelet derived growth factor (PDGF) B plays a role in recruiting pericytes to form walls around newly formed vessels. In PDGFB deficient mice, the number of pericytes is decreased and blood vessels are dilated and develop microaneurysms, resulting in embryonic lethality [62]. The angiopoietins (Ang-1 and -2) and their receptor Tie2 also play an important role in the maturation of blood vessels. The Ang-1/Tie2 signaling cascade lowers vascular permeability by promoting the association of pericytes with the endothelium [63]. Further, in Tie2 knockout mice, the process of capillary maturation is disturbed, resulting in embryonic lethality [64]. Overall, the process of angiogenesis is coordinated by several classes of growth factors and their receptors in both endothelial cells and mural cells and each step is tightly regulated and necessary for the successful development of new blood vessels.

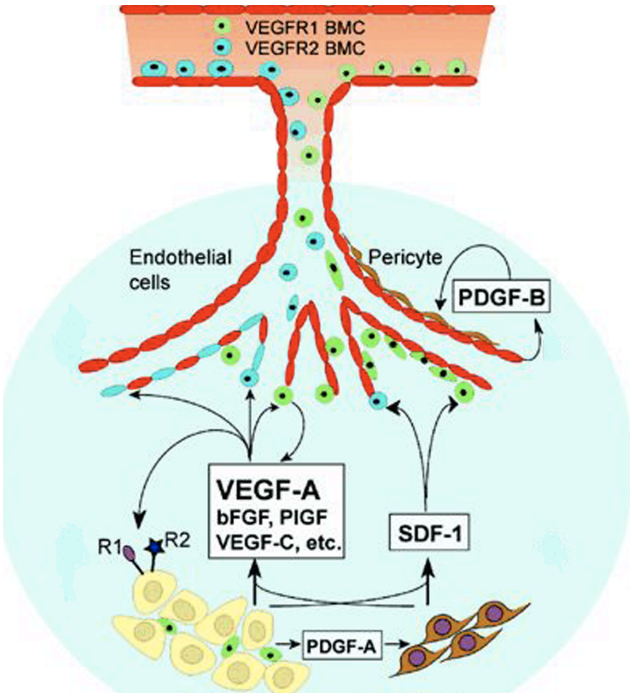

Figure 1-4. Schematic illustrating the basic mechanism of angiogenesis. Angiogenic stimulants are secreted by cells in response to a change in environmental conditions. The basement membrane of the surrounding vasculature is degraded and endothelial cells migrate in the direction of the angiogenic stimulus and form a nascent endothelial sprout [65].

1.2.2 VEGF

VEGF-A is an approximately 45 KDa glycoprotein that acts as both a permeability and angiogenic growth factor [66, 67]. VEGF-A belongs to a family of associated genes that includes VEGF-B, -C, -D, and placental growth factor (PLGF). While the other members of the VEGF family have been found to control the growth and differentiation of the vascular system, VEGF-A is widely recognized as the key regulator of blood vessel growth and development *in vivo*. VEGF-A has been demonstrated to stimulate growth, prevent apoptosis, and promote the migration of endothelial cells *in vitro* [68]. The human VEGF-A gene is comprised of eight exons and seven introns and can be alternatively spliced to generate four VEGF-A isoforms, VEGF-A_{121}, VEGF-A_{165}, VEGF-A_{189}, and VEGF-A_{206} [69, 70]. VEGF-A isoforms 189 and 206 contain all eight exons and

are bound to the extracellular matrix (ECM) through a heparin-binding domain. VEGF-A_{121} does not contain exons six or seven and is freely diffusible within the ECM, while VEGF-A_{165}, the most abundant isoform, does not contain exon six and has intermediate ECM binding properties [71]. The expression of VEGF-A by cells is regulated by several mechanisms, including oxygen tension and growth factors. The VEGF-A gene contains a hypoxia response element (HRE) and its expression is activated in response to activation of the HIF pathway [72]. Numerous growth factors have also been found to stimulate VEGF-A gene expression including TGF-α and -β, insulin-like growth factor, FGF, and PDGF [68].

VEGF-A binds two receptor tyrosine kinases located on the cell surface, VEGFR1 (Flt1) and VEGFR2 (Flk1/KDR). VEGFR1 was the first receptor to be identified for VEGF-A [73]. In response to VEGF-A binding, VEGFR1 undergoes weak tyrosine autophosphorylation [73, 74], and it is thought that VEGFR1 is not the primary receptor responsible for VEGF-A effects, but rather is a decoy receptor, allowing for negative regulation of VEGF-A on the vascular endothelium [75]. VEGFR2 is recognized as the primary mediator of the mitogenic effects of VEGF-A during neo-vascularization. Upon binding, VEGFR2 dimerizes and undergoes strong autophosphorylation, inducing the downstream phosphorylation of multiple proteins in endothelial cells, including phospholipase C-γ, PI-3 kinase, Ras, and members of the Src family [76, 77]. The importance of VEGFR2 in neo-vascularization is highlighted by the fact that VEGFR2 null mice die in early embryogenesis due to a failure to develop blood islands and organized blood vessels [78]. Further, VEGFR2 but not VEGFR1 is necessary for the anti-apoptotic effects of VEGF-A in human umbilical vein endtothelial cells [58].

1.2.3 FGF-2

Basic fibroblast growth factor (FGF-2) belongs to a large family of protein growth factors that currently includes 22 members based on the homology of their amino acid sequences [79]. Five isoforms of FGF-2 have been identified that occur through alternative splicing of the same gene resulting in protein products with molecular weights of 18, 22, 22.5, 24, and 34 KDa [80]. FGF-2 has the capacity to increase the migrational ability of endothelial and smooth muscle cells [81]. FGF-2 has also been found to stimulate the proliferation of endothelial cells and plays a role in the remodeling of the extracellular matrix during angiogenesis by stimulating the proteolysis of ECM components [82, 83]. FGF-2 exerts its effects through four structurally releated proteins receptors, FGF receptors (FGFR) 1-4 which contain immunoglobulin-like amino acid sequences in their extracellular ligand binding domain [84]. FGF-2 is one of the most important growth factors involved in tumor angiogenesis and plays an important role in the regulation of physiological angiogenesis *in vivo*.

1.2.4 Angiopoietin-1

Angiopoietin-1 (Ang-1) is an approximately 70 KDa glycoprotein that belongs to a family of four proteins (Ang-1, -2, -3, and -4) that are grouped together based on the homology of the amino acid sequences [85]. Ang-1 plays an important role in the later stages of angiogenesis through stabilization of the new capillary sprout. Inactivation of the Ang-1 gene in mice results in a decrease in the number of large vessels, thinning of the walls of larger blood vessels, and disintegration of the blood vessel network [64]. Ang-1 signaling has been found to promote endothelial cell survival by promoting the expression of the anti-apoptotic protein survivin [86] and acts to recruit pericytes and smooth muscle cells in the peri-vascular space to newly formed endothelial cell sprouts. Ang-1 exerts its effects on endothelial cells through binding with its cognate receptor tyrosine kinase, Tie2.

1.3 Biomaterials

Biomaterials are generally divided into four major classes of materials: metals, ceramics, polymers, and natural materials [87]. Orthopaedic biomaterials have been very successful in restoring mobility and quality of life to millions of individuals, and represent a large segment of the biomaterials industry. In 2002, orthopaedic biomaterial sales were approximately $14 billion and the orthopaedic biomaterial market is expected to grow at a rate of nearly 10% annually [88].

Metals and metal alloys are the most commonly used materials in orthopaedic and dental implants because of their tensile strength, stiffness, and resistance to wear [89]. Titanium (Ti) and its alloys (Ti6Al4V), stainless steel, and cobalt alloys (CoCrMo) are the primary metals used in orthopaedics [88]. Titanium and Ti6Al4V are commonly used in total joint replacements because of their high corrosion resistance compared to stainless steel and CoCrMo alloys. This resistance is due to the formation of a passive oxide film (TiO_2) that forms on their surface. Ti and Ti alloys also possess mechanical properties closer to those of native bone. In dental applications, commercially pure Ti (cpTi) is predominantly used because it is more biocompatible than Ti alloys and fatigue and wear resistance are not as big of an issue. Regardless of the material used, all biomaterials elicit a host response when implanted *in vivo*.

1.3.1 Host Response to Biomaterials

Biocompatibility is defined as the ability of a material to perform with an appropriate response in a specific application [90]. Upon the implantation of a biomaterial into the body, there is generally a well-defined sequence of events that occurs involving inflammation, wound healing, and foreign-body reaction in response to injury.

The first event to occur in response to injury to vascularized tissue is the development of a provisional matrix through the formation of a haematoma at the implant site [91]. The provisional matrix consists of fibrin, produced by activation of blood coagulation and contains mitogens, cytokines, and growth factors to initiate and control the subsequent wound healing process. The first inflammatory cells to come into contact with a biomaterial surface are neutrophils [92]. The acute inflammatory phase typically only lasts the first few days after implantation of a biomaterial and the major role of neutrophils during the acute inflammatory phase is to phagocytose microorganisms and foreign materials.

The formation of granulation tissue occurs as early as 3-5 days after implantation of a biomaterial and can last several weeks [91]. Granulation tissue is characteristic of the wound healing response and is a highly vascularized tissue containing numerous small blood vessels formed by angiogenesis. Granulation tissue is also characterized by proliferating fibroblasts that are active in creating a matrix containing collagens and proteglycans [91]. Monocytes and macrophages are also characteristic of granulation tissue.

Materials that have poor biocompatibility elicit a foreign body reaction where foreign body giant cells and components of the granulation tissue, including fibroblasts and macrophages persist at the implant/tissue interface. The long-term presence of a foreign body reaction leads to fibrous encapsulation of the implanted biomaterial, and can lead to implant loosening and ultimately implant failure.

The goal of any implant in orthopaedics and dentistry is osseointegration of the implant with the surrounding host tissue. Osseointegration is defined as the direct contact of bone to the surface of a biomaterial, without the formation of a fibrous layer [93]. During peri-implant healing, new bone is formed as a result of the recruitment and

migration of osteogenic cells to the implant surface, resulting in the apparent growth of new bone tissue along the implant surface, termed bone-to-implant-contact [94]. The degree of bone-to-implant contact can be measured histologically and is effected by the surface topography and chemistry of the implant [95].

1.3.2 Cell Response to Ti

The surface properties of materials contribute to host cellular response and ultimately determine the overall success or failure of an implanted biomaterial. Cells interact with the surface of a material through an adsorbed layer of proteins, ions, sugars, and lipids present in the blood and tissue fluid. The surface properties of materials are largely responsible for this interaction, and the surface properties that affect this process include topography, surface energy, chemistry, and surface charge [96]. *In vitro* studies have shown that Ti surface microtopography and energy can affect the selective adsorption of proteins including albumin, fibronectin, and vitronectin onto the surface [97, 98].

Osteoblasts interact with their substrate primarily via integrin binding to extracellular matrix (ECM) proteins [99]. Integrins are heterodimeric transmembrane glycoprotein receptor complexes consisting of non-covalently associated α and β subunits. Integrin receptors bind ECM proteins on the outside of the cell and associate with the cytoskeleton and signaling complexes inside the cell to transduce signals. Osteoblasts express several integrin α and β subunits including α_1, α_2, α_3, α_4, α_5, α_6, α_v, β_1, and β_3 [100-102]. The expression of integrin subunits by osteoblast-like cells is regulated by surface chemical composition and topography [103, 104]

Upon binding, integrin molecules cluster into focal adhesions, where they initiate intracellular signaling cascades to control proliferation and differentiation. Focal adhesion complexes are comprised of structural proteins such as vinculin and talin, and

signaling molecules including focal adhesion kinase (FAK) and Src [105]. Bound integrins, along with growth factors can also activate the MAPK signal transduction pathway [106-108].

In vitro, it has been shown that modifications to Ti substrate microarchitecture has an effect on the attachment and differentiation of osteoblast-like cells, including MG63 and MC3T3-E1 cell lines, as well as fetal rat calvarial cells and normal human osteoblasts [109]. MG63 cells exhibit stronger attachment to Ti substrates with average roughness values (R_a) between 4–7 μm than do cells cultured on smooth Ti substrates. While cell attachment appears to be stronger on rough Ti substrates, cell proliferation is decreased and differentiation is increased, as these cells display increased alkaline phosphatase specific activity and osteocalcin production [110]. Further, MG63 osteoblast-like cells cultured on rough Ti surfaces release increased levels of local bone regulatory factors, including osteoprotegerin (OPG), prostaglandin E_2 (PGE_2), and transforming growth factor β1 (TGF-β1). Taken together, these results indicate that rough Ti substrates promote osteoblast differentiation and maturation to a greater extent than smooth Ti surfaces.

In addition to surface roughness, surface free energy of Ti substrates also plays a role in regulating bone cell responsiveness. Ti surfaces naturally have a low surface free energy due to the adsorption of hydrocarbons and carbonates from the ambient atmosphere onto the TiO_2 surface layer. This adsorption also makes the Ti surfaces hydrophobic. Modification of Ti surfaces can be done to create a more hydrophilic surface with a high surface free energy [111]. MG63 cells cultured on high surface free energy substrates show an enhanced response to Ti surface microtopography. On microrough, high surface free energy Ti substrates, these cells show increases in

alkaline phosphatase specfic activity, osteocalcin production, and levels of TGF-β1 and OPG compared to rough Ti surfaces alone [112].

In vivo, Ti substrates with a rough microtopography support greater bone-to-implant contact than smooth surfaces do, resulting in greater removal torque strength [[113-115]]. Preliminary studies have indicated that high surface free energy Ti surfaces have the potential to improve the early stages of soft- and hard tissue integration of implants *in vivo* [116].

1.4 Bone Graft Substitutes

The biological processes involved in bone regeneration generally require three critical components: (1) an ostegenic potential capable of providing progenitor cells to the newly forming bone, (2) osteoinductive factors, and (3) an osteoconductive scaffold to promote neovascularization and support new bone growth [117]. Autologous bone grafts are considered the "gold standard" in the field of bone graft substitutes, however limited donor availability and donor site morbidity and pain have necessitated the use of other materials including ceramics, allografts, osteoinductive factors, and demineralized bone matrix for use in filling osseous defects.

1.4.1 Demineralized bone matrix

Demineralized bone matrices (DBM) are generated by acid extraction of bone, resulting in the loss of much of the mineralized component of bone but retaining collagen I and other non-collagenous proteins [117]. DBM is known to possess both osteoconductive and osteoinductive factors. Among the osteoinductive factors in DBM are the bone morphogenic proteins (BMPs). It is well documented that the levels of BMPs in DBM vary from donor to donor resulting in differences in osteogenic potential *in vivo* [118-120]. While DBM is known to be osteoinductive, the particulate, powdery nature of DBM results in poor handling qualities and a lack of structural strength for use

in bone defects. To improve its handling qualities for use in surgical procedures, DBM is often combined other materials, including calcium sulfate, glycerol, gelatin, and hyaluronic acid [121, 122].

1.4.2 Hyaluronic acid

Hyaluronic acid is a high molecular weight (10^4 – 10^7 Da), negatively charged, non-sulfated glycosaminoglycan consisting of repeating units of *N*-acetylglucosamine and D-glucuronic acid [123]. It is a component of the extracellular matrix (ECM) expressed in nearly all tissue types [123] and plays an important role in tissue morphogenesis and healing [124, 125]. During wound healing, native hyaluronic acid serves as an anti-angiogenic molecule, inhibiting endothelial cell proliferation and migration [126]. These observations have lead to the use of the sodium salt of hyaluronic acid (NaHY) in a number of wound healing applications [127]. Although NaHY inhibits capillary formation in a three dimensional collagen gel [126, 128], low molecular weight degradation products of NaHY have been demonstrated to stimulate vascular endothelial cell proliferation [129-133], migration [134], collagen synthesis [135], sprout formation [136], and new blood vessel formation [137].

1.5 Thesis Objective

It is well known that Ti surface microarchitecture and chemical composition affect osteoblast differentiation *in vitro* and bone formation *in vivo*. Ti substrates that present a microrough surface topography combined with a high surface free energy reduce the proliferation of osteoblasts and increase their production of osteocalcin, a late marker of osteoblast differentiation. In addition, cells cultured on microrough Ti substrates show enhanced production of local factors that generate an osteogenic microenvironment including prostaglandin E_2, TGF-β1 and osteoprotegerin. However, the clinical success of implanted materials is dependent not only upon osseointegration but also on

neovascularization in the peri-implant bone. Bone is a highly vascularized tissue, and osteoblasts express and secrete several growth factors that are known to play a role in neovascularization, including VEGF-A, FGF-2, and Ang-1. How biomaterial properties may influence the response of cells to enhance neovascularization in the peri-implant space is not well known. An understanding of this process could allow bioengineers to better design orthopaedic materials to promote both osteogenesis as well as neovascularization, potentially resulting in better implant fixation and longer implant lifetimes.

The purpose of this thesis is to develop an understanding as to how biomaterials regulate cellular response to elicit a pro-vasculogenic environment at the cell-surface interface, and the mechanism by which this process occurs. In addition, one aim of this thesis is to understand the specific role of VEGF-A in osteoblast cell response to biomaterial surface features. Finally, this thesis aims to investigate the host vascular response to implanted biomaterials *in vivo*.

The first aim of this thesis (Chapter 2) uses *in vitro* cell culture techniques and a novel *in vivo* bone formation model, the murine femoral press-fit model, to examine whether biomaterial surface topography or surface free energy affects the angiogenic response of cells or tissues at the bone/implant interface. The results indicate that a rough surface microtopography combined with a high surface free energy enhance the secretion of pro-angiogenic growth factors by osteoblast-like cells *in vitro* and enhance both bone formation and neovascularization *in vivo*. Further, this aim uses shRNA techniques to specifically knockdown several integrin subunits expressed by osteoblasts to determine if signaling through integrin receptor complexes mediates the expression of pro-angiogenic growth factors (Chapter 3). Silencing of the α_2, α_5, or β_1 integrin subunits resulted in an increase in the production of VEGF-A compared to wild-type MG63 cells

while silencing of the α_1 integrin subunit decreased production of VEGF-A. The results suggest that signaling through specific integrin receptors affects the production of angiogenic growth factors by osteoblast-like cells.

The second aim of this thesis (Chapter 4) uses molecular biology techniques, including shRNA transduction to silence VEGF-A and treatments with neutralization antibodies and exogenous growth factors to determine the specific role of VEGF-A in osteoblast-like cell response to surface microtopography and surface energy. The results indicate that VEGF-A produced by osteoblast-like cells has both an autocrine and paracrine effect. VEGF-A silenced cells exhibited reduced production of both pro-angiogenic and osteogenic growth factors in response to surface microtopgraphy and surface energy, and conditioned media from VEGF-A silenced osteoblast-like cell cultures failed to stimulate endothelial cell differentiation in an *in vitro* model.

The third aim of this thesis (Chapter 5) uses the *in vivo* bone marrow ablation model to determine whether neovascularization in response to an implanted osteogenic biomaterial can be modulated *in vivo* using three-dimensional micro-computed tomography (μCT) to analyze vascular morphology and bone formation during healing. The results show that a combination of low molecular weight sodium hyaluronate (NaHY), an angiogenic biomaterial, as a carrier for demineralized bone matrix, an osteogenic stimulus, can enhance both neovascularization and bone formation during healing.

The results of this thesis demonstrate that biomaterial properties affect the angigogenic response of cells *in vitro* and can enhance neovascularization *in vivo*. However, the results of this thesis raise further questions as to the specific interactions between cells and the biomaterial that elicit this response as well as how osteoblasts and endothelial cells interact during bone formation following implant insertion. Overall,

the results further the understanding of how biomaterials regulate cell and tissue response and can help to improve biomaterial design and implant success in compromised bone.

1.6 References

1. Woolf AD, Pfleger B. Burden of major musculoskeletal conditions. Bull World Health Organ 2003;81(9):646-656.

2. Yelin EH. U.S. Department of Health and Human Services, Agency for Healthcare Research and Quality, Medical Expenditures Panel Survery, 1996-2004. San Francisco, CA: Institute for Health Policy and Studies; 2004.

3. United States Bone and Joint Initiative. [cited March 20, 2011]; Available from: http://www.usbjd.org/about/index.cfm?pg=fast.cfm#_ednref1

4. Donos N, Mardas N, Chadha V. Clinical outcomes of implants following lateral bone augmentation: systematic assessment of available options (barrier membranes, bone grafts, split osteotomy). J Clin Periodontol 2008 Sep;35(8 Suppl):173-202.

5. Esposito M, Grusovin MG, Willings M, Coulthard P, Worthington HV. The effectiveness of immediate, early, and conventional loading of dental implants: a Cochrane systematic review of randomized controlled clinical trials. Int J Oral Maxillofac Implants 2007 Nov-Dec;22(6):893-904.

6. Palmquist A, Omar OM, Esposito M, Lausmaa J, Thomsen P. Titanium oral implants: surface characteristics, interface biology and clinical outcome. J R Soc Interface Oct 6;7 Suppl 5:S515-527.

7. Deng F, Zhang H, Shao H, He Q, Zhang P. A comparison of clinical outcomes for implants placed in fresh extraction sockets versus healed sites in periodontally compromised patients: a 1-year follow-up report. Int J Oral Maxillofac Implants Sep-Oct; 25(5):1036-1040.

8. Hernandez CJ, Keaveny TM. A biomechanical perspective on bone quality. Bone 2006 Dec;39(6):1173-1181.

9. Kaplan FS, Hayes WC, Keaveny TM, Boskey A, Einhorn TA, JP L. Form and Function of Bone. In: SR S, editor. Orthopaedic Basic Science. 1 ed. Rosemont, IL: American Academy of Orthopaedic Surgeons, 1994.

10. Boron WF, Boulpaep EL. Medical Physiology. 1 ed: Saunders, 2003.

11. Choi K, Kuhn JL, Ciarelli MJ, Goldstein SA. The elastic moduli of human subchondral, trabecular, and cortical bone tissue and the size-dependency of cortical bone modulus. J Biomech 1990;23(11):1103-1113.

12. Buckwalter JA, Cooper RR. Bone structure and function. Instr Course Lect 1987;36:27-48.

13. Goldstein SA. The mechanical properties of trabecular bone: dependence on anatomic location and function. J Biomech 1987;20(11-12):1055-1061.

14. Boskey AL. Mineral-matrix interactions in bone and cartilage. Clin Orthop Relat Res 1992 Aug(281):244-274.

15. Allori AC, Sailon AM, Warren SM. Biological basis of bone formation, remodeling, and repair-part II: extracellular matrix. Tissue Eng Part B Rev 2008 Sep;14(3):275-283.

16. Rho JY, Kuhn-Spearing L, Zioupos P. Mechanical properties and the hierarchical structure of bone. Med Eng Phys 1998 Mar;20(2):92-102.

17. Nakashima T, Takayanagi H. Osteoclasts and the immune system. J Bone Miner Metab 2009;27(5):519-529.

18. Yavropoulou MP, Yovos JG. Osteoclastogenesis--current knowledge and future perspectives. J Musculoskelet Neuronal Interact 2008 Jul-Sep;8(3):204-216.

19. Panetta NJ, Gupta DM, Longaker MT. Bone regeneration and repair. Curr Stem Cell Res Ther Jun;5(2):122-128.

20. Bone Health and Osteoporosis: A Report of the Surgeon General. [cited 2011 March 25]; Available from: http://www.surgeongeneral.gov/library/bonehealth/chapter_2.html

21. Marie PJ. Transcription factors controlling osteoblastogenesis. Arch Biochem Biophys 2008 May 15;473(2):98-105.

22. Wagner EF, Karsenty G. Genetic control of skeletal development. Curr Opin Genet Dev 2001 Oct;11(5):527-532.

23. Liu W, Toyosawa S, Furuichi T, Kanatani N, Yoshida C, Liu Y, et al. Overexpression of Cbfa1 in osteoblasts inhibits osteoblast maturation and causes osteopenia with multiple fractures. J Cell Biol 2001 Oct 1;155(1):157-166.

24. Winslow MM, Pan M, Starbuck M, Gallo EM, Deng L, Karsenty G, et al. Calcineurin/NFAT signaling in osteoblasts regulates bone mass. Dev Cell 2006 Jun;10 (6):771-782.

25. Day TF, Guo X, Garrett-Beal L, Yang Y. Wnt/beta-catenin signaling in mesenchymal progenitors controls osteoblast and chondrocyte differentiation during vertebrate skeletogenesis. Dev Cell 2005 May;8(5):739-750.

26. Hill TP, Spater D, Taketo MM, Birchmeier W, Hartmann C. Canonical Wnt/beta-catenin signaling prevents osteoblasts from differentiating into chondrocytes. Dev Cell 2005 May;8(5):727-738.

27. Glass DA, 2nd, Karsenty G. Molecular bases of the regulation of bone remodeling by the canonical Wnt signaling pathway. Curr Top Dev Biol 2006;73:43-84.

28. Krishnan V, Moore TL, Ma YL, Helvering LM, Frolik CA, Valasek KM, et al. Parathyroid hormone bone anabolic action requires Cbfa1/Runx2-dependent signaling. Mol Endocrinol 2003 Mar;17(3):423-435.

29. Wang BL, Dai CL, Quan JX, Zhu ZF, Zheng F, Zhang HX, et al. Parathyroid hormone regulates osterix and Runx2 mRNA expression predominantly through protein kinase A signaling in osteoblast-like cells. J Endocrinol Invest 2006 Feb;29(2):101-108.

30. Viereck V, Siggelkow H, Tauber S, Raddatz D, Schutze N, Hufner M. Differential regulation of Cbfa1/Runx2 and osteocalcin gene expression by vitamin-D3, dexamethasone, and local growth factors in primary human osteoblasts. J Cell Biochem 2002;86(2):348-356.

31. Lee MH, Kim YJ, Kim HJ, Park HD, Kang AR, Kyung HM, et al. BMP-2-induced Runx2 expression is mediated by Dlx5, and TGF-beta 1 opposes the BMP-2-induced osteoblast differentiation by suppression of Dlx5 expression. J Biol Chem 2003 Sep 5;278(36):34387-34394.

32. Miyama K, Yamada G, Yamamoto TS, Takagi C, Miyado K, Sakai M, et al. A BMP-inducible gene, dlx5, regulates osteoblast differentiation and mesoderm induction. Dev Biol 1999 Apr 1;208(1):123-133.

33. Ahdjoudj S, Lasmoles F, Holy X, Zerath E, Marie PJ. Transforming growth factor beta2 inhibits adipocyte differentiation induced by skeletal unloading in rat bone marrow stroma. J Bone Miner Res 2002 Apr;17(4):668-677.

34. Kim HJ, Kim JH, Bae SC, Choi JY, Ryoo HM. The protein kinase C pathway plays a central role in the fibroblast growth factor-stimulated expression and transactivation activity of Runx2. J Biol Chem 2003 Jan 3;278(1):319-326.

35. Lian JB, Stein GS. Concepts of osteoblast growth and differentiation: basis for modulation of bone cell development and tissue formation. Crit Rev Oral Biol Med 1992;3(3):269-305.

36. Owen TA, Holthuis J, Markose E, van Wijnen AJ, Wolfe SA, Grimes SR, et al. Modifications of protein-DNA interactions in the proximal promoter of a cell-growth-regulated histone gene during onset and progression of osteoblast differentiation. Proc Natl Acad Sci U S A 1990 Jul;87(13):5129-5133.

37. Owen TA, Aronow M, Shalhoub V, Barone LM, Wilming L, Tassinari MS, et al. Progressive development of the rat osteoblast phenotype in vitro: reciprocal relationships in expression of genes associated with osteoblast proliferation and differentiation during formation of the bone extracellular matrix. J Cell Physiol 1990 Jun; 143(3):420-430.

38. Haller A. Experimentorum de ossiem formatione. Francisci Grasset 1763;2.

39. Hunter J. Treatise on the Blood, Inflammation and Gunshot Wounds. In: Nicol. G, editor. London, 1794.

40. Kanczler JM, Oreffo RO. Osteogenesis and angiogenesis: the potential for engineering bone. Eur Cell Mater 2008;15:100-114.

41. Marks S, Hermey D. The structure and development of bone. In: Bilezekian J, Raisz L, Rodan G, editors. Principles of Bone Biology. San Diego: Academic Press, 1996. p. 3-24.

42. Hunziker EB. Mechanism of longitudinal bone growth and its regulation by growth plate chondrocytes. Microsc Res Tech 1994 Aug 15;28(6):505-519.

43. Gerber HP, Ferrara N. Angiogenesis and bone growth. Trends Cardiovasc Med 2000 Jul;10(5):223-228.

44. Yabsley RH, Harris WR. The Effect of Shaft Fractures and Periosteal Stripping on the Vascular Supply to Epiphyseal Plates. J Bone Joint Surg Am 1965 Apr;47:551-566.

45. Uchida S, Sakai A, Kudo H, Otomo H, Watanuki M, Tanaka M, et al. Vascular endothelial growth factor is expressed along with its receptors during the healing process of bone and bone marrow after drill-hole injury in rats. Bone 2003 May;32(5): 491-501.

46. Glowacki J. Angiogenesis in fracture repair. Clin Orthop Relat Res 1998 Oct(355 Suppl):S82-89.

47. Karamysheva AF. Mechanisms of angiogenesis. Biochemistry (Mosc) 2008 Jul; 73(7):751-762.

48. Carmeliet P. Angiogenesis in health and disease. Nat Med 2003 Jun;9(6): 653-660.

49. Shomento SH, Wan C, Cao X, Faugere MC, Bouxsein ML, Clemens TL, et al. Hypoxia-inducible factors 1alpha and 2alpha exert both distinct and overlapping functions in long bone development. J Cell Biochem Jan 1;109(1):196-204.

50. Pugh CW, Ratcliffe PJ. Regulation of angiogenesis by hypoxia: role of the HIF system. Nat Med 2003 Jun;9(6):677-684.

51. Ben-Yosef Y, Lahat N, Shapiro S, Bitterman H, Miller A. Regulation of endothelial matrix metalloproteinase-2 by hypoxia/reoxygenation. Circ Res 2002 Apr 19;90(7): 784-791.

52. Currie MJ, Gunningham SP, Turner K, Han C, Scott PA, Robinson BA, et al. Expression of the angiopoietins and their receptor Tie2 in human renal clear cell carcinomas; regulation by the von Hippel-Lindau gene and hypoxia. J Pathol 2002 Dec; 198(4):502-510.

53. Gleadle JM, Ebert BL, Firth JD, Ratcliffe PJ. Regulation of angiogenic growth factor expression by hypoxia, transition metals, and chelating agents. Am J Physiol 1995 Jun;268(6 Pt 1):C1362-1368.

54. Kuwabara K, Ogawa S, Matsumoto M, Koga S, Clauss M, Pinsky DJ, et al. Hypoxia-mediated induction of acidic/basic fibroblast growth factor and platelet-derived growth factor in mononuclear phagocytes stimulates growth of hypoxic endothelial cells. Proc Natl Acad Sci U S A 1995 May 9;92(10):4606-4610.

55. Liu Y, Cox SR, Morita T, Kourembanas S. Hypoxia regulates vascular endothelial growth factor gene expression in endothelial cells. Identification of a 5' enhancer. Circ Res 1995 Sep;77(3):638-643.

56. Tuder RM, Flook BE, Voelkel NF. Increased gene expression for VEGF and the VEGF receptors KDR/Flk and Flt in lungs exposed to acute or to chronic hypoxia. Modulation of gene expression by nitric oxide. J Clin Invest 1995 Apr;95(4):1798-1807.

57. Gerber HP, Dixit V, Ferrara N. Vascular endothelial growth factor induces expression of the antiapoptotic proteins Bcl-2 and A1 in vascular endothelial cells. J Biol Chem 1998 May 22;273(21):13313-13316.

58. Gerber HP, McMurtrey A, Kowalski J, Yan M, Keyt BA, Dixit V, et al. Vascular endothelial growth factor regulates endothelial cell survival through the phosphatidylinositol 3'-kinase/Akt signal transduction pathway. Requirement for Flk-1/ KDR activation. J Biol Chem 1998 Nov 13;273(46):30336-30343.

59. Heo SH, Choi YJ, Ryoo HM, Cho JY. Expression profiling of ETS and MMP factors in VEGF-activated endothelial cells: role of MMP-10 in VEGF-induced angiogenesis. J Cell Physiol Sep;224(3):734-742.

60. Sinescu C, Popa F, Grigorean VT, Onose G, Sandu AM, Popescu M, et al. Molecular basis of vascular events following spinal cord injury. J Med Life Jul-Sep;3(3): 254-261.

61. Gerhardt H, Golding M, Fruttiger M, Ruhrberg C, Lundkvist A, Abramsson A, et al. VEGF guides angiogenic sprouting utilizing endothelial tip cell filopodia. J Cell Biol 2003 Jun 23;161(6):1163-1177.

62. Lindahl P, Johansson BR, Leveen P, Betsholtz C. Pericyte loss and microaneurysm formation in PDGF-B-deficient mice. Science 1997 Jul 11;277(5323): 242-245.

63. Armulik A, Abramsson A, Betsholtz C. Endothelial/pericyte interactions. Circ Res 2005 Sep 16;97(6):512-523.

64. Suri C, Jones PF, Patan S, Bartunkova S, Maisonpierre PC, Davis S, et al. Requisite role of angiopoietin-1, a ligand for the TIE2 receptor, during embryonic angiogenesis. Cell 1996 Dec 27;87(7):1171-1180.

65. Ruan J, Hajjar K, Rafii S, Leonard JP. Angiogenesis and antiangiogenic therapy in non-Hodgkin's lymphoma. Ann Oncol 2009 Mar;20(3):413-424.

66. Gospodarowicz D, Abraham JA, Schilling J. Isolation and characterization of a vascular endothelial cell mitogen produced by pituitary-derived folliculo stellate cells. Proc Natl Acad Sci U S A 1989 Oct;86(19):7311-7315.

67. Senger DR, Galli SJ, Dvorak AM, Perruzzi CA, Harvey VS, Dvorak HF. Tumor cells secrete a vascular permeability factor that promotes accumulation of ascites fluid. Science 1983 Feb 25;219(4587):983-985.

68. Ferrara N, Davis-Smyth T. The biology of vascular endothelial growth factor. Endocr Rev 1997 Feb;18(1):4-25.

69. Houck KA, Ferrara N, Winer J, Cachianes G, Li B, Leung DW. The vascular endothelial growth factor family: identification of a fourth molecular species and characterization of alternative splicing of RNA. Mol Endocrinol 1991 Dec;5(12): 1806-1814.

70. Tischer E, Mitchell R, Hartman T, Silva M, Gospodarowicz D, Fiddes JC, et al. The human gene for vascular endothelial growth factor. Multiple protein forms are encoded through alternative exon splicing. J Biol Chem 1991 Jun 25;266(18): 11947-11954.

71. Park JE, Keller GA, Ferrara N. The vascular endothelial growth factor (VEGF) isoforms: differential deposition into the subepithelial extracellular matrix and bioactivity of extracellular matrix-bound VEGF. Mol Biol Cell 1993 Dec;4(12):1317-1326.

72. Dor Y, Porat R, Keshet E. Vascular endothelial growth factor and vascular adjustments to perturbations in oxygen homeostasis. Am J Physiol Cell Physiol 2001 Jun;280(6):C1367-1374.

73. de Vries C, Escobedo JA, Ueno H, Houck K, Ferrara N, Williams LT. The fms-like tyrosine kinase, a receptor for vascular endothelial growth factor. Science 1992 Feb 21;255(5047):989-991.

74. Waltenberger J, Claesson-Welsh L, Siegbahn A, Shibuya M, Heldin CH. Different signal transduction properties of KDR and Flt1, two receptors for vascular endothelial growth factor. J Biol Chem 1994 Oct 28;269(43):26988-26995.

75. Park JE, Chen HH, Winer J, Houck KA, Ferrara N. Placenta growth factor. Potentiation of vascular endothelial growth factor bioactivity, in vitro and in vivo, and high

affinity binding to Flt-1 but not to Flk-1/KDR. J Biol Chem 1994 Oct 14;269(41): 25646-25654.

76. Eliceiri BP, Paul R, Schwartzberg PL, Hood JD, Leng J, Cheresh DA. Selective requirement for Src kinases during VEGF-induced angiogenesis and vascular permeability. Mol Cell 1999 Dec;4(6):915-924.

77. Guo D, Jia Q, Song HY, Warren RS, Donner DB. Vascular endothelial cell growth factor promotes tyrosine phosphorylation of mediators of signal transduction that contain SH2 domains. Association with endothelial cell proliferation. J Biol Chem 1995 Mar 24;270(12):6729-6733.

78. Shalaby F, Rossant J, Yamaguchi TP, Gertsenstein M, Wu XF, Breitman ML, et al. Failure of blood-island formation and vasculogenesis in Flk-1-deficient mice. Nature 1995 Jul 6;376(6535):62-66.

79. Ornitz DM, Itoh N. Fibroblast growth factors. Genome Biol 2001;2 (3):REVIEWS3005.

80. Arnaud E, Touriol C, Boutonnet C, Gensac MC, Vagner S, Prats H, et al. A new 34-kilodalton isoform of human fibroblast growth factor 2 is cap dependently synthesized by using a non-AUG start codon and behaves as a survival factor. Mol Cell Biol 1999 Jan;19(1):505-514.

81. Gospodarowicz D, Ferrara N, Schweigerer L, Neufeld G. Structural characterization and biological functions of fibroblast growth factor. Endocr Rev 1987 May;8(2):95-114.

82. Presta M, Maier JA, Rusnati M, Ragnotti G. Basic fibroblast growth factor: production, mitogenic response, and post-receptor signal transduction in cultured normal and transformed fetal bovine aortic endothelial cells. J Cell Physiol 1989 Dec;141(3): 517-526.

83. Schweigerer L, Neufeld G, Friedman J, Abraham JA, Fiddes JC, Gospodarowicz D. Capillary endothelial cells express basic fibroblast growth factor, a mitogen that promotes their own growth. Nature 1987 Jan 15-21;325(6101):257-259.

84. Cross MJ, Claesson-Welsh L. FGF and VEGF function in angiogenesis: signalling pathways, biological responses and therapeutic inhibition. Trends Pharmacol Sci 2001 Apr;22(4):201-207.

85. Reiss Y. Angiopoietins. Recent Results Cancer Res;180:3-13.

86. Papapetropoulos A, Fulton D, Mahboubi K, Kalb RG, O'Connor DS, Li F, et al. Angiopoietin-1 inhibits endothelial cell apoptosis via the Akt/survivin pathway. J Biol Chem 2000 Mar 31;275(13):9102-9105.

87. Hoffman A. Classes of Materials Used in Medicine. In: Ratner B, Hoffman A, Schoen F, Lemons J, editors. Biomaterials Science. 2 ed. New York: Elsevier Academic Press, 2004. p. 67.

88. Hallab N, Jacobs J, Katz J. Application of Materials in Medicine, Biology, and Artificial Organs. In: Ratner B, Hoffman A, Schoen F, Lemons J, editors. Biomaterials Science. 2 ed. New York: Elsevier Academic Press, 2004. p. 526-555.

89. Brunski J. Metals. In: Ratner B, Hoffman A, Schoen F, Lemons J, editors. Biomaterials Science. 2 ed. New York: Elsevier Academic Press, 2004. p. 137-153.

90. Definitions in Biomaterials. Progress in Biomedical Engineering. 4 ed. Amsterdam: Elsevier, 1987.

91. Anderson JM. Inflammation, Wound Healing, and the Foreign-Body Response. In: Ratner B, Hoffman A, Schoen F, Lemons J, editors. Biomaterials Science. 2 ed. New York: Elsevier, 2004. p. 296-304.

92. Inflammation and Repair. In: Cotran RZ, Kumar V, Robbins SL, editors. Pathologic Basis of Disease. 6 ed. Philadelphia: WB Saunders. p. 50-112.

93. Branemark PI, Hansson BO, Adell R, Breine U, Lindstrom J, Hallen O, et al. Osseointegrated implants in the treatment of the edentulous jaw. Experience from a 10-year period. Scand J Plast Reconstr Surg Suppl 1977;16:1-132.

94. Davies JE, Hosseini MM. Histodynamics of Endosseous Wound Healing. In: Davies JE, editor. Bone Engineering. Toronto: em squared incorporated, 2000.

95. Boyan BD, Hummert TW, Dean DD, Schwartz Z. Role of material surfaces in regulating bone and cartilage cell response. Biomaterials 1996 Jan;17(2):137-146.

96. Ratner BD HA, Schoen FJ, Lemons JE, editor. Biomaterials Science: An Introduction to Materials in Medicine. 2 ed. San Diego: Elsevier Academic Press, 2004.

97. Ellingsen JE. A study on the mechanism of protein adsorption to TiO2. Biomaterials 1991 Aug;12(6):593-596.

98. Kieswetter K, Schwartz Z, Dean DD, Boyan BD. The role of implant surface characteristics in the healing of bone. Crit Rev Oral Biol Med 1996;7(4):329-345.

99. Hynes RO. Integrins: bidirectional, allosteric signaling machines. Cell 2002 Sep 20;110(6):673-687.

100. Gronthos S, Simmons PJ, Graves SE, Robey PG. Integrin-mediated interactions between human bone marrow stromal precursor cells and the extracellular matrix. Bone 2001 Feb;28(2):174-181.

101. Moursi AM, Globus RK, Damsky CH. Interactions between integrin receptors and fibronectin are required for calvarial osteoblast differentiation in vitro. J Cell Sci 1997 Sep;110 (Pt 18):2187-2196.

102. Siebers MC, ter Brugge PJ, Walboomers XF, Jansen JA. Integrins as linker proteins between osteoblasts and bone replacing materials. A critical review. Biomaterials 2005 Jan;26(2):137-146.

103. Gronowicz G, McCarthy MB. Response of human osteoblasts to implant materials: integrin-mediated adhesion. J Orthop Res 1996 Nov;14(6):878-887.

104. Raz P, Lohmann CH, Turner J, Wang L, Poythress N, Blanchard C, et al. 1alpha, 25(OH)2D3 regulation of integrin expression is substrate dependent. J Biomed Mater Res A 2004 Nov 1;71(2):217-225.

105. Garcia AJ. Get a grip: integrins in cell-biomaterial interactions. Biomaterials 2005 Dec;26(36):7525-7529.

106. Dedhar S. Integrin mediated signal transduction in oncogenesis: an overview. Cancer Metastasis Rev 1995 Sep;14(3):165-172.

107. Egan SE, Weinberg RA. The pathway to signal achievement. Nature 1993 Oct 28;365(6449):781-783.

108. Seger R, Krebs EG. The MAPK signaling cascade. FASEB J 1995 Jun;9(9): 726-735.

109. Goto T, Yoshinari M, Kobayashi S, Tanaka T. The initial attachment and subsequent behavior of osteoblastic cells and oral epithelial cells on titanium. Biomed Mater Eng 2004;14(4):537-544.

110. Martin JY, Schwartz Z, Hummert TW, Schraub DM, Simpson J, Lankford J, Jr., et al. Effect of titanium surface roughness on proliferation, differentiation, and protein synthesis of human osteoblast-like cells (MG63). J Biomed Mater Res 1995 Mar;29(3): 389-401.

111. Rupp F, Scheideler L, Olshanska N, de Wild M, Wieland M, Geis-Gerstorfer J. Enhancing surface free energy and hydrophilicity through chemical modification of microstructured titanium implant surfaces. J Biomed Mater Res A 2006 Feb;76(2): 323-334.

112. Zhao G, Schwartz Z, Wieland M, Rupp F, Geis-Gerstorfer J, Cochran DL, et al. High surface energy enhances cell response to titanium substrate microstructure. J Biomed Mater Res A 2005 Jul 1;74(1):49-58.

113. Buser D, Schenk RK, Steinemann S, Fiorellini JP, Fox CH, Stich H. Influence of surface characteristics on bone integration of titanium implants. A histomorphometric study in miniature pigs. J Biomed Mater Res 1991 Jul;25(7):889-902.

114. Gotfredsen K, Wennerberg A, Johansson C, Skovgaard LT, Hjorting-Hansen E. Anchorage of TiO2-blasted, HA-coated, and machined implants: an experimental study with rabbits. J Biomed Mater Res 1995 Oct;29(10):1223-1231.

115. Cochran DL, Schenk RK, Lussi A, Higginbottom FL, Buser D. Bone response to unloaded and loaded titanium implants with a sandblasted and acid-etched surface: a histometric study in the canine mandible. J Biomed Mater Res 1998 Apr;40(1):1-11.

116. Schwarz F, Wieland M, Schwartz Z, Zhao G, Rupp F, Geis-Gerstorfer J, et al. Potential of chemically modified hydrophilic surface characteristics to support tissue integration of titanium dental implants. J Biomed Mater Res B Appl Biomater 2009 Feb; 88(2):544-557.

117. Miyazaki M, Tsumura H, Wang JC, Alanay A. An update on bone substitutes for spinal fusion. Eur Spine J 2009 Jun;18(6):783-799.

118. Lee YP, Jo M, Luna M, Chien B, Lieberman JR, Wang JC. The efficacy of different commercially available demineralized bone matrix substances in an athymic rat model. J Spinal Disord Tech 2005 Oct;18(5):439-444.

119. Peterson B, Whang PG, Iglesias R, Wang JC, Lieberman JR. Osteoinductivity of commercially available demineralized bone matrix. Preparations in a spine fusion model. J Bone Joint Surg Am 2004 Oct;86-A(10):2243-2250.

120. Wang JC, Alanay A, Mark D, Kanim LE, Campbell PA, Dawson EG, et al. A comparison of commercially available demineralized bone matrix for spinal fusion. Eur Spine J 2007 Aug;16(8):1233-1240.

121. Acarturk TO, Hollinger JO. Commercially available demineralized bone matrix compositions to regenerate calvarial critical-sized bone defects. Plast Reconstr Surg 2006 Sep 15;118(4):862-873.

122. Kohles SS, Vernino AR, Clagett JA, Yang JC, Severson S, Holt RA. A morphometric evaluation of allograft matrix combinations in the treatment of osseous defects in a baboon model. Calcif Tissue Int 2000 Aug;67(2):156-162.

123. Slevin M, Krupinski J, Gaffney J, Matou S, West D, Delisser H, et al. Hyaluronan-mediated angiogenesis in vascular disease: uncovering RHAMM and CD44 receptor signaling pathways. Matrix Biol 2007 Jan;26(1):58-68.

124. Aslan M, Simsek G, Dayi E. The effect of hyaluronic acid-supplemented bone graft in bone healing: experimental study in rabbits. J Biomater Appl 2006 Jan;20(3): 209-220.

125. Jung M, Tuischer JS, Sergi C, Gotterbarm T, Pohl J, Richter W, et al. Local application of a collagen type I/hyaluronate matrix and growth and differentiation factor 5 influences the closure of osteochondral defects in a minipig model by enchondral ossification. Growth Factors 2006 Dec;24(4):225-232.

126. Rooney P, Kumar S, Ponting J, Wang M. The role of hyaluronan in tumour neovascularization (review). Int J Cancer 1995 Mar 3;60(5):632-636.

127. Jiang D, Liang J, Noble PW. Hyaluronan in tissue injury and repair. Annu Rev Cell Dev Biol 2007;23:435-461.

128. West DC, Kumar S. Tumour-associated hyaluronan: a potential regulator of tumour angiogenesis. Int J Radiat Biol 1991 Jul-Aug;60(1-2):55-60.

129. Deed R, Rooney P, Kumar P, Norton JD, Smith J, Freemont AJ, et al. Early-response gene signalling is induced by angiogenic oligosaccharides of hyaluronan in endothelial cells. Inhibition by non-angiogenic, high-molecular-weight hyaluronan. Int J Cancer 1997 Apr 10;71(2):251-256.

130. Slevin M, Krupinski J, Kumar S, Gaffney J. Angiogenic oligosaccharides of hyaluronan induce protein tyrosine kinase activity in endothelial cells and activate a cytoplasmic signal transduction pathway resulting in proliferation. Lab Invest 1998 Aug; 78(8):987-1003.

131. Slevin M, Kumar S, Gaffney J. Angiogenic oligosaccharides of hyaluronan induce multiple signaling pathways affecting vascular endothelial cell mitogenic and wound healing responses. J Biol Chem 2002 Oct 25;277(43):41046-41059.

132. Slevin M, West D, Kumar P, Rooney P, Kumar S. Hyaluronan, angiogenesis and malignant disease. Int J Cancer 2004 May 1;109(5):793-794; author reply 795-796.

133. West DC, Kumar S. The effect of hyaluronate and its oligosaccharides on endothelial cell proliferation and monolayer integrity. Exp Cell Res 1989 Jul;183(1): 179-196.

134. Sattar A, Rooney P, Kumar S, Pye D, West DC, Scott I, et al. Application of angiogenic oligosaccharides of hyaluronan increases blood vessel numbers in rat skin. J Invest Dermatol 1994 Oct;103(4):576-579.

135. Rooney P, Wang M, Kumar P, Kumar S. Angiogenic oligosaccharides of hyaluronan enhance the production of collagens by endothelial cells. J Cell Sci 1993 May;105 (Pt 1):213-218.

136. Montesano R, Kumar S, Orci L, Pepper MS. Synergistic effect of hyaluronan oligosaccharides and vascular endothelial growth factor on angiogenesis in vitro. Lab Invest 1996 Aug;75(2):249-262.

137. West DC, Hampson IN, Arnold F, Kumar S. Angiogenesis induced by degradation products of hyaluronic acid. Science 1985 Jun 14;228(4705):1324-1326.

CHAPTER 2: Regulation of Angiogenesis During Osseointegration by Titanium Surface Microstructure and Energy

2.1 Introduction

Biomaterial surface properties play a significant role in determining host cellular responses to implant materials used in tissue engineering and regenerative medicine applications. Modifications to surface microarchitecture, chemistry, or energy can alter cell adhesion, proliferation, and gene expression [1-3]. By designing materials to present specific surface properties, there is the potential to control cell responses to achieve the desired application.

Titanium (Ti) is a widely used biomaterial in the orthopaedic and dental industries because of the biocompatibility and resistance to wear of the Ti oxide layer that forms on its surface. *In vitro* studies have shown that modifications to Ti surface microtopography affect the attachment and differentiation of osteoblasts, including MG63 and MC3T3-E1 cell lines, as well as fetal rat calvarial cells and normal human osteoblasts [4]. MG63 cells cultured on Ti surfaces with microrough topographies that resemble osteoclast resorption pits display a more differentiated phenotype than cells grown on smooth Ti substrates, characterized by decreased alkaline phosphatase specific activity and higher levels of osteocalcin [5]. The combination of microstructure and high surface energy further enhances osteoblast differentiation on Ti surfaces [6]. *In vivo*, microstructured implant surfaces support greater bone-to-implant contact than smooth surfaces do, resulting in greater removal torque strength [7-9].

The overall success of biomaterial implants in orthopaedic and dental applications however, is not only dependent on achieving the desired cellular response at the host tissue/implant interface but also by the integration of the implant into the

surrounding host tissue. Angiogenesis, the sprouting of new capillary blood vessels from the pre-existing vasculature, is a critical process during embryonic development and in several physiological conditions, including the formation of new bone and bone fracture healing [15,16], as well as during bone regeneration and osseointegration of implanted materials [17]. This suggests that materials that support peri-implant bone formation may support angiogenesis as well as osteogenesis.

The formation of blood vessels *in vivo* is a complex process and involves the coordination of multiple growth factors and events. Among the many identified growth factors that serve to initiate and control angiogenesis are vascular endothelial growth factor-A (VEGF-A) [18], basic fibroblast growth factor (FGF-2) [19], epidermal growth factor (EGF) [20], and angiopoietin-1 (Ang-1) [21]. Both VEGF-A and FGF-2 are two of the growth factors necessary for initiating angiogenesis and both are chemotactic for endothelial cells [22]. VEGF-A is produced by multiple cell types, including osteoblasts [23] and hypertrophic chondrocytes [24], and affects vascular permeability *in vivo* [25]. The interaction of VEGF with its receptors Flt-1 and Flk-1/KDR is one of the first signal transduction pathways activated during angiogenesis in endothelial cells [26]. FGF-2 is a heparin-binding polypeptide that induces proliferation, migration, and protease production in cultured endothelial cells and promotes neovascularization *in vivo* [27]. EGF has also been implicated in angiogenesis by stimulating the proliferation of endothelial cells through its interaction with the tyrosine kinase EGF receptor [28]. EGF treatment of prostate cancer cells increases VEGF mRNA expression suggesting that EGF may also exert its effect by stimulating VEGF production [29]. Ang-1, a member of the angiopoietin family of signaling molecules, binds to its cognate receptor tyrosine kinase Tie1 present on the surface of endothelial cells, inducing signaling events that

serve to control later stages of blood vessel formation, such as the stabilization of the endothelial sprout and its interaction with pericytes [30].

Recent studies suggest that osteoblasts may play a role in directly stimulating endothelial cells. Osteoblasts produce VEGF-A [31] and FGF-2 [32], and levels of these angiogenic factors are regulated by factors that stimulate osteogenesis *in vivo*, including 1,25 dihydroxyvitamin D_3 [$1,25(OH)_2D_3$] [33], 17β-estradiol [34], and bone morphogenetic protein-2 (BMP-2) [35]. Others have noted that neovascularization is increased in peri-implant bone when microstructured Ti implants are used [36].

Mesenchymal stem cells (MSCs) that have been induced to become osteoblasts produce greater levels of angiogenic factors than unstimulated MSCs [37]. This suggests that this is a function of mature secretory cells and those factors that enhance osteoblast differentiation may also enhance their ability to promote angiogenesis. While it has been established that Ti surface properties influence osteoblast maturation and differentiation and enhance osseointegration *in vivo*, the potential role that surface properties may have in enhancing angiogenesis surrounding the implant surface through the secretion of angiogenic stimulators by osteoblasts has not been investigated.

In this study, we examined the production of the pro-angiogenic growth factors VEGF-A, FGF-2, EGF and Ang-1 by MG63 human osteoblast-like cells and normal human osteoblasts cultured on Ti surfaces with varying microtopographies and surface energies. In addition, we investigated whether surface-dependent production of those factors is sensitive to systemic regulation by treating the cells with $1α,25(OH)_2D_3$. We verified that factors produced by the cells were angiogenic by assessing endothelial cell differentiation in response to the conditioned media from MG63 cell cultures from the different Ti substrates. The specific contribution of VEGF-A was determined by treating the endothelial cell cultures with conditioned media in the presence of a neutralization

antibody to VEGF-A. Finally, the effect of titanium substrate microtopography and surface energy on bone formation and vascularization *in vivo* was examined using a novel murine femoral press-fit model.

2.2 Materials and Methods

2.2.1 Ti Surfaces

Ti disks were prepared from 1 mm thick sheets of grade 2 unalloyed commercially pure Ti punched into 15mm diameter disks and supplied by Institut Straumann AG (Basel, Switzerland). The production and characterization of smooth pretreatment (PT), sand blasted and acid etched (SLA), and modified SLA (modSLA) surfaces have been described previously [6]. PT surfaces were degreased by washing Ti disks in acetone and processed in a 2% ammonium fluoride/2% hydrofluoric acid/10% nitric acid solution. SLA surfaces were made by coarse grit-blasting of the PT surfaces with 0.25-0.50 mm corundum grit followed by acid etching. modSLA surfaces were made using the same procedure as SLA surfaces under nitrogen rinsing to prevent exposure to air and were then stored under aqueous conditions under nitrogen to retain high surface free energy. The PT surface has an overall average roughness (Ra) of less than 0.7 μm. SLA and modSLA surfaces have a complex microtopography with craters varying from 30 to 100 μm in diameter overlaid with pits from 1 to 3 μm in diameter. The acid etch creates sharp edges approximately 700 nm in height, resulting in an overall Ra of approximately 4 μm. PT, SLA and modSLA Ti disks all have a TiO_2 surface layer, with the PT and SLA surfaces being hydrophobic due to the adsorption of atmospheric hydrocarbons while the modSLA surface is hydrophilic. Advancing contact angles were used to calculate the hydrophilicity of the surfaces as PT (95.8°), SLA (139.80°), and modSLA (~0°). Surface free energy for PT, SLA, and modSLA surfaces was calculated

according to Zisman (critical surface tension), Equation of State (EOS), and Geometric Mean approaches and is described in detail elsewhere [38].

Surface treatments for Ti implants for *in vivo* studies were prepared in a manner similar to those for Ti surfaces described above. Ti implants consisted of two parts: a handling device and the Ti implant rod [46]. Cylindrical Ti implants were manufactured to be 5 mm in length and 0.9 mm in diameter. All implants were sterilized by gamma irradiation at 25 kGy prior to use.

2.2.2 Cell Culture

Human MG63 osteoblast like cells were cultured in 24-well tissue culture plates on tissue culture treated polystyrene (TCPS, used as a control for all studies), PT, SLA, and modSLA surfaces using Dulbecco's modified Eagle's medium (DMEM) supplemented with 10% fetal bovine serum and 1% penicillin/streptomycin. Cells were seeded at an initial density of 10,000 cells/cm^2 and media were exchanged 24 hours after seeding and every 48 hours thereafter. When the cells were confluent on TCPS, media from all cultures were collected and examined for VEGF-A, FGF-2, EGF, Ang-1 and osteocalcin levels. Additionally, conditioned media from MG63 cell cultures were used to assess differentiation of human aortic endothelial cells as described below.

Primary human osteoblasts (HOB cells) were isolated from the mandible of a 50 year old male donor by use of an explant culture. Briefly, isolated bone chips were cleaned of all soft and connective tissues and cut into approximately 1.5 mm fragments. The bone fragments were then cultured in DMEM containing 10% fetal bovine serum and 1% penicillin/streptomycin for two weeks to allow cells to migrate out of the tissue. The migrated osteoblasts were then collected and cultured in DMEM containing 10% FBS and 1% penicillin/streptomycin. Fourth passage human osteoblasts were used for experiments.

2.2.3 Effect of $1,25(OH)_2D_3$

Confluent MG63 cell cultures were treated with 10^{-8}M or 10^{-9}M $1\alpha,25(OH)_2D_3$ or vehicle for 24 hours prior to harvest.

2.2.4 Cell Number

Cell number was determined for all cell types at time of harvest. At confluence or after 24 hour treatment with $1\alpha,25(OH)_2D_3$, cells were released from TCPS and Ti surfaces using two sequential incubations with 0.25% trypsin for 10 minutes at 37°C to ensure that no cells remained on the rough Ti surfaces and counted using an automated cell counter (Z1 Particle counter, Beckman Coulter, Fullerton, CA).

2.2.5 Alkaline Phosphatase Specific Activity

Alkaline phosphatase specific activity (orthophosphoric monoester phosphohydrolase, alkaline; E.C. 3.1.3.1) was measured in the cell lysates as a marker of osteoblastic differentiation. Enzyme activity was determined using a colorimetric assay measuring the release of *p*-nitrophenol from *p*-nitrophenylphosphate at 37°C. Samples were read on a plate reader at 415nm [39].

2.2.6 Osteocalcin

Osteocalcin levels in the conditioned medium of MG63 cells and human osteoblasts grown on Ti surfaces were determined as a marker of osteoblast maturation using a commercially available radioimmunoassay (Biomedical Technologies, Inc., Stoughton, MA) following the manufacturer's protocol.

2.2.7 VEGF-A, FGF-2, EGF, Ang-1

The levels of the angiogenic growth factors VEGF-A, FGF-2, EGF, and Ang-1 were determined in the conditioned medium using commercially available sandwich ELISA assays (Duoset ELISA Development Systems, R&D Systems, Minneapolis, MN) following the manufacturer's protocols.

2.2.8 Endothelial Cell Differentiation

To determine if the conditioned media were angiogenic, we examined their ability to support endothelial tube formation. Human aortic endothelial cells (HAEC) were purchased from Lonza (Walkersville, MD) and grown in 75cm^2 tissue culture flasks using endothelial cell basal medium (EGM-2, Lonza). At confluence, cells were passaged and used for the endothelial tube formation assay. Endothelial cell differentiation was assessed using two separate assays; a Matrigel tube formation assay (Millipore, St. Charles, MO), and a fibrin gel assay (Millipore).

2.2.9 Matrigel Tube Formation Assay

Briefly, 50 μL ECMatrix™ was added to each well of a 96-well tissue culture plate and allowed to solidify for 1 hour at 37^{o}C. HAECs were then seeded at a density of 1 X 10^4 cells/well using a mixture of 100μL conditioned medium from MG63 cells cultured on TCPS, PT, SLA, and modSLA surfaces and 50μL EGM-2 for growth maintenance. Cells were cultured for 24 hours, and at 4, 8, 12, and 24 hours after seeding, pictures were taken for morphometric analysis to determine the total endothelial tube length and total number of branch points.

To assess the specific role of VEGF-A, endothelial cell differentiation in the presence of a competitive VEGF-A blocking antibody was determined. Goat anti-human VEGF-A neutralization antibody was purchased from R&D Systems (Minneapolis, MN) and was added to the culture medium at a concentration of 5 μg/mL.

2.2.10 Fibrin Gel Assay

Endothelial cell differentiation was further assessed with the use of a fibrin gel assay. 30 μL of fibrinogen solution and 20 μL of thrombin solution were added to each well of a 96-well plate and the mixture was allowed to polymerize for 30 minutes at 37^{o}C. HAECs were plated in 100 μL of EGM-2 at a density of 5 x 10^3 cells/well and cultured at

37°C for 24h. At 24h, media were removed and a second layer of fibrin was added on top of cells by again mixing 30 μL of fibrinogen and 20μL of thrombin. The mixture was allowed to polymerize for 5 minutes before 100 μL of conditioned media from MG63 cell cultures on Ti substrates was added. At 12, 24, 36, and 48h after the addition of conditioned media, images were taken for morphometric analysis to determine total endothelial tube length.

2.2.11 *In vivo* model

All animal handling and procedures were approved by the Georgia Institute of Tehnology IACUC review board and conducted in accordance with NIH guidelines. Custom-made Ti implants were inserted into the femoral medullary canal of mice via a medial parapatellar arthrotomy. Briefly, male C57/Bl6 mice (ages 8 weeks or 9 months) were anesthetized with 5% isoflurane gas inhalation. The right hind limb of animals was shaved and cleaned using ethanol and chlorhexidine. Anesthetization was maintained with 2% isoflurane gas inhalation for the duration of the surgical procedure. Cleaned, anesthetized animals were placed in a supine position and covered with a sterile surgical drape. Using a scalpel, an 8 mm incision was made over the distal side of the knee. Blunt dissection was used to move aside the ligament and patella to expose the intercondyler notch of the distal femur. Once the femoral cartilage was exposed, a 1 mm round dental bur was used to penetrate the distal intercondylar notch of the femur to access the medullary cavity. A 22G needle was gently pushed into the femur to confirm penetration of the medullary cavity. Cylindrical Ti implants were inserted into the femoral medullary canal and broken from the handling device. To confirm successful insertion of the implant into the femoral medullary canal, x-ray imaging was done prior to closure of the surgical incision. If the Ti implant was not inserted into the medullary canal or if insertion of the Ti implant resulted in a broken femur, the mouse was removed from the

study and euthanized using CO_2 inhalation. This was done to ensure an appropriate number of successful surgeries for each Ti implant type. Following successful implant insertion, periosteal tissue was closed using resorbable sutures and the surgical incision was closed with wound clips. After recovery from anesthesia, mice were injected with 0.03 mg/kg buprenorphine to relieve post-operative pain. Animals were monitored every 12 hours for 48 hours post-surgery and once per day thereafter for the duration of the study. Wound clips were removed 10-14 post-surgery. All animals had access to food and water *ad libitum* for the duration of the study.

2.2.12 Vascular Perfusion

At 28 days post-surgery, 9 month-old animals were euthanized via CO_2 inhalation. Immediately after euthanization, the thoracic cavity was opened and a 22G butterfly needle was inserted into the left ventricle. The inferior vena cava was severed to allow for the vasculature to be flushed. Heparanized saline (100 U/mL) was used to flush the vasculature followed by perfusion with 10% neutral buffered formalin to fix the tissue specimens. The vasculature was perfused using a radio-opaque silicone rubber compound (Microfil, Flow Tech Inc., Carver, MA) consisting of a 9:1 ratio of Microfil:curing agent. Following vascular perfusion, the injected Microfil compound was allowed to polymerize overnight at 4^{o}C.

2.2.12 Implant Harvest

At 28 days (9 month mice) or 35 days (8 week mice) limbs containing Ti implants were collected and stored in 10% neutral buffered formalin for histological processing. Sagittal tissue sections were cut and polished to a final thickness of 10 – 20 μm and stained with haematoxylin and eosin for histological analysis.

Using commercially available image analysis software (Image-Pro, MediaCybernetics, Bethesda, MD) stained tissue sections were analyzed for bone to implant contact (both 8

week and 9 month old animals) as well as total blood vessel number (9 month old animals).

2.2.13 Statistical Analysis

The data presented here are from one of two separate sets of experiments. Both sets of experiments yielded comparable observations. For any given experiment, each data point represents the mean ± standard error of six individual cultures. Data were analyzed by ANOVA and when statistical differences were detected, Student's *t*-test for multiple comparisons using Bonferroni's modification was used. p-values < 0.05 were considered significant.

2.3 Results

2.3.1 MG63 and HOB Cell Response

As noted previously [6], MG63 cell differentiation was increased on the SLA and modSLA substrates compared to cells on TCPS and PT, validating the model. Total cell number was comparable on TCPS and smooth PT surfaces, whereas cells cultured on microrough SLA Ti surfaces demonstrated a significant decrease ($p<0.05$) in cell number when compared to TCPS and smooth PT Ti surfaces (Figure 2-1A). The addition of high surface energy on modSLA Ti surfaces did not result in any further decrease in overall cell number. MG63 cells exhibited a more differentiated phenotype when grown on Ti substrates compared to TCPS. Alkaline phosphatase specific activity on all three Ti substrates was significantly reduced (Figure 2-1B). Osteocalcin, a late marker of osteoblast differentiation was found to be similar on TCPS and smooth PT substrates, and was increased 212% in MG63 cell cultures on SLA (Figure 2-1C). The combination of high surface energy and microstructure on modSLA surfaces resulted in a further increase in osteocalcin levels compared to SLA.

Secretion of angiogenic factors by MG63 cells was differentially regulated as a function of substrate morphology and surface energy. Secreted levels of VEGF-A on TCPS and PT substrates were comparable (Figure 2-2A). Levels of secreted VEGF-A increased nearly 2-fold on SLA while MG63 cell cultures produced almost 3-fold higher levels of VEGF-A on modSLA. Secretion of FGF-2 and EGF exhibited similar substrate-dependent effects. FGF-2 levels were similar on both TCPS and PT substrates; secreted levels observed on SLA were approximately 10-fold higher than TCPS levels; and the combination of a hydrophilic surface with the rough surface microstructure observed on modSLA resulted in a further enhancement of FGF-2 production (Figure 2-2B). EGF production on SLA and modSLA was significantly higher than on either TCPS or PT (Figure 2-2C). In contrast to secreted levels of VEGF-A, FGF-2, and EGF, the levels of Ang-1 were comparable on all surfaces examined (Figure 2-2D).

HOB cells cultured on TCPS as well as on all three Ti surfaces exhibited similar responses to those observed in MG63 cell cultures. Total cell number on TCPS was significantly higher than that observed on all three Ti substrates (Figure 2-3A). Further, a rough microstructure reduced total cell number compared to smooth pre-treated Ti surfaces. High surface energy further reduced total cell number on modSLA surfaces.

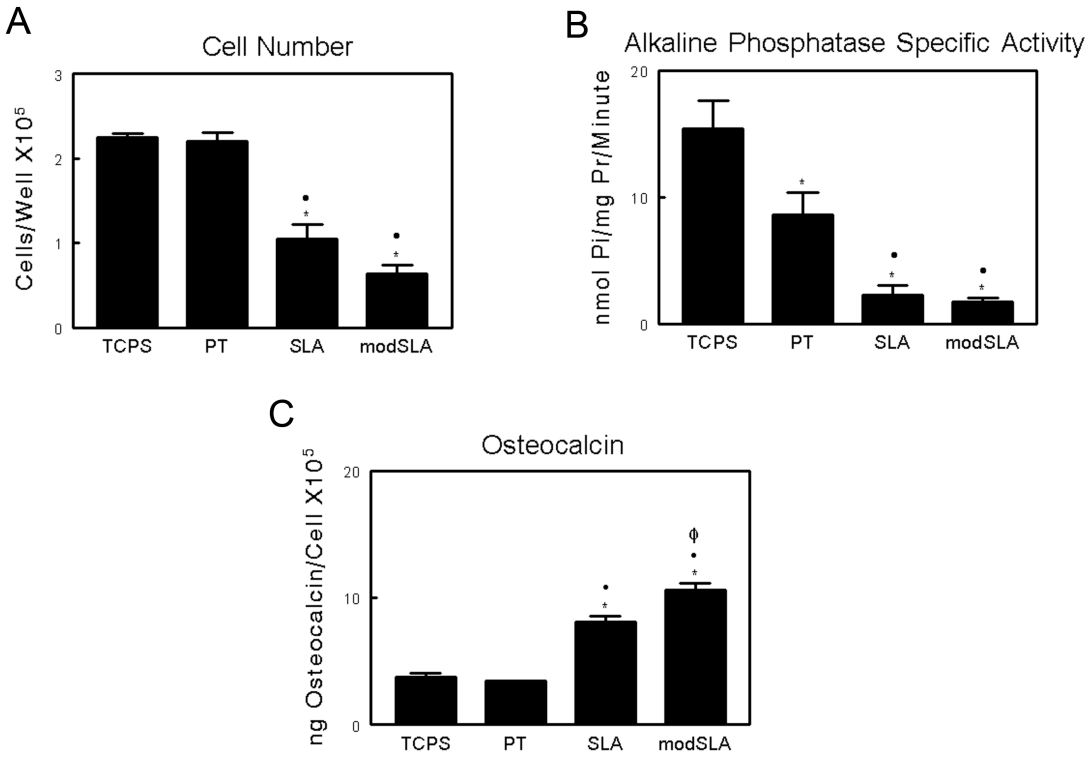

Figure 2-1. Response of MG63 cells cultured on tissue culture polystyrene and Ti surfaces: (A) cell number, (B) alkaline phosphatase specific activity in the cell lysate, and (C) osteocalcin levels in the conditioned medium. Cells were cultured on control (TCPS), PT, SLA, and modSLA Ti surfaces. Values presented are mean $\pm$ SEM of six independent cultures. The data presented are from one of two separate experiments with comparable results. Data were analyzed using ANOVA and statistical significance between groups was determined using Bonferroni's modification of Student's t-test. *$p< 0.05$ vs. TCPS; ·$p<0.05$ vs. PT; Φ$p<0.05$ vs. SLA.

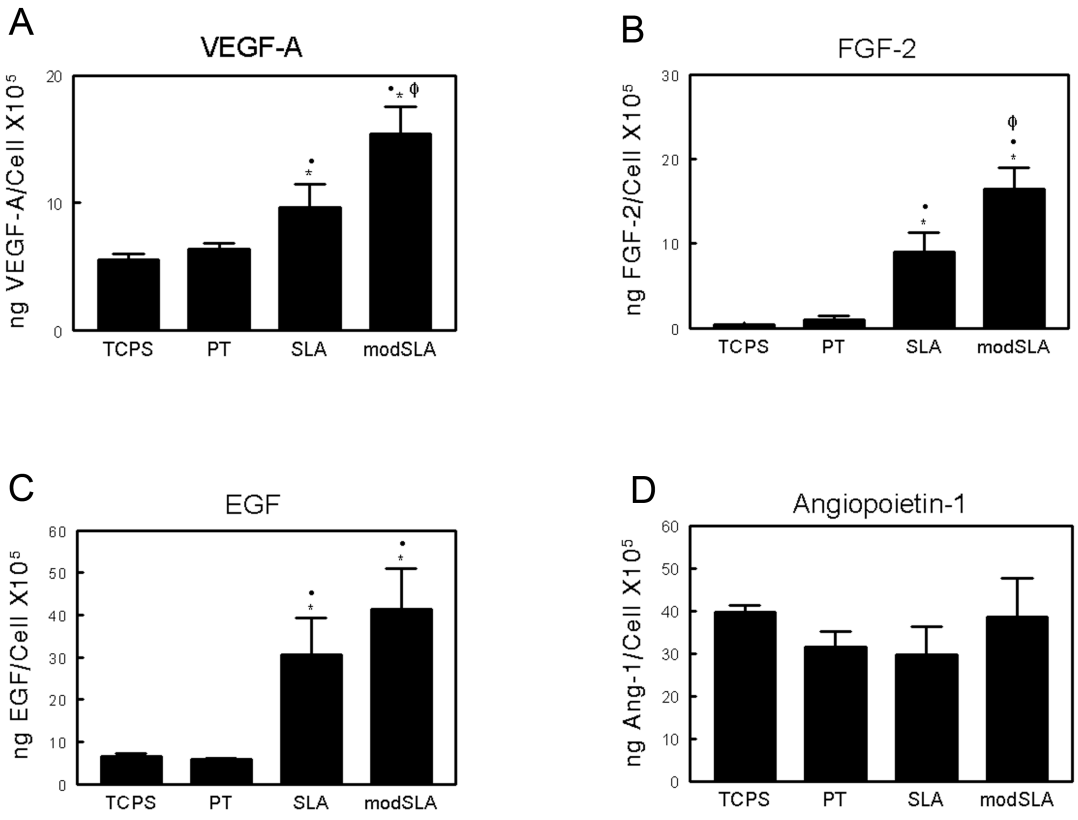

Figure 2-2. Production of angiogenic growth factors by MG63 cells on tissue culture polystyrene and Ti surfaces: (A) VEGF-A, (B) FGF-2, (C) EGF, and (D) Ang-1 levels were determined in the conditioned medium by ELISA. Cells were cultured on control (TCPS), PT, SLA, and modSLA Ti surfaces. Values presented are mean $\pm$ SEM of six independent cultures. The data presented are from one of two separate experiments with comparable results. Data were analyzed using ANOVA and statistical significance between groups was determined using Bonferroni's modification of Student's t-test. *$p < 0.05$, vs. TCPS; ·$p<0.05$, vs. PT; Φ$p<0.05$, vs. SLA.

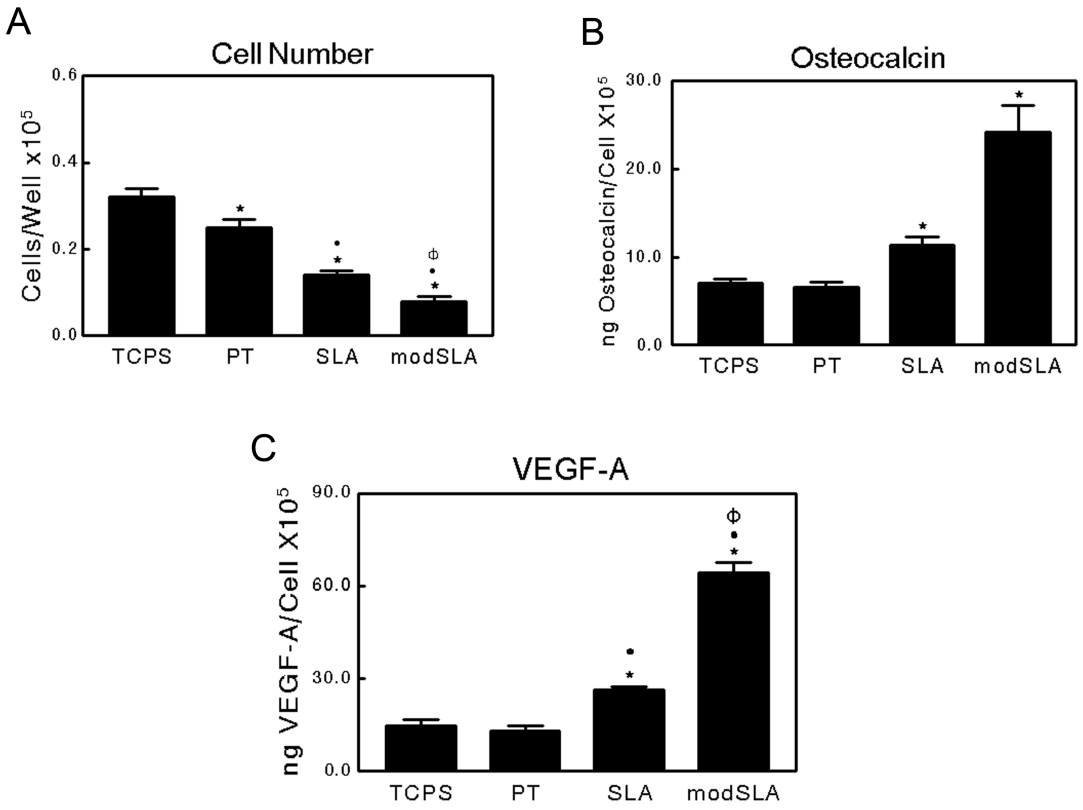

Figure 2-3. Characterization of normal human osteoblasts cultured on TCPS, PT, SLA, and modSLA Ti surfaces: (A) cell number, (B) osteocalcin, and (C) VEGF-A levels in the conditioned medium. Values presented are mean ± SEM of six independent cultures. The data presented are from one of two separate experiments with comparable results. Data were analyzed using ANOVA and statistical significance between groups was determined using Bonferroni's modification of Student's t-test. *$p < 0.05$ vs. TCPS; ·$p<0.05$ vs. PT; Φ$p<0.05$ vs. SLA.

Osteocalcin production by HOB cells on TCPS and PT substrates was comparable, while osteocalcin levels increased approximately 1.6 fold and 3.5 fold on SLA and modSLA surfaces, respectively (Figure 2-3B). Similarly, VEGF-A levels were comparable on TCPS and PT. Secreted VEGF-A levels were doubled on SLA substrates, while cultures on modSLA surfaces showed increased levels over SLA (Figure 2-3C). Levels of FGF-2 and EGF in the conditioned media of cells grown on all substrates were undetectable by ELISA (data not shown).

Treatment of MG63 cells with the vitamin D metabolite 1α,25$(OH)_2$D3 caused a dose dependent increase in both osteocalcin (Figure 2-4A) and VEGF-A (Figure 2-4B) on all surfaces in addition to the increase observed in response to Ti surface microstructure. The effects of surface roughness and 1α,25$(OH)_2D_3$ were synergistic for both osteocalcin and VEGF-A. No effect of 1α,25$(OH)_2D_3$ on FGF-2 and EGF was observed regardless of substrate (data not shown).

2.3.2 Endothelial Cell Differentiation

Conditioned media from MG63 cell cultures affected endothelial tube formation in a Matrigel® tube formation assay in a substrate dependent manner. Conditioned media from all three Ti substrates caused a greater degree of endothelial cell differentiation than conditioned media from cells grown on TCPS based on total endothelial tube length (Figure 2-6A). Moreover, surface energy had a further stimulating effect. Using the number of branch points (the number of points where endothelial networks split into two or more tube like structures) as another marker of endothelial cell differentiation, we found that at 4h of culture, the number of branch points induced by conditioned media from all Ti substrates was significantly higher than those observed in the presence of TCPS media. Media from cultures grown on SLA increased the number of endothelial

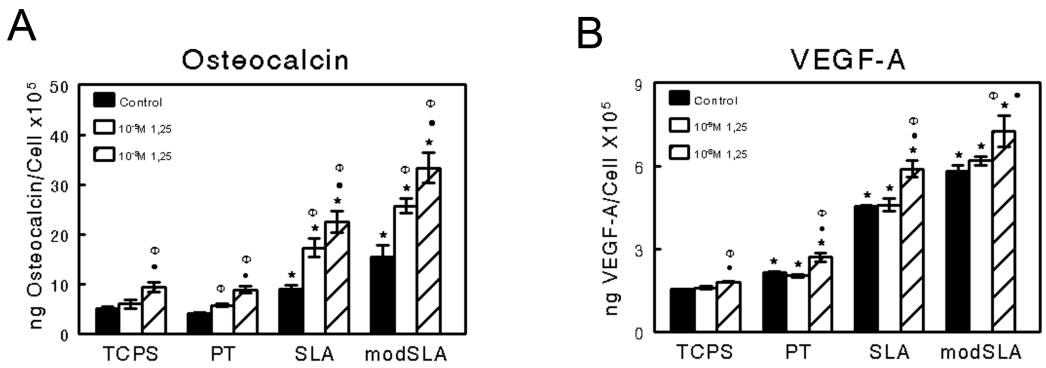

Figure 2-4. Effect of 1α,25 $(OH)_2D_3$ treatment on MG63 cell differentiation. MG63 cells were cultured on TCPS, PT, SLA, and modSLA Ti surfaces. At confluence, cultures were treated with 10^{-9}M or 10^{-8}M 1α,25 $(OH)_2$D3 for 24 hours. (A) Osteocalcin and (B) VEGF-A levels in the conditioned medium were determined. Values are mean $\pm$ SEM of six independent cultures. The data presented are from one of two experiments with comparable results. Data were analyzed using ANOVA and statistical significance between groups was determined using Bonferroni's modification of Student's t-test. *p< 0.05 vs. TCPS; ·p<0.05 vs. PT; Φp<0.05 vs. SLA.

branch points observed versus media from PT substrates (SLA vs. PT), and media from cultures on the high surface energy substrate caused a further increase in endothelial branch points (modSLA vs. SLA).

The increase in endothelial cell differentiation seen at earlier time points in response to conditioned media from cultures grown on SLA and modSLA surfaces was due in part to an increase in the levels of VEGF-A. Addition of a VEGF-A neutralization antibody to conditioned media from these cultures reduced endothelial cell differentiation to levels observed using conditioned media from TCPS cultures in the absence of antibody (Figure 2-6B). Results from the fibrin gel assay further demonstrate that there were increased levels of pro-angiogenic growth factors in the conditioned media of MG63 cell cultures on Ti substrates. Similar to the Matrigel® assay, endothelial cells cultured in media from all three Ti substrates exhibited a greater degree of differentiation as determined by tubular network length after 36h of cultured within a fibrin gel network (Figure 2-5 and Figure 2-6C). There were no significant differences in total tube length between the different Ti substrates however.

2.3.3 *In vivo* results

Bone formation and osseointegration surrounding PT, SLA, and modSLA implants was examined using a femoral intramedullary bone formation model. Implants were designed and manufactured to fit into the medullary canal of C57/Bl6 mice (Figure 2-7A). Implants were successfully inserted into the medullary space without breaking the femur (Figure 2-7B,C). After 35 days (8 week-old mice) or 28 days (9 month-old mice), limbs were harvested and cut for histological analysis of new bone formation as well as neovascularization (Figure 2-8). New bone formation around PT, SLA, and modSLA implants *in vivo* was affected by the age of the animals. For both 8 week and 9 month-old mice, neither surface microstructure nor surface energy had an effect on bone

to implant contact where the implant surface came in direct contact with the femoral cortical bone surface (Table 2-1).

Table 2-1: Cortical Surface Bone to Implant Contact

Surface Type	*8 Week*	*9 Month*
PT	0.88 $\pm$ 0.06	0.89 $\pm$ 0.06
SLA	0.87 $\pm$ 0.05	0.89 $\pm$ 0.07
modSLA	0.92 $\pm$ 0.07	0.93 $\pm$ 0.07

Ti surface microstructure nor surface energy had an effect on the marrow bone to implant contact (BIC) in 8 week old, male, C57/Bl6 mice, which are young, physically mature animals (Figure 2-7A). In 9 month-old C57/Bl6 male mice, which are considered an aged animal model, increased surface microtopography alone had no effect on total BIC within the femoral marrow cavity, however total BIC was significantly increased in response to the surface microtopography and high surface energy seen on modSLA Ti implants compared to smooth PT Ti implants (Figure 2-7A). Additionally, the total number of blood vessels within the marrow space surrounding Ti implants was also increased in the modSLA implant group relative to smooth PT controls (Figure 2-7B).

2.4 Discussion

Angiogenesis is an essential process for the clinically successful integration of orthopaedic and dental implants. Here we demonstrate that the surface properties of biomaterials affect cellular response with regard to the production of pro-angiogenic growth factors and show that these factors stimulate endothelial cell differentiation. These observations suggest that microstructured, high energy surfaces induce angiogenesis during osseointegration.

Our results show that in addition to producing increased levels of VEGF-A on SLA and modSLA [40], MG63 cells also produce increased FGF-2 levels on these

substrates. Part of the increase is due to microstructure and part is due to surface energy. MG63 cells produce elevated levels of EGF as well, but this effect is due primarily to substrate microstructure since no further increase was seen on modSLA. Not all angiogenic factors are regulated in this manner, however, either as a function of surface chemistry or surface microarchitecture. Levels of angiopoeitin-1 were comparable in the conditioned media of all cultures examined.

The human osteoblasts used in the present study exhibited marked increases in VEGF-A when grown on SLA and further increases when grown on modSLA, but unlike the MG63 cells they did not exhibit substrate dependent changes in FGF-2 or EGF. We examined cells from only a single human donor. Numerous studies demonstrate the variability among donors as a function of sex, age, and donor site [41,42]. In addition, it is likely that failure to observe such changes was because these factors were below the limits of detection of the assay kits we used.

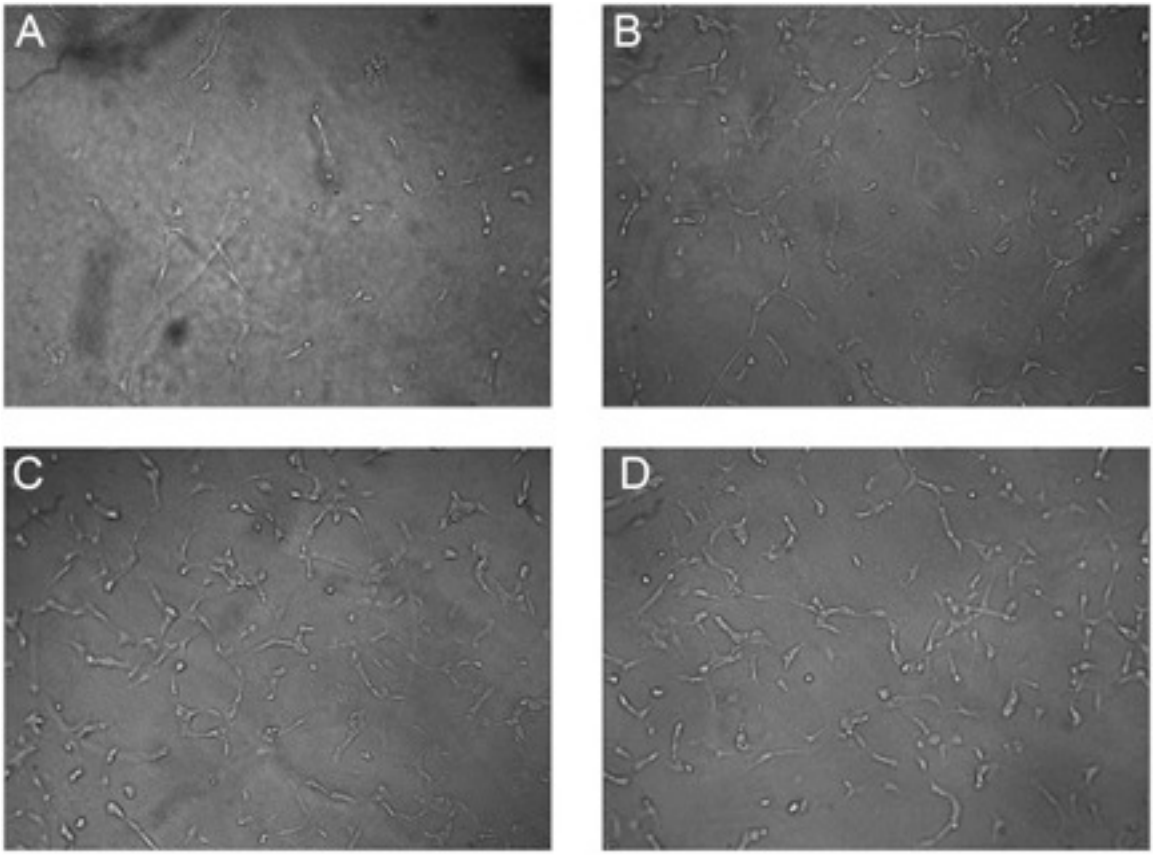

Figure 2-5. Endothelial cell differentiation. Representative images of endothelial cells cultured on a fibrin gel matrix with conditioned media from (A) TCPS, (B) PT, (C) SLA, and (D) modSLA cultures of MG63 cells.

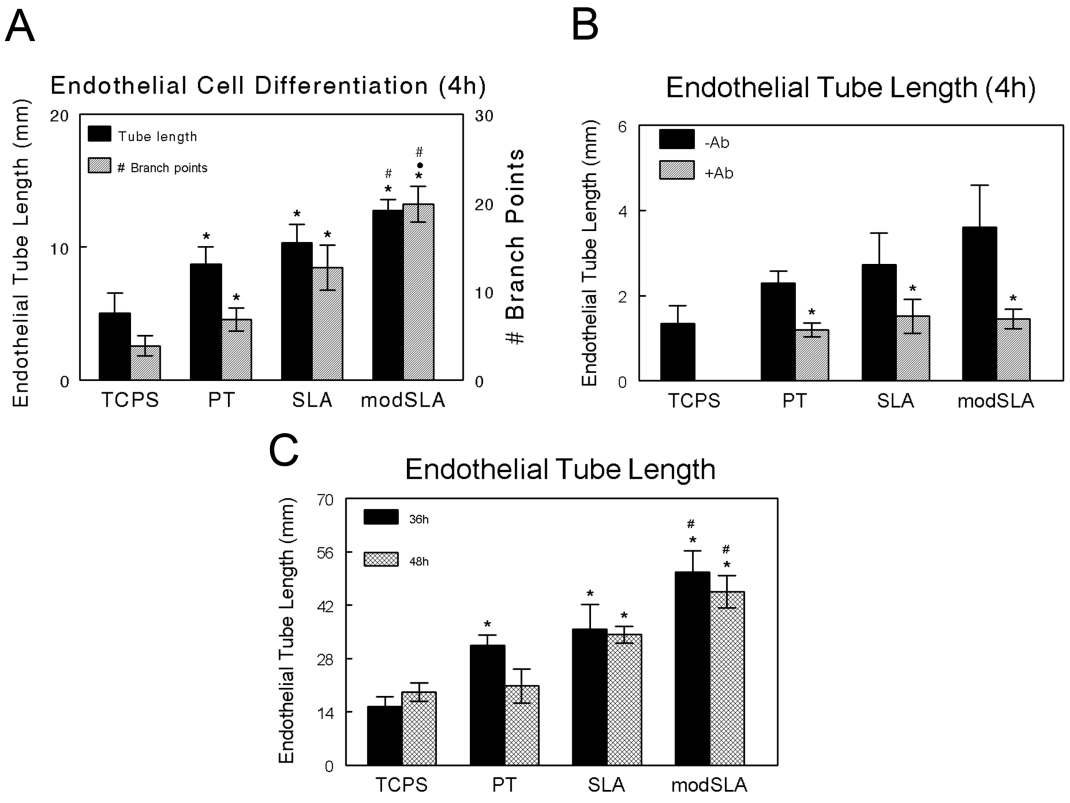

Figure 2-6. Endothelial cell differentiation. Endothelial tube formation was assessed using both a Matrigel® tube formation assay and a fibrin gel assay with conditioned medium from MG63 cells cultured on TCPS, PT, SLA, and modSLA surfaces. (A) Total endothelial tube length and total number of branch points at 4h. *p< 0.05 vs. TCPS; ·p<0.05 vs. PT; #p<0.05 vs. SLA. (B) Addition of VEGF-A neutralization antibody inhibits endothelial cell differentiation in response to MG63 conditioned media. Endothelial tube formation was assessed using conditioned medium from MG63 cells cultured on TCPS, PT, SLA, and modSLA surfaces in the presence of a VEGF-A neutralization antibody. Total endothelial tube length is presented for cultures with and without the addition of neutralization antibody. *p<0.05 vs. no antibody. (C)Fibrin gel assay total endothelial tube length at 24 and 36 hours. *p< 0.05 vs. TCPS; #p<0.05 vs. PT.

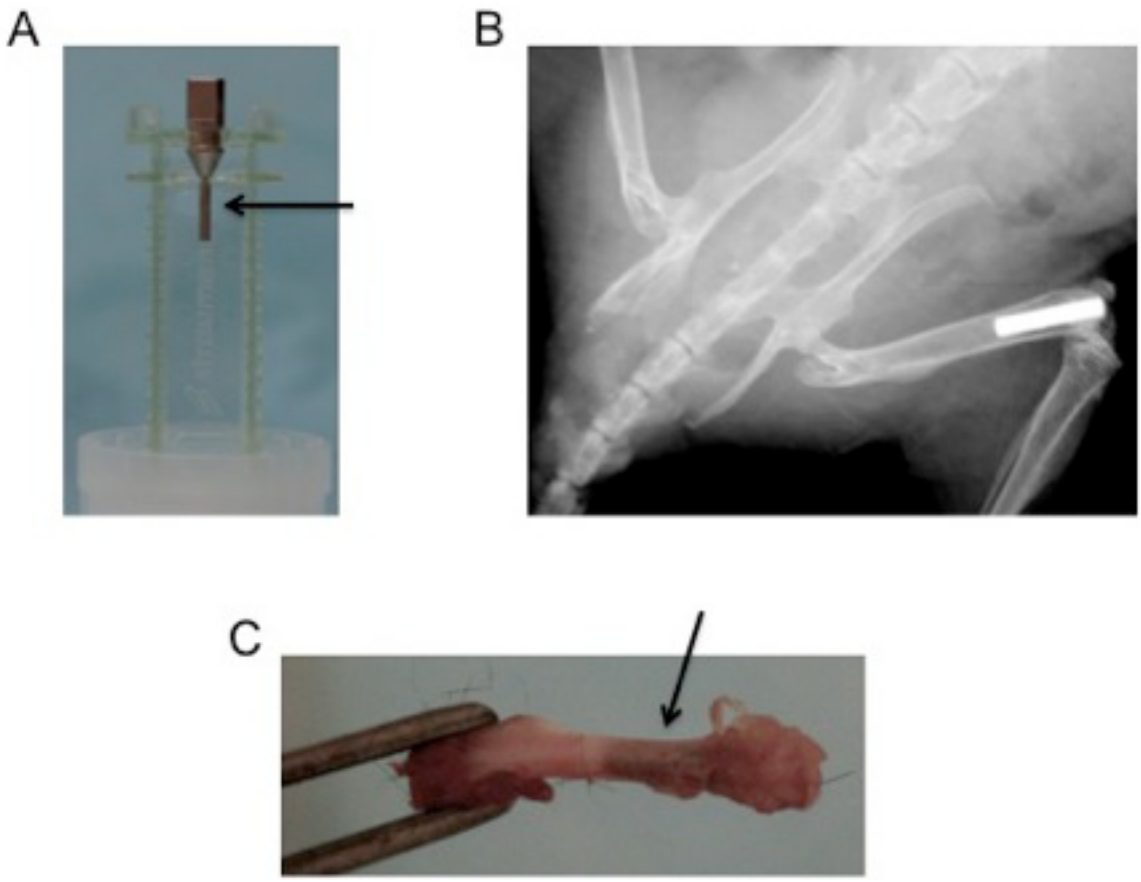

Figure 2-7. Representative images demonstrating feasibility of the mouse femoral intramedullary bone formation model. (A) Image showing the implant (arrow) and handling device for an SLA implant. (B) X-ray image showing an implant that has been inserted into the femoral medullary space without breaking of the bone. (C) Gross morphology of a mouse femur with an implant (arrow).

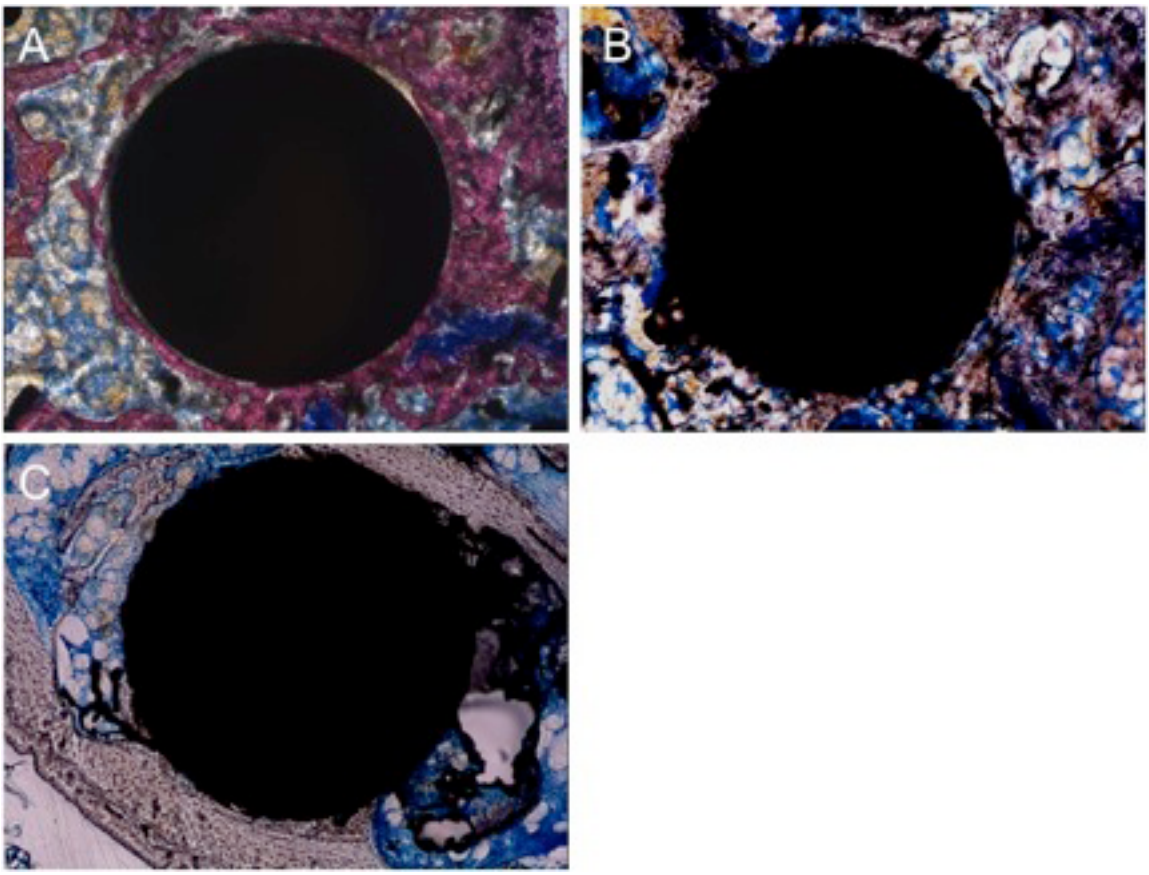

Figure 2-8. Representative histology sections for (A) PT, (B) SLA, and (C) modSLA titanium implants. Marrow and cortical bone to implant contact (BIC) as well as the number of blood vessels in the marrow were determined for all the implant types.

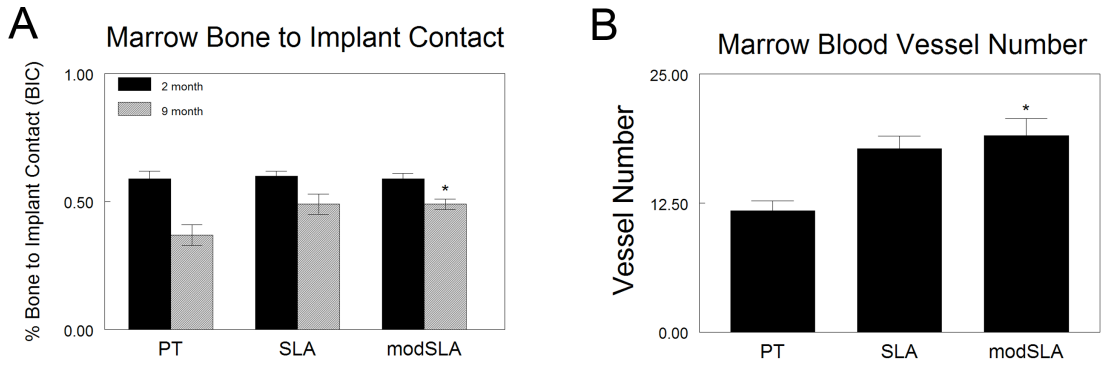

Figure 2-9. *In vivo* bone formation. Bone formation and neovascularization surrounding PT, SLA, and modSLA Ti implants was examined using a novel murine intramedullary bone formation model. (A) The percent bone to implant contact (% BIC) was measured for both 2 month old and 9 month old animals. *$p<0.05$ vs. PT. (B) The total number of blood vessels within the marrow space of 9 month old animals. $P<0.05$ vs. PT. Values presented are the mean $\pm$ SEM of six implants per group. Data were analyzed using ANOVA and statistical significance between groups was determined using Bonferroni's modification of Student's t-test.

Our results support the hypothesis that production of angiogenic factors is related to the state of osteogenic maturation of the osteoblasts. MG63 cells and normal human osteoblasts exhibited a more differentiated phenotype on SLA and modSLA than on TCPS and PT, with reduced alkaline phosphatase and increased osteocalcin typical of secretory cells. These cells also exhibited increased production of angiogenic factors, suggesting that this is linked to the acquisition of a more differentiated phenotype.

The systemic osteotropic hormone $1\alpha,25(OH)_2D_3$ is a key regulator of bone metabolism [33]. Treatment of late-stage osteoblast cultures with $1\alpha,25(OH)_2D_3$ upregulates expression of both alkaline phosphatase and type I collagen, markers of osteoblast differentiation [43]. Previous results from our laboratory have shown that treatment of MG63 cells cultures with $1\alpha,25(OH)_2D_3$ enhances cell response to Ti surface microstructure [44]. Our results here support this data and further show that production of VEGF-A is regulated in the same manner.

Substrates that presented a microrough surface topography and high surface energy enhanced the synthesis of several pro-angiogenic growth factors, which subsequently resulted in an enhancement of the differentiation of human aortic endothelial cells *in vitro*. This supports the hypothesis that more mature osteoblasts produce the angiogenic factors needed to recruit a vascular supply. The addition of a VEGF-A neutralization antibody to endothelial cell cultures inhibited this increase in endothelial cell differentiation, indicating that the increased levels of VEGF-A produced by MG63 cells on SLA and modSLA substrates contributes to endothelial cell differentiation.

Using the murine intramedullary bone formation model, a novel, *in vivo* bone formation model, we observed that both age as well as biomaterial surface features affect osseointegration and neovascularization. In young, skeletally mature C57/Bl6

mice, neither Ti surface roughness nor wettability had a significant effect on osseointegration, as determined by histological examination of total bone to implant contact at 35 days post-implantation. However, in 9-month old C57/Bl6 mice, which are an aged model representing compromised bone, the combination of a rough surface microtopography and high surface energy on modSLA substrates resulted in a significant increase in total bone to implant contact surrounding these implants. In addition, when the vasculature of these animals was perfused and the total number of blood vessels surrounding the implants within the marrow space were determined, it was found that modSLA implants significantly increased the total vessel number. These results are consistent with results found previously demonstrating that healing abilities are diminished with age [47].

In a clinical setting, establishment of a vasculature preceding or concomitant with bone formation allows for not only the delivery of oxygen, systemic hormones, and nutrients to the injury site but also the migration of mesenchymal stem cells. In the absence of neovascularization, the implant may be surrounded by a fibrous capsule, resulting in implant loosening and ultimately failure, demonstrating the importance of the initial reaction of the first cells to come in contact with an implanted material.

We show here that substrate microstructure and surface energy regulate the production of angiogenic growth factors by osteoblasts. The increase in endothelial cell differentiation observed in response to conditioned media from SLA and modSLA cultures further demonstrate that Ti substrate features control osseointegration by enhancing angiogenesis at the material/tissue interface.

2.5 References

1. Hench LL, Polak JM. Third-generation biomedical materials. Science 2002;295:1014-7.

2. Jell G, Stevens MM. Gene activation by bioactive glasses. J Mater Sci Mater Med 2006;17:997-1002.

3. Kriparamanan R, Aswath P, Zhou A, Tang L, Nguyen KT. Nanotopography: cellular responses to nanostructured materials. J Nanosci Nanotechnol 2006;6:1905-19.

4. Goto T, Yoshinari M, Kobayashi S, Tanaka T. The initial attachment and subsequent behavior of osteoblastic cells and oral epithelial cells on titanium. Biomed Mater Eng 2004;14:537-44.

5. Boyan BD, Schwartz Z, Lohmann CH, Sylvia VL, Cochran DL, Dean DD, Puzas JE. Pretreatment of bone with osteoclasts affects phenotypic expression of osteoblast-like cells. J Orthop Res 2003;21:638-47.

6. Zhao G, Schwartz Z, Wieland M, Rupp F, Geis-Gerstorfer J, Cochran DL, Boyan BD. High surface energy enhances cell response to titanium substrate microstructure. J Biomed Mater Res A 2005;74:49-58.

7. Buser D, Schenk RK, Steinemann S, Fiorellini JP, Fox CH, Stich H. Influence of surface characteristics on bone integration of titanium implants. A histomorphometric study in miniature pigs. J Biomed Mater Res 1991;25:889-902.

8. Gotfredsen K, Wennerberg A, Johansson C, Skovgaard LT, Hjorting-Hansen E. Anchorage of TiO2-blasted, HA-coated, and machined implants: an experimental study with rabbits. J Biomed Mater Res 1995;29:1223-31.

9. Cochran DL, Schenk RK, Lussi A, Higginbottom FL, Buser D. Bone response to unloaded and loaded titanium implants with a sandblasted and acid-etched surface: a histometric study in the canine mandible. J Biomed Mater Res 1998;40:1-11.

10. Hynes RO. Integrins: bidirectional, allosteric signaling machines. Cell 2002;110:673-87.

11. Gronowicz G, McCarthy MB. Response of human osteoblasts to implant materials: integrin-mediated adhesion. J Orthop Res 1996;14:878-87.

12. Raz P, Lohmann CH, Turner J, Wang L, Poythress N, Blanchard C, Boyan BD, Schwartz Z. 1alpha,25(OH)2D3 regulation of integrin expression is substrate dependent. J Biomed Mater Res A 2004;71:217-25.

13. Olivares-Navarrete R, Raz P, Zhao G, Chen J, Wieland M, Cochran DL, Chaudhri RA, Ornoy A, Boyan BD, Schwartz Z. Integrin alpha2beta1 plays a critical role in osteoblast response to micron-scale surface structure and surface energy of titanium substrates. Proc Natl Acad Sci U S A 2008;105:15767-72.

14. Wang L, Zhao G, Olivares-Navarrete R, Bell BF, Wieland M, Cochran DL, Schwartz Z, Boyan BD. Integrin beta1 silencing in osteoblasts alters substrate-dependent responses to 1,25-dihydroxy vitamin D3. Biomaterials 2006;27:3716-25.

15. Duvall CL, Taylor WR, Weiss D, Wojtowicz AM, Guldberg RE. Impaired angiogenesis, early callus formation, and late stage remodeling in fracture healing of osteopontin-deficient mice. J Bone Miner Res 2007;22:286-97.

16. Geris L, Gerisch A, Sloten JV, Weiner R, Oosterwyck HV. Angiogenesis in bone fracture healing: a bioregulatory model. J Theor Biol 2008;251:137-58.

17. Abshagen K, Schrodi I, Gerber T, Vollmar B. In vivo analysis of biocompatibility and vascularization of the synthetic bone grafting substitute NanoBone(R). J Biomed Mater Res A 2008.

18. Connolly DT, Heuvelman DM, Nelson R, Olander JV, Eppley BL, Delfino JJ, Siegel NR, Leimgruber RM, Feder J. Tumor vascular permeability factor stimulates endothelial cell growth and angiogenesis. J Clin Invest 1989;84:1470-8.

19. Schweigerer L, Neufeld G, Friedman J, Abraham JA, Fiddes JC, Gospodarowicz D. Capillary endothelial cells express basic fibroblast growth factor, a mitogen that promotes their own growth. Nature 1987;325:257-9.

20. Mehta VB, Besner GE. HB-EGF promotes angiogenesis in endothelial cells via PI3-kinase and MAPK signaling pathways. Growth Factors 2007;25:253-63.

21. Koblizek TI, Weiss C, Yancopoulos GD, Deutsch U, Risau W. Angiopoietin-1 induces sprouting angiogenesis in vitro. Curr Biol 1998;8:529-32.

22. Deckers MM, Karperien M, van der Bent C, Yamashita T, Papapoulos SE, Lowik CW. Expression of vascular endothelial growth factors and their receptors during osteoblast differentiation. Endocrinology 2000;141:1667-74.

23. Clarkin CE, Emery RJ, Pitsillides AA, Wheeler-Jones CP. Evaluation of VEGF-mediated signaling in primary human cells reveals a paracrine action for VEGF in osteoblast-mediated crosstalk to endothelial cells. J Cell Physiol 2008;214:537-44.

24. Carlevaro MF, Cermelli S, Cancedda R, Descalzi Cancedda F. Vascular endothelial growth factor (VEGF) in cartilage neovascularization and chondrocyte differentiation: auto-paracrine role during endochondral bone formation. J Cell Sci 2000;113:59-69.

25. Collins PD, Connolly DT, Williams TJ. Characterization of the increase in vascular permeability induced by vascular permeability factor in vivo. Br J Pharmacol 1993;109:195-9.

26. Stoelcker B, Echtenacher B, Weich HA, Sztajer H, Hicklin DJ, Mannel DN. VEGF/Flk-1 interaction, a requirement for malignant ascites recurrence. J Interferon Cytokine Res 2000;20:511-7.

27. Baffour R, Berman J, Garb JL, Rhee SW, Kaufman J, Friedmann P. Enhanced angiogenesis and growth of collaterals by in vivo administration of recombinant basic fibroblast growth factor in a rabbit model of acute lower limb ischemia: dose-response effect of basic fibroblast growth factor. J Vasc Surg 1992;16:181-91.

28. Wakui S. Epidermal growth factor receptor at endothelial cell and pericyte interdigitation in human granulation tissue. Microvasc Res 1992;44:255-62.

29. Ravindranath N, Wion D, Brachet P, Djakiew D. Epidermal growth factor modulates the expression of vascular endothelial growth factor in the human prostate. J Androl 2001;22:432-43.

30. Cai J, Kehoe O, Smith GM, Hykin P, Boulton ME. The angiopoietin/Tie-2 system regulates pericyte survival and recruitment in diabetic retinopathy. Invest Ophthalmol Vis Sci 2008;49:2163-71.

31. Wang DS, Miura M, Demura H, Sato K. Anabolic effects of 1,25-dihydroxyvitamin D3 on osteoblasts are enhanced by vascular endothelial growth factor produced by osteoblasts and by growth factors produced by endothelial cells. Endocrinology 1997;138:2953-62.

32. Hurley MM, Abreu C, Gronowicz G, Kawaguchi H, Lorenzo J. Expression and regulation of basic fibroblast growth factor mRNA levels in mouse osteoblastic MC3T3-E1 cells. J Biol Chem 1994;269:9392-6.

33. St-Arnaud R. The direct role of vitamin D on bone homeostasis. Arch Biochem Biophys 2008;473:225-30.

34. McMillan J, Kinney RC, Ranly DM, Fatehi-Sedeh S, Schwartz Z, Boyan BD. Osteoinductivity of demineralized bone matrix in immunocompromised mice and rats is decreased by ovariectomy and restored by estrogen replacement. Bone 2007;40:111-21.

35. Cole BJ, Bostrom MP, Pritchard TL, Sumner DR, Tomin E, Lane JM, Weiland AJ. Use of bone morphogenetic protein 2 on ectopic porous coated implants in the rat. Clin Orthop Relat Res 1997:219-28.

36. Schwartz Z, Raz P, Zhao G, Barak Y, Tauber M, Yao H, Boyan BD. Effect of micrometer-scale roughness of the surface of Ti6Al4V pedicle screws in vitro and in vivo. J Bone Joint Surg Am 2008;90:2485-98.

37. Mayer H, Bertram H, Lindenmaier W, Korff T, Weber H, Weich H. Vascular endothelial growth factor (VEGF-A) expression in human mesenchymal stem cells: autocrine and paracrine role on osteoblastic and endothelial differentiation. J Cell Biochem 2005;95:827-39.

38. Rupp F, Scheideler L, Olshanska N, de Wild M, Wieland M, Geis-Gerstorfer J. Enhancing surface free energy and hydrophilicity through chemical modification of microstructured titanium implant surfaces. J Biomed Mater Res A 2006;76:323-34.

39. Martin JY, Schwartz Z, Hummert TW, Schraub DM, Simpson J, Lankford J, Jr., Dean DD, Cochran DL, Boyan BD. Effect of titanium surface roughness on proliferation, differentiation, and protein synthesis of human osteoblast-like cells (MG63). J Biomed Mater Res 1995;29:389-401.

40. Rausch-fan X, Qu Z, Wieland M, Matejka M, Schedle A. Differentiation and cytokine synthesis of human alveolar osteoblasts compared to osteoblast-like cells (MG63) in response to titanium surfaces. Dent Mater 2008;24:102-10.

41. Siddappa R, Licht R, van Blitterswijk C, de Boer J. Donor variation and loss of multipotency during in vitro expansion of human mesenchymal stem cells for bone tissue engineering. J Orthop Res 2007;25:1029-41.

42. Katopodi T, Tew SR, Clegg PD, Hardingham TE. The influence of donor and hypoxic conditions on the assembly of cartilage matrix by osteoarthritic human articular chondrocytes on Hyalograft matrices. Biomaterials 2009;30:535-40.

43. Owen TA, Aronow MS, Barone LM, Bettencourt B, Stein GS, Lian JB. Pleiotropic effects of vitamin D on osteoblast gene expression are related to the proliferative and differentiated state of the bone cell phenotype: dependency upon basal levels of gene expression, duration of exposure, and bone matrix competency in normal rat osteoblast cultures. Endocrinology 1991;128:1496-504.

44. Boyan BD, Lossdorfer S, Wang L, Zhao G, Lohmann CH, Cochran DL, Schwartz Z. Osteoblasts generate an osteogenic microenvironment when grown on surfaces with rough microtopographies. Eur Cell Mater 2003;6:22-7.

45. Siebers MC, ter Brugge PJ, Walboomers XF, Jansen JA. Integrins as linker proteins between osteoblasts and bone replacing materials. A critical review. Biomaterials 2005;26:137-46.

46. Zhao G. Interaction of surface energy and microarchitecture in determining cell and tisse response to biomaterials. Ph.D. Thesis. Georgia Institute of Technology 2007.

47. Fisher M, Hyzy S, Guldberg RE, Schwartz Z, Boyan BD. Regeneration of bone marrow after tibial ablation in immunocompromised rats is age dependent. Bone 2009;46:396-401.

CHAPTER 3: Integrin Mediated Signaling Regulates the Angiogenic Response of Osteoblasts to Titanium Substrate Features

3.1 Introduction

The initial interaction of cells with a biomaterial surface plays a significant role in determining host tissue response to an implanted material. Upon implantation into the body, the surface of a biomaterial is conditioned with an adsorbed layer of proteins, ions, sugars and lipids present in the surrounding blood and tissue fluid [1, 2]. The surface properties of the implanted material help to determine which biological molecules adsorb. The orientation of the adsorbed biological molecules directly influences the attachment, proliferation, and differentiation of surrounding cells [3]. The adhesion of cells with a biomaterial surface involves several classes of proteins including extracellular matrix proteins, cytoskeletal proteins, cadherins, and integrins [4].

Osteoblasts interact with their substrate primarily via integrin binding to extracellular matrix (ECM) proteins [5]. Integrins are heterodimeric transmembrane glycoprotein receptor complexes consisting of non-covalently associated α and β subunits. Integrin receptors bind ECM proteins on the outside of the cell and associate with the cytoskeleton and signaling complexes inside the cell to transduce signals. Osteoblasts express several integrin α and β subunits including α_1, α_2, α_3, α_4, α_5, α_6, α_v, β_1, and β_3 [6-8]. The expression of integrin subunits by osteoblast-like cells is regulated by surface chemical composition and topography [9, 10]

Upon binding, integrin molecules cluster into focal adhesions, where they initiate intracellular signaling cascades to control proliferation and differentiation. Focal

adhesion complexes are comprised of structural proteins such as vinculin and talin, and signaling molecules including focal adhesion kinase (FAK) and Src [11]. Bound integrins, along with growth factors can also activate the MAPK signal transduction pathway [12-14].

Titanium (Ti) is a commonly used material in the orthopaedic and dental fields and Ti surface microtopography and chemical composition affect osteoblast differentiation *in vitro* and bone formation *in vivo*. Ti substrates that present a microrough surface topography combined with a high surface free energy increase production of osteocalcin, a late marker of osteoblast differentiation *in vivo* and enhance bone-to-implant contact and removal torque strength *in vivo* [15-17].

On tissue culture polystyrene surfaces, osteoblasts primarily express the $\alpha_5\beta_1$ integrin [9]. However, when grown on Ti substrates, expression of α_2 and β_1 integrin subunits is increased [10], suggesting that the surface roughness dependent differentiation of osteoblasts may be mediated specifically through $\alpha_2\beta_1$ signaling. Knockdown of either the α_2 or β_1 integrin subunits in MG63 cells blocks surface roughness dependent differentiation of those cells [18, 19], and has an effect on the production of pro-angiogenic growth factors [20].

Integrins also play an important role in neovascularization. Vascular endothelial cells, similar to osteoblasts, express several integrin α and β subunits in a differential manner [21]. In quiescent vessels, many integrins are either not expressed or are in an inactive state. During neovascularization, endothelial cells upregulate expression of integrin pairs that are also expressed during osteoblastic differentiation, including $\alpha_1\beta_1$, $\alpha_2\beta_1$, and $\alpha_5\beta_1$ [22].

Angiogenic growth factor receptors, including the VEGF receptor Flk-1 and the PDGFβ receptor have been found to interact with integrins on the surface of endothelial

cells during neovascularization [23]. Endothelial cell integrin pairs have also been found to interact directly with angiogenic growth factors including VEGF-A and FGF-2 [24, 25].

While it is known that signaling through integrin receptors in osteoblasts has an effect on the differentiation and expression of osteogenic markers in response to Ti surface roughness and energy, whether or not integrin signaling in osteoblasts affects the production of angiogenic growth factors in these cells is not known. In this study, we investigated the role that signaling through specific integrin receptors has on the production of pro-angiogenic growth factors in osteoblast-like cells in response to substrate microtopography and surface free energy. In order to elucidate the effect of different integrin α and β subunits, we transduced shRNA specific for integrin subunits α_1, α_2, α_5, and β_1 into an MG63 osteoblast like cell line to knockdown expression of these integrins. We cultured wild-type MG63 cells and specific integrin silenced MG63 cells on Ti surfaces presenting varying topographies and surface free energies and examined the production of both osteogenic and angiogenic growth factors.

3.2 Materials and Methods

3.2.1 Titanium substrate preparation

Ti disks were prepared from 1 mm thick sheets of grade 2 unalloyed commercially pure Ti punched into 15mm diameter disks and supplied by Institut Straumann AG (Basel, Switzerland). The production and characterization of smooth pretreatment (PT), sand blasted and acid etched (SLA), and modified SLA (modSLA) surfaces have been described previously [[26]]. PT surfaces were degreased by washing Ti disks in acetone and processed in a 2% ammonium fluoride/2% hydrofluoric acid/10% nitric acid solution. SLA surfaces were made by coarse grit-blasting of the PT surfaces with 0.25-0.50 mm corundum grit followed by a dual acid etching procedure with hydrochloric acid and hydrofluoric acid. modSLA surfaces were made using the

same procedure as SLA surfaces under nitrogen rinsing to prevent exposure to air and were then stored under aqueous conditions under nitrogen to retain high surface free energy. The PT surface has an overall average roughness (Ra) of less than 0.7 μm. SLA and modSLA surfaces have a complex microtopography with craters varying from 30 to 100 μm in diameter overlaid with pits from 1 to 3 μm in diameter. The acid etch creates sharp edges approximately 700 nm in height, resulting in an overall Ra of approximately 4 μm. PT, SLA and modSLA Ti disks all have a TiO_2 surface layer, with the PT and SLA surfaces being hydrophobic due to the adsorption of atmospheric hydrocarbons while the modSLA surface is hydrophilic. Advancing contact angles were used to calculate the hydrophilicity of the surfaces as PT (95.8°), SLA (139.80°), and modSLA (~0°). Surface free energy for PT, SLA, and modSLA surfaces was calculated according to Zisman (critical surface tension), Equation of State (EOS), and Geometric Mean approaches and is described in detail elsewhere[27].

3.2.2 Generation of integrin silenced cell lines

Integrin α_2: Stably silenced MG63 osteoblast-like cells for integrin α_2 were generated by transfection with α_2 integrin shRNA using a P-suppressor-neo vector system and shown to have a 70% reduction in α_2 protein as described in detail previously[[18]]. Integrin α_2-silenced MG63 cells were maintained in media containing geneticin (G418; Invitrogen, Carlsbad, CA) at a concentration of 600 μg/mL for the duration of cell culture.

Integrins α_1, α_5, and β_1: MG63 osteoblast-like cells were transduced using Mission® lentiviral transduction particles (Sigma-Aldrih, St. Louis, MO) with shRNA specific for each target gene of interest following the manufacturer's recommended

protocol. Verification of silencing for each integrin subunit was done using western blot analysis and real-time qPCR.

3.2.3 Cell Culture

Non-transduced MG63 cells and MG63 cells silenced for integrins α_1, α_2, α_5, and β_1 were plated in 24-well tissue culture plates on tissue culture treated polystyrene (TCPS, used as a control for all studies), PT, SLA, and modSLA surfaces using Dulbecco's modified Eagle's medium (DMEM) supplemented with 10% fetal bovine serum and 1% penicillin/streptomycin. Cells were seeded at an initial density of 10,000 cells/cm^2 and media were exchanged 24 hours after seeding and every 48 hours thereafter. When the cells were confluent on TCPS, media from all cultures were collected and examined for VEGF-A, FGF-2, Ang-1 and osteocalcin levels.

3.2.4 Cell Number

Cell number was determined for all cell types at time of harvest. At confluence, cells were released from TCPS and Ti surfaces using two sequential incubations with 0.25% trypsin for 10 minutes at 37^{o}C to ensure that no cells remained on the rough Ti surfaces and counted using an automated cell counter (Z1 Particle counter, Beckman Coulter, Fullerton, CA).

3.2.5 Alkaline Phosphatase Specific Activity

Alkaline phosphatase specific activity (orthophosphoric monoester phosphohydrolase, alkaline; E.C. 3.1.3.1) was measured in the cell lysates as a marker of osteoblastic differentiation. Enzyme activity was determined using a colorimetric assay measuring the release of *p*-nitrophenol from *p*-nitrophenylphosphate at 37^{o}C. Samples were read on a plate reader at 415nm.

3.2.6 Osteocalcin

Osteocalcin levels in the conditioned medium of MG63 cells and human osteoblasts grown on Ti surfaces were determined as a marker of osteoblast maturation using a commercially available radioimmunoassay (Biomedical Technologies, Inc., Stoughton, MA) following the manufacturer's protocol.

3.2.7 VEGF-A, FGF-2, Ang-1

The levels of the angiogenic growth factors VEGF-A, FGF-2, and Ang-1 were determined in the conditioned medium using commercially available sandwich ELISA assays (Duoset ELISA Development Systems, R&D Systems, Minneapolis, MN) following the manufacturer's protocols.

3.2.8 Statistical Analysis

The data presented here are from one of at least two separate sets of experiments. Both sets of experiments yielded comparable observations. For any given experiment, each data point represents the mean $\pm$ standard error of six individual cultures. Data were analyzed by ANOVA and when statistical differences were detected, Student's *t*-test for multiple comparisons using Bonferroni's modification was used. p-values < 0.05 were considered significant.

3.3 Results

3.3.1 MG63 cell response

Consistent with previously published results, for all experiments, MG63 cells exhibited a decrease in total cell number and an increase in secreted levels of osteocalcin, VEGF-A, and FGF-2 with increasing surface roughness and hydrophilicity, while secreted levels of Angiopoietin-1 were unaffected by either surface roughness or energy[20] (Figures 1-4).

3.3.2 Integrin α_1 silencing

Silencing of the α_1 integrin subunit resulted in no significant differences in measured cell number on any of the substrates examined (Figure 3-1A). Osteocalcin production increased in response to surface roughness and energy in both wild-type MG63 cells and integrin α_1 silenced cells, however this increase was significantly attenuated in integrin α_1 silenced cells (Figure 3-1B) The secreted levels of angiogenic growth factors were affected in response to specific integrin silencing. Secreted levels of VEGF-A by integrin α_1 cell cultures increased in response to the surface microroughness and hydrophilicity observed on modSLA substrates compared to TCPS control cultures, however, secreted levels of VEGF-A in integrin α_1 silenced cell cultures were significantly reduced on all substrates relative to MG63 cell cultures (Figure 3-1C). Integrin α_1 silencing had no effect on the secreted levels of FGF-2 or Ang-1 compared to MG63 cell cultures on TCPS, PT, or SLA substrates (Figure 3-1D,E). On modSLA substrates, FGF-2 production was significantly reduced compared to MG63 cultures (Figure 3-1D). In contrast, secreted levels of Ang-1 were significantly increased in integrin α_1 cell cultures compared to both MG63 cell cultures on modSLA and α_1 silenced cells on TCPS (Figure 3-1E).

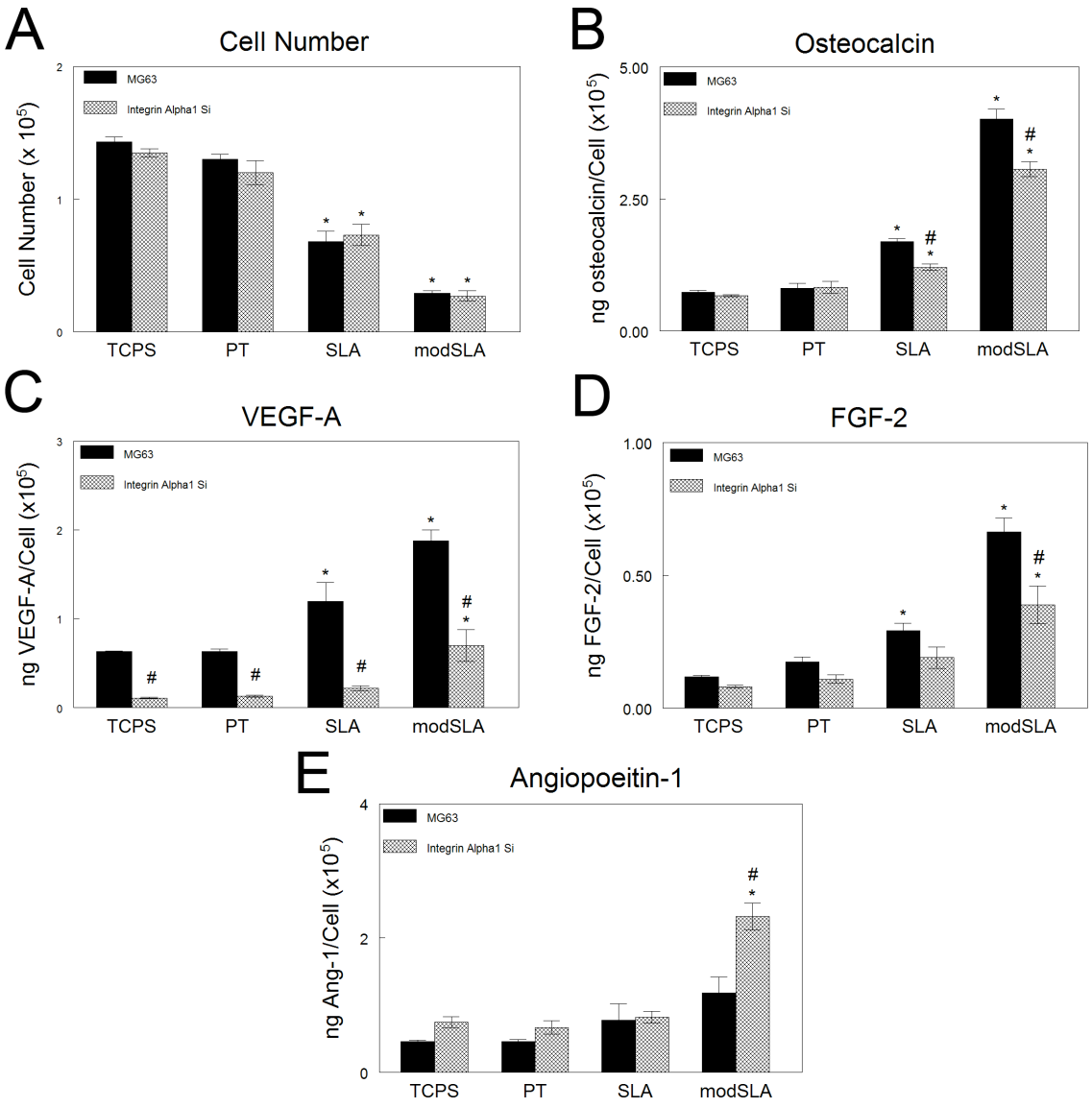

Figure 3-1. Integrin α_1 silenced cell response to Ti substrate features. (A) Total cell number of integrin α_1 silenced cells and MG63 wild-type cells were determined. (B) Osteocalcin, (C) VEGF-A, (D) FGF-2, and (E) Ang-1 levels in the conditioned media of both MG63 cells and integrin α_1 silenced MG63 cells were determined. Values presented are mean $\pm$ SEM of six independent cultures. Data were analyzed using ANOVA and statistical significance between groups was determined using Bonferroni's modification of Student's t-test. *p<0.05 vs. TCPS; #p<0.05 vs. MG63 cultures.

3.3.3 Integrin α_2 silencing

Total cell number for integrin α_2 silenced cells were comparable to MG63 cell numbers on TCPS, PT, and SLA substrates. On microrough, hydrophilic modSLA substrates, α_2 silenced cell numbers were higher than those observed for MG63 cell cultures (Figure 3-2A). Integrin α_2 silencing attenuated the surface roughness and energy dependent increases in osteocalcin production observed in MG63 cells but had no effect on secreted levels of osteocalcin on smooth TCPS or PT substrates or (Figure 3-2B). Unlike integrin α_1 silenced cells, production of VEGF-A by integrin α_2 silenced cells was increased nearly 2 fold on all substrates examined (Figure 3-2C). Integrin α_2 silencing had no effect on FGF-2 production in response to increasing surface microstructure but it reduced FGF-2 levels significantly compared to MG63 cells on modSLA substrates (Figure 3-2D). Similar to α_1 silenced cells, secreted levels of Ang-1 were significantly increased by α_2 silenced cells on modSLA substrates compared to levels observed on TCPS and MG63 cells on modSLA, but α_1 silencing had no effect on Ang-1 levels on any other substrates examined (Figure 3-2E).

3.3.4 Integrin α_5 silencing

Similar to the results for α_2 silenced cells, integrin α_5 silenced cells had comparable cell number to MG63 cells on TCPS, PT, and SLA substrates while cell number was increased on modSLA surfaces in α_5 silenced cells compared to MG63 cell cultures (Figure 3-3A). Secreted levels of osteocalcin, a late marker of osteoblast maturation, in α_5 silenced cells was similar to secreted levels by MG63 cell cultures on all substrates (Figure 3-3B). Silencing of the integrin α_5 subunit significantly increased secretion of VEGF-A by cells compared to MG63 cell cultures on TCPS, PT, and modSLA substrates, but no differences in secreted levels by α_5 silenced cells were

observed on SLA substrates compared to MG63 cells (Figure 3-3C). No differences in FGF-2 and Ang-1 production by integrin α_5 silenced cell cultures were observed compared to MG63 cell cultures on any substrates examined (Figure 3-3D,E). However, Ang-1 production by α_5 silenced cells was significantly higher on microrough, hydrophilic modSLA substrates compared to smooth TCPS substrates (Figure 3-3E).

3.3.5 Integrin β_1 silencing

Total cell number in integrin β_1 silenced cells was less than that observed in MG63 cell cultures on smooth TCPS and PT substrates but cell number was not affected in response to surface roughness and hydrophilicity on SLA and modSLA substrates (Figure 3-4A). Similar to α_2 silencing, the surface roughness and hydrophilicity dependent increase in osteocalcin production seen in MG63 cells was blocked by silencing of the β_1 integrin (Figure 3-4B). VEGF-A production was significantly increased in integrin β_1 silenced cells on all substrates (Figure 3-4C). FGF-2 and Ang-1 production in β_1 cells was not changed on smooth TCPS, PT or SLA substrates but was significantly increased on microrough, hydrophilic modSLA substrates (Figure 3-4D,E). Secreted levels of FGF-2 by β_1 silenced cells were similar to levels in MG63 cells on all substrates (Figure 3-4D). Ang-1 production on modSLA substrates was significantly higher in β_1 silenced cell cultures compared to MG63 cells (Figure 3-4E).

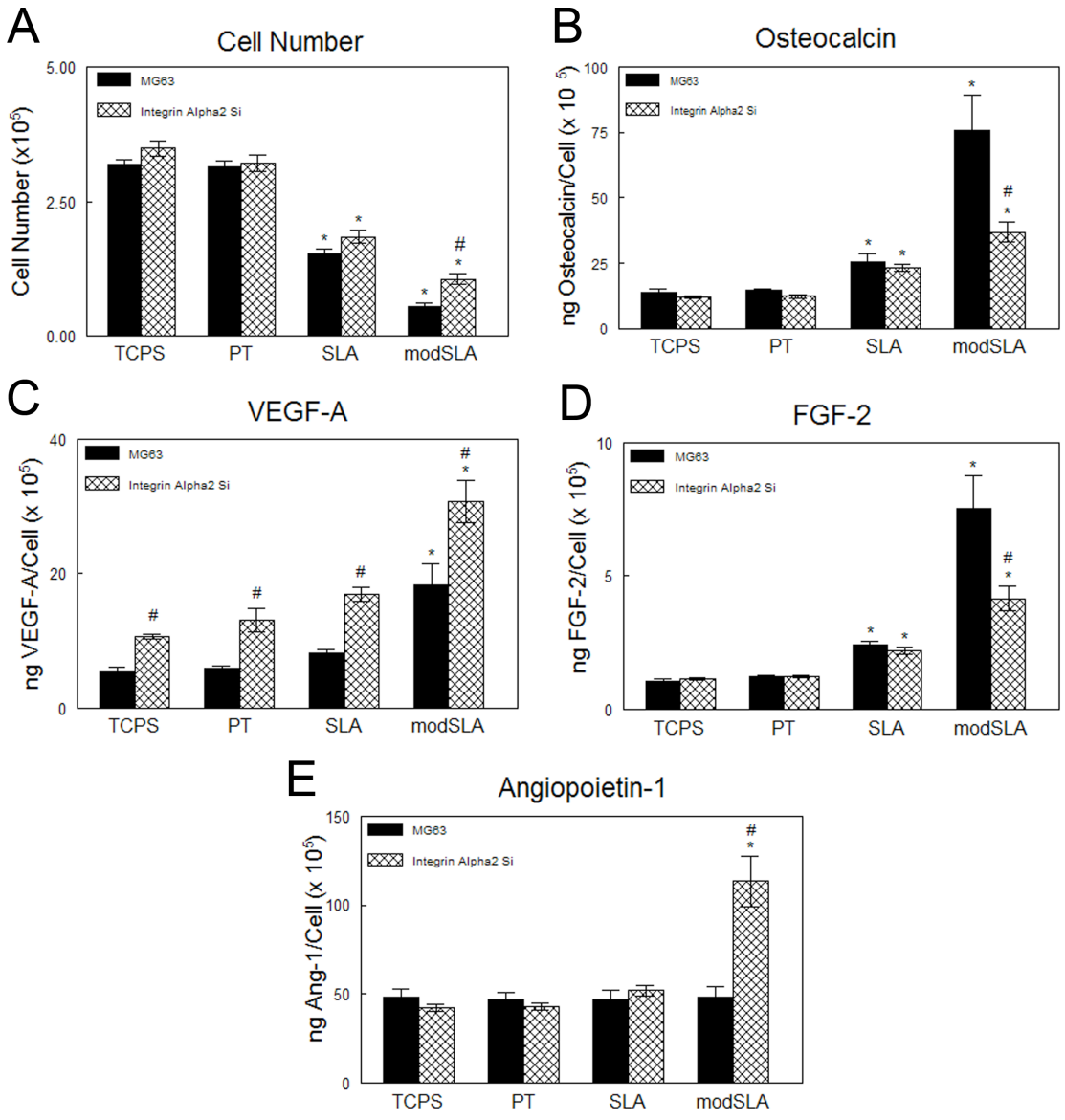

Figure 3-2. Integrin α_2 silenced cell response to Ti substrate features. (A) Total cell number of integrin α_2 silenced cells and MG63 cells were counted. (B) Osteocalcin, (C) VEGF-A, (D) FGF-2, and (E) Ang-1 levels in the conditioned media of both MG63 cells and integrin α_2 silenced MG63 cells were determined. Values presented are mean $\pm$ SEM of six independent cultures. Data were analyzed using ANOVA and statistical significance between groups was determined using Bonferroni's modification of Student's t-test. *p<0.05 vs. TCPS; #p<0.05 vs. MG63 cultures.

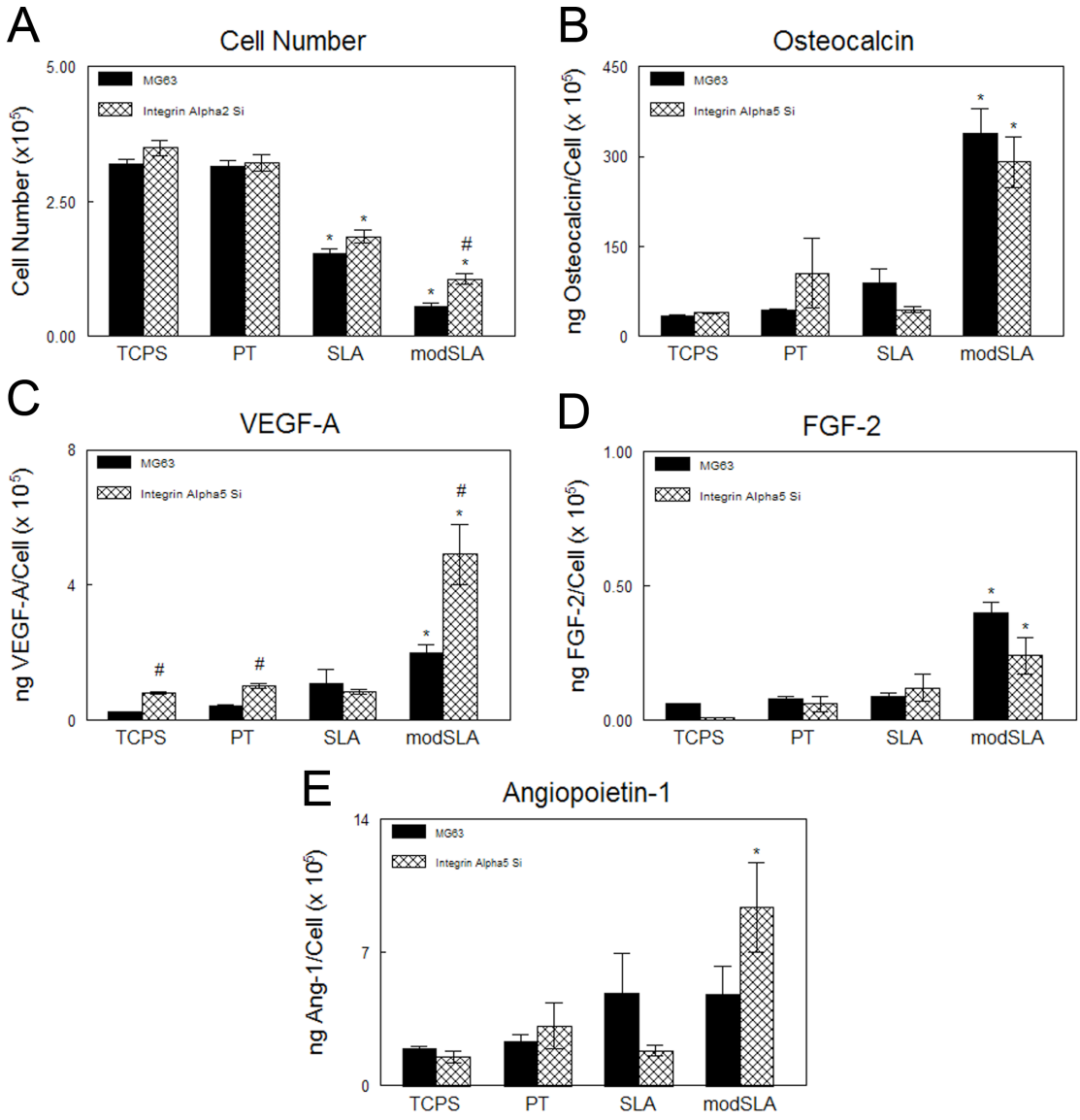

Figure 3-3. Integrin α_5 silenced cell response to Ti substrate features. (A) Total cell number of integrin α_5 silenced cells and MG63 cells were counted. (B) Osteocalcin, (C) VEGF-A, (D) FGF-2, and (E) Ang-1 levels in the conditioned media of both MG63 cells and integrin α_5 silenced MG63 cells were determined. Values presented are mean $\pm$ SEM of six independent cultures. Data were analyzed using ANOVA and statistical significance between groups was determined using Bonferroni's modification of Student's t-test. *p<0.05 vs. TCPS; #p<0.05 vs. MG63 cultures.

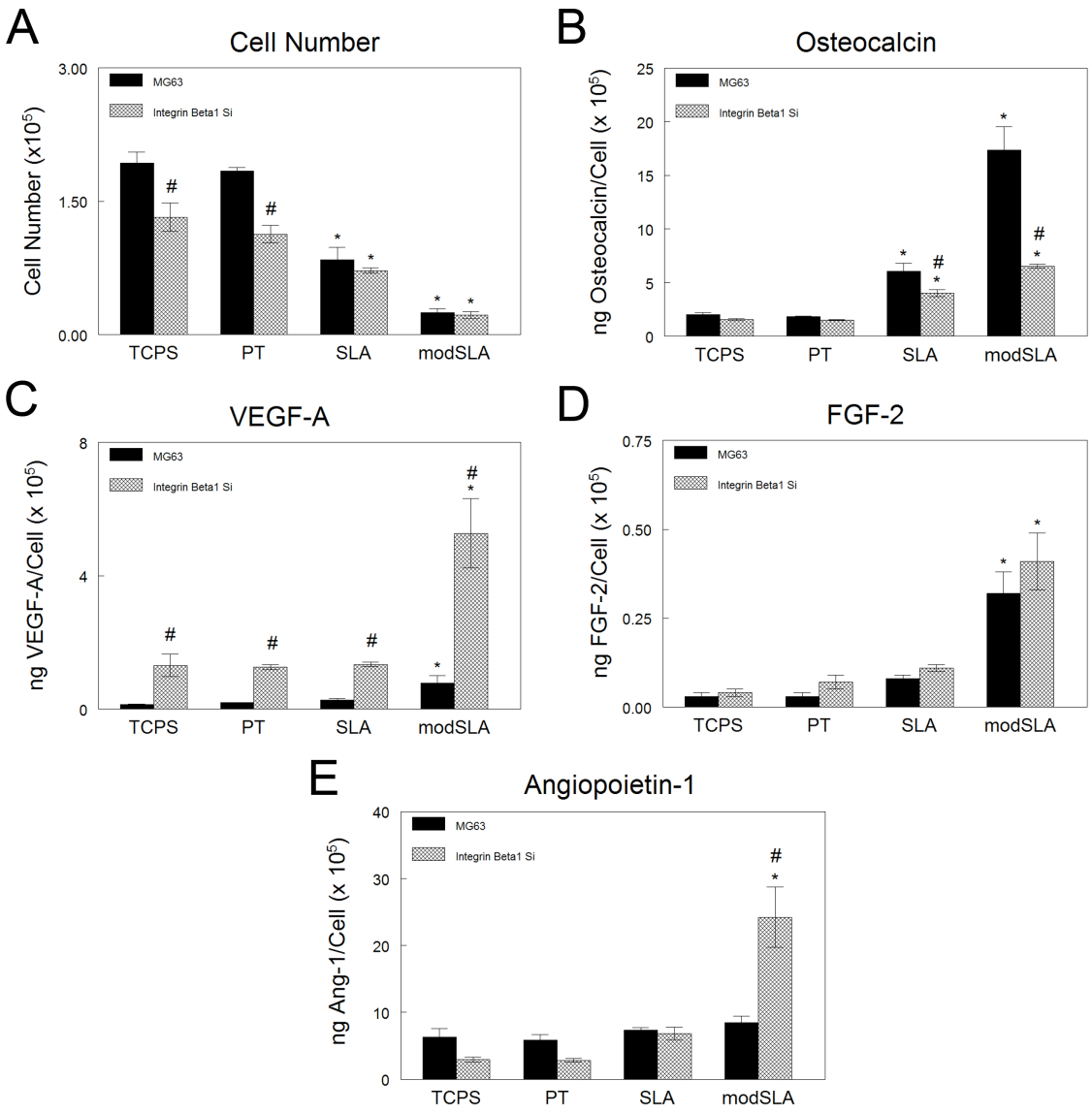

Figure 3-4. Integrin β_1 silenced cell response to Ti substrate features. (A) Total cell number of integrin β_1 silenced cells and MG63 cells were counted. (B) Osteocalcin, (C) VEGF-A, (D) FGF-2, and (E) Ang-1 levels in the conditioned media of both MG63 cells and integrin β_1 silenced MG63 cells were determined. Values presented are mean $\pm$ SEM of six independent cultures. Data were analyzed using ANOVA and statistical significance between groups was determined using Bonferroni's modification of Student's t-test. *p<0.05 vs. TCPS; #p<0.05 vs. MG63 cultures.

3.4 Discussion

Integrin binding to titanium substrates is important in triggering osteoblastic differentiation of cells in response to surface microstructure and energy. A number of integrins have been identified as being involved in osteoblast attachment and differentiation [28, 29]. In the present study, we found that knockdown of specific integrin subunits in an MG63 osteoblast-like cell line not only affects the differentiation of these cells in response to Ti surface topography and energy, but also affects the production of pro-angiogenic growth factors.

We found that the expression of integrin receptor subunits involved in osteoblastic differentiation is affected in response to Ti surface features. Our results are consistent with those found previously where expression of integrins α_2 and β_1 are increased on rough Ti surfaces and expression of integrin α_5 is decreased [10, 18]. Similar to integrins α_2 and β_1, we observed that expression of integrin α_1 is increased on microrough Ti surfaces compared to smooth Ti and TCPS control surfaces.

Cells cultured on Ti substrates presenting a rough surface morphology and high surface energy have a more differentiated phenotype displaying increased levels of osteocalcin, osteoprotegerin, and the local factor prostaglandin E2 [26]. Knockdown of either the α_2 or β_1 integrin subunits in these cells resulted in the loss of differentiation in response to Ti surface microstructure [18, 19] whereas knockdown of the α_5 subunit did not result in any significant changes in the differentiation of MG63 osteoblast-like cells [30].

The mechanism by which Ti surface microstructure and energy regulate the production of pro-angiogenic growth factors by osteoblasts is unclear. We found here that knockdown of several integrin receptor subunits differentially regulated the production of VEGF-A, FGF-2, and Ang-1. In particular, secreted levels of VEGF-A were

increased in cells silenced for integrins α_2, α_5, and β_1 whereas silencing of integrin α_1 resulted in a decrease in VEGF-A production in response to Ti surface topography and energy. Levels of FGF-2 were only affected in response to knockdown of either α_1 or α_2, and were decreased on modSLA Ti surfaces in these cells. In contrast, secretion of Ang-1 was increased on modSLA Ti surfaces in α_1, α_2, and β_1 silenced cells compared to wild-type MG63 cells. Taken together, these results suggest that signaling events through integrin adhesion receptors may regulate the production of pro-angiogenic growth factors to induce endothelial cell migration and subsequent vascular formation during peri-implant healing.

Integrin $\alpha_5\beta_1$ binds fibronectin [5] and has been suggested to promote early osteoblast proliferation and differentiation events and shRNA targeting endogenous integrin α_5 has been found to inhibit osteoblastic differentiation of mesenchymal stromal cells [31], potentially explaining why α_5 silencing did not have a largely significant effect on the expression of osteogenic or angiogenic markers in MG63 cells. Both $\alpha_1\beta_1$ and $\alpha_2\beta_1$ bind collagen I in the extracellular matrix [32] and both integrin receptors recognize and bind the same GFOGER motif [33]. However, in our study we found that silencing of the α_1 integrin subunit resulted in a decrease in the production of VEGF-A by MG63 cells in response to Ti surface features while knockdown of the α_2 integrin subunit increased VEGF-A production. This data suggests that activation of the $\alpha_1\beta_1$ integrin is necessary for the production of VEGF-A in MG63 osteoblast like cells whereas $\alpha_2\beta_1$ integrin binding and activation serves to downregulate VEGF-A expression. This may indicate that downstream signaling events differ between $\alpha_1\beta_1$ and $\alpha_2\beta_1$ integrins, resulting in the different effects induced by knockdown of each integrin.

Overall, our results indicate that in addition to promoting differentiation, signaling through integrin receptor complexes regulates the angiogenic response of osteoblasts to implant surface features. Further examination of the effect of conditioned media from knockdown cell cultures is necessary to determine if the differences in production of these growth factors influences endothelial cell differentiation. Also, it is possible that signaling events through other integrin adhesion receptors such as α_v and β_3 may modulate the production of angiogenic growth factors by osteoblasts.

3.5 References

1. Ellingsen JE. A study on the mechanism of protein adsorption to TiO2. Biomaterials 1991 Aug;12(6):593-596.

2. Kieswetter K, Schwartz Z, Dean DD, Boyan BD. The role of implant surface characteristics in the healing of bone. Crit Rev Oral Biol Med 1996;7(4):329-345.

3. Boyan BD, Hummert TW, Dean DD, Schwartz Z. Role of material surfaces in regulating bone and cartilage cell response. Biomaterials 1996 Jan;17(2):137-146.

4. Anselme K. Osteoblast adhesion on biomaterials. Biomaterials 2000 Apr;21(7): 667-681.

5. Hynes RO. Integrins: bidirectional, allosteric signaling machines. Cell 2002 Sep 20;110(6):673-687.

6. Gronthos S, Simmons PJ, Graves SE, Robey PG. Integrin-mediated interactions between human bone marrow stromal precursor cells and the extracellular matrix. Bone 2001 Feb;28(2):174-181.

7. Moursi AM, Globus RK, Damsky CH. Interactions between integrin receptors and fibronectin are required for calvarial osteoblast differentiation in vitro. J Cell Sci 1997 Sep;110 (Pt 18):2187-2196.

8. Siebers MC, ter Brugge PJ, Walboomers XF, Jansen JA. Integrins as linker proteins between osteoblasts and bone replacing materials. A critical review. Biomaterials 2005 Jan;26(2):137-146.

9. Gronowicz G, McCarthy MB. Response of human osteoblasts to implant materials: integrin-mediated adhesion. J Orthop Res 1996 Nov;14(6):878-887.

10. Raz P, Lohmann CH, Turner J, Wang L, Poythress N, Blanchard C, et al. 1alpha, 25(OH)2D3 regulation of integrin expression is substrate dependent. J Biomed Mater Res A 2004 Nov 1;71(2):217-225.

11. Garcia AJ. Get a grip: integrins in cell-biomaterial interactions. Biomaterials 2005 Dec;26(36):7525-7529.

12. Dedhar S. Integrin mediated signal transduction in oncogenesis: an overview. Cancer Metastasis Rev 1995 Sep;14(3):165-172.

13. Egan SE, Weinberg RA. The pathway to signal achievement. Nature 1993 Oct 28;365(6449):781-783.

14. Seger R, Krebs EG. The MAPK signaling cascade. FASEB J 1995 Jun;9(9): 726-735.

15. Schwartz Z, Raz P, Zhao G, Barak Y, Tauber M, Yao H, et al. Effect of micrometer-scale roughness of the surface of Ti6Al4V pedicle screws in vitro and in vivo. J Bone Joint Surg Am 2008 Nov;90(11):2485-2498.

16. Zhao G, Zinger O, Schwartz Z, Wieland M, Landolt D, Boyan BD. Osteoblast-like cells are sensitive to submicron-scale surface structure. Clinical oral implants research 2006 Jun;17(3):258-264.

17. Zinger O, Zhao G, Schwartz Z, Simpson J, Wieland M, Landolt D, et al. Differential regulation of osteoblasts by substrate microstructural features. Biomaterials 2005 May;26(14):1837-1847.

18. Olivares-Navarrete R, Raz P, Zhao G, Chen J, Wieland M, Cochran DL, et al. Integrin alpha2beta1 plays a critical role in osteoblast response to micron-scale surface structure and surface energy of titanium substrates. Proceedings of the National Academy of Sciences of the United States of America 2008 Oct 14;105(41): 15767-15772.

19. Wang L, Zhao G, Olivares-Navarrete R, Bell BF, Wieland M, Cochran DL, et al. Integrin beta1 silencing in osteoblasts alters substrate-dependent responses to 1,25-dihydroxy vitamin D3. Biomaterials 2006 Jul;27(20):3716-3725.

20. Raines AL, Olivares-Navarrete R, Wieland M, Cochran DL, Schwartz Z, Boyan BD. Regulation of angiogenesis during osseointegration by titanium surface microstructure and energy. Biomaterials Jun;31(18):4909-4917.

21. Enenstein J, Kramer RH. Confocal microscopic analysis of integrin expression on the microvasculature and its sprouts in the neonatal foreskin. J Invest Dermatol 1994 Sep;103(3):381-386.

22. Max R, Gerritsen RR, Nooijen PT, Goodman SL, Sutter A, Keilholz U, et al. Immunohistochemical analysis of integrin alpha vbeta3 expression on tumor-associated vessels of human carcinomas. Int J Cancer 1997 May 2;71(3):320-324.

23. Soldi R, Mitola S, Strasly M, Defilippi P, Tarone G, Bussolino F. Role of alphavbeta3 integrin in the activation of vascular endothelial growth factor receptor-2. EMBO J 1999 Feb 15;18(4):882-892.

24. Hutchings H, Ortega N, Plouet J. Extracellular matrix-bound vascular endothelial growth factor promotes endothelial cell adhesion, migration, and survival through integrin ligation. FASEB J 2003 Aug;17(11):1520-1522.

25. Rusnati M, Tanghetti E, Dell'Era P, Gualandris A, Presta M. alphavbeta3 integrin mediates the cell-adhesive capacity and biological activity of basic fibroblast growth factor (FGF-2) in cultured endothelial cells. Mol Biol Cell 1997 Dec;8(12):2449-2461.

26. Zhao G, Schwartz Z, Wieland M, Rupp F, Geis-Gerstorfer J, Cochran DL, et al. High surface energy enhances cell response to titanium substrate microstructure. J Biomed Mater Res A 2005 Jul 1;74(1):49-58.

27. Rupp F, Scheideler L, Olshanska N, de Wild M, Wieland M, Geis-Gerstorfer J. Enhancing surface free energy and hydrophilicity through chemical modification of microstructured titanium implant surfaces. J Biomed Mater Res A 2006 Feb;76(2): 323-334.

28. Brighton CT, Albelda SM. Identification of integrin cell-substratum adhesion receptors on cultured rat bone cells. J Orthop Res 1992 Nov;10(6):766-773.

29. Saito T, Albelda SM, Brighton CT. Identification of integrin receptors on cultured human bone cells. J Orthop Res 1994 May;12(3):384-394.

30. Bell BF. Mechanisms regulating osteoblast response to surface microtopography and vitamin D. Atlanta: Georgia Institute of Technology; 2009.

31. Hamidouche Z, Fromigue O, Ringe J, Haupl T, Vaudin P, Pages JC, et al. Priming integrin alpha5 promotes human mesenchymal stromal cell osteoblast differentiation and osteogenesis. Proceedings of the National Academy of Sciences of the United States of America 2009 Nov 3;106(44):18587-18591.

32. McCall-Culbreath KD, Zutter MM. Collagen receptor integrins: rising to the challenge. Curr Drug Targets 2008 Feb;9(2):139-149.

33. Knight CG, Morton LF, Peachey AR, Tuckwell DS, Farndale RW, Barnes MJ. The collagen-binding A-domains of integrins alpha(1)beta(1) and alpha(2)beta(1) recognize the same specific amino acid sequence, GFOGER, in native (triple-helical) collagens. J Biol Chem 2000 Jan 7;275(1):35-40.

CHAPTER 4. The Role of VEGF-A in Cell Response to Titanium Surface Microstructure and Energy

4.1 Introduction

The surface properties of biomaterials directly influence the attachment, proliferation, and phenotypic expression of cells both *in vitro* and *in vivo* [1-5]. The first events after implantation of a material into the body involve the adsorption of proteins onto the surface of the material from the surrounding blood and tissue fluid [REF]. The topography, chemistry, and energy of a biomaterial surface are all known to affect this process and the subsequent cellular response.

In orthopaedics and dentistry, titanium (Ti) is a commonly used material due to its biocompatibility, good mechanical properties and resistance to wear. The biocompatibility and wear resistance of Ti is due to the thin oxide layer (TiO_2) that forms on its surface. Substrates fabricated from commercially pure Ti can be used to assess osteoblast response *in vitro* and bone formation *in vivo*. It is well known that Ti substrates presenting a rough micron-scale topography affect the attachment and differentiation of osteoblasts *in vitro* [6]. Cells cultured on these substrates display a more differentiated phenotype with a reduction in proliferation and an increase in the production of factors that generate an osteogenic microenvironment, including osteocalcin, PGE_2, $TGF\beta_1$, and osteoprotegerin [7]. Combining a rough surface microtopography with a high surface energy further enhances the differentiation of osteoblasts on Ti surfaces [8]. Rough Ti substrates support greater bone to implant contact and have higher torque removal strengths *in vivo* [9, 10].

In addition to promoting osteoblast differentiation and bone formation, the establishment of a vascular supply is of critical importance in orthopaedic and dental applications. Angiogenesis, the sprouting of new capillary blood vessels from the pre-existing vasculature, is an important part of bone formation and bone fracture healing [11]. Vascularization of the cartilage template precedes ossification during both intramembranous and endochondral ossification [12-14]. Bone remodeling, regeneration, and osseintegration of implanted biomaterials is also dependent on the delivery of osteoprogenitor cells via a vascular supply [15, 16].

Osteoblast and osteoblast progenitor cells have been demonstrated to produce and secrete several pro-angiogenic growth factors, including vascular endothelial growth factor-A (VEGF-A), basic fibroblast growth factor (FGF-2), and angiopoietin-1 (Ang-1), and that the expression of these growth factors is dependent on the state of maturation of the cell [17-20]. Further, we and others have also found that the expression of these growth factors is dependent on Ti surface microtopography and energy [21-23].

VEGF-A has been identified as a particularly important growth factor during bone formation and remodeling. VEGF-A is a member of the VEGF family of proteins that include VEGF members -A, -B, -C, -D, and PlGF-1 and -2. These growth factors all have the ability to stimulate endothelial cell proliferation and differentiation [24, 25]. VEGF-A is expressed by hypertrophic chondrocytes and may be involved directly in osteoblast differentiation [26, 27].

VEGF-A exerts its effects through two tyrosine kinase receptors, VEGFR1/Flt-1 and VEGFR2/KDR. Both VEGF receptors have been found to be expressed by osteoblasts during their differentiation [17, 28, 29].

While it is known that osteoblasts express VEGF-A and the receptors for VEGF-A and that disruption of VEGF-A signaling in osteoblasts inhibits bone formation during

endochondral ossification, it is not known whether VEGF-A production by osteoblasts in response to Ti surface microtopography and energy has an effect on the differentiation of these cells. In the present study, we sought to determine the potential role that VEGF-A has in mediating the differentiation of osteoblasts to Ti surface microtopography and energy. To do this, we stably silenced VEGF-A in an MG63 osteoblast-like cell line using shRNA targeting VEGF-A. We cultured wild-type MG63 cells and VEGF-A silenced MG63 cells on Ti surfaces presenting different surface roughness and energy and examined the production of osteogenic and angiogenic growth factors in these cells. To determine if VEGF-A produced by MG63 cells has a paracrine effect on endothelial cells, we used conditioned media from wild-type MG63 and VEGF-A silenced MG63 cell cultures in an *in vitro* fibrin gel assay to assess endothelial tubule formation. To see if endogenous VEGF-A produced by MG63 cells in response to Ti surface roughness and energy has an autocrine effect on MG63 cell differentiation through interaction with VEGFR2/Flk-1, we used a monoclonal antibody against human VEGFR2/Flk-1 in wild-type MG63 cell cultures on Ti substrates. We also treated MG63 cells on Ti surfaces with rhVEGF-A or rhFGF-2 to determine if osteoblastic differentiation is enhanced with treatment of either of these growth factors. Finally, to see if the production of osteogenic and angiogenic growth factors in VEGF-A silenced MG63 cells could be restored to wild-type levels, we treated VEGF-A silenced MG63 cells with exogenous rhVEGF-A or rhFGF-2.

4.2 Materials & Methods

4.2.1 Preparation of Ti substrates

Ti disks were prepared from 1 mm thick sheets of grade 2 unalloyed commercially pure Ti punched into 15mm diameter disks and supplied by Institut Straumann AG (Basel, Switzerland). The production and characterization of smooth

pretreatment (PT), sand blasted and acid etched (SLA), and modified SLA (modSLA) surfaces have been described previously [8]. PT surfaces were degreased by washing Ti disks in acetone and processed in a 2% ammonium fluoride/2% hydrofluoric acid/10% nitric acid solution. SLA surfaces were made by coarse grit-blasting of the PT surfaces with 0.25-0.50 mm corundum grit followed by acid etching. modSLA surfaces were made using the same procedure as SLA surfaces under nitrogen rinsing to prevent exposure to air and were then stored under aqueous conditions under nitrogen to retain high surface free energy. The PT surface has an overall average roughness (Ra) of less than 0.7 μm. SLA and modSLA surfaces have a complex microtopography with craters varying from 30 to 100 μm in diameter overlaid with pits from 1 to 3 μm in diameter. The acid etch creates sharp edges approximately 700 nm in height, resulting in an overall Ra of approximately 4 μm. PT, SLA and modSLA Ti disks all have a TiO_2 surface layer, with the PT and SLA surfaces being hydrophobic due to the adsorption of atmospheric hydrocarbons while the modSLA surface is hydrophilic. Advancing contact angles were used to calculate the hydrophilicity of the surfaces as PT (95.8°), SLA (139.80°), and modSLA (~0°). Surface free energy for PT, SLA, and modSLA surfaces was calculated according to Zisman (critical surface tension), Equation of State (EOS), and Geometric Mean approaches and is described in detail elsewhere [30].

4.2.2 General Cell Culture

MG63 osteoblast-like osteosarcoma cells were maintained in culture using Dulbecco's Modified Eagle's Medium (DMEM) supplemented with 10% fetal calf serum and 1% penicillin/streptomycin. Stably silenced MG63 cells for VEGF-A were cultured in DMEM containing 10% fetal calf serum, 1% penicillin/streptomycin and 0.5 μg/mL puromycin for selection of successfully transduced cells. For experiments, both MG63 cells and VEGF-A silenced MG63 cells were plated at an initial seeding density of

10,000 cells/cm^2 in 24-well standard tissue culture plates. Media were changed 24 hours after plating and every 48 hours thereafter until the cells were 100% confluent. When cells reached 100% confluent on TCPS, media from all cultures were collected and examined for secreted levels of VEGF-A, FGF-2, Ang-1, OPG, and osteocalcin where appropriate.

Human aortic endothelial cells (HAEC), for use in endothelial tubule formation assays, were maintained in culture using Endothelial Cell Growth Medium-2 (EGM-2, Lonza, Walkersville, MD). For experiments, HAEC were plated at a density of 5,000 cells/cm^2 on fibrin gel coated 96-well plates as described in detail in section 4.2.11.

4.2.3 Generation of VEGF-A silenced MG63 cells

To generate stably silenced MG63 cells for VEGF-A, we used MISSION® shRNA lentiviral transduction particles targeting the VEGF-A gene (Sigma-Aldrich, St. Louis, MO). 5 separate shRNA clones were designed and packaged into self-inactivating replication incompetent lentiviral particles for transduction. The sequences for the 5 clones are described below:

Clone H1
CCGGAGGGCAGAATCATCACGAAGTCTCGAGACTTCGTGATGATTCTGCCCTTTTTT
Clone H2
CCGGCGAACGTACTTGCAGATGTGACTCGAGTCACATCTGCAAGTACGTTCGTTTTT
Clone H3
CCGGGCGCAAGAAATCCCGGTATAACTCGAGTTATACCGGGATTTCTTGCGCTTTTT
Clone H4
CCGGGACGTGTAAATGTTCCTGCAACTCGAGTTGCAGGAACATTTACACGTCTTTTT
Clone H5
CCGGATGCGGATCAAACCTCACCAACTCGAGTTGGTGAGGTTTGATCCGCATTTTTT

In additioned to the 5 clones described above, an empty shRNA vector, not containing a hairpin insert (PLK0.1) and an shRNA sequence not targeting any gene in the human genome (NT) were used as controls.

To transduce cells, MG63 cells were plated at a density of 10,000 cells/cm^2. After reaching 60 – 70% confluency, cells were transduced with lentiviral particles at a multiplicity of infection (MOI) of 5. After 18 hours, media containing lentiviral particles were discarded into a bleach solution and cells were fed with DMEM containing 10% fetal calf serum and 1% penicillin/streptomycin. The following day, 0.5 μg/mL puromycin were added to transduced MG63 cell cultures to select for successfully transduced cells. Transduced cells were maintained in medium containing 0.5 μg/mL puromycin until plating for experiments.

4.2.4 Flk-1/IgG Antibody Treatment

MG63 cells plated on tissue culture polystyrene (TCPS, control for all studies), PT, SLA, and modSLA Ti substrates were treated with 100 ng/mL of an Flk-1 mouse anti-human monoclonal neutralization antibody (R&D Systems, Minneapolis, MN) or 100 ng/mL of a rabbit anti-human nonspecific IgG polyclonal antibody (NeoMarkers, Fremond, CA) for the duration of cell culture.

4.2.5 rhVEGF-A Treatment

For studies examining the effect of addition of exogenous VEGF-A to cells on Ti substrates, cell culture media were supplemented with 20 ng/mL rhVEGF-A_{165} (R&D Systems, Minneapolis, MN) and MG63 cells and VEGF-A silenced MG63 cells were treated with VEGF-A supplemented media for the duration of cell culture.

4.2.6 rhFGF-2 Treatment

For studies examining the effect of addition of exogenous FGF-2 to cells on Ti substrates, cell culture media were supplemented with 10 ng/mL rhFGF-2 (R&D Systems, Minneapolis, MN) and MG63 cells and VEGF-A silenced MG63 cells were treated with FGF-2 supplemented media for the duration of cell culture.

4.2.7 Cell Number

Total cell number were determined for all cell types and treatments at time of harvest. At confluence, cells were released from TCPS and Ti surfaces using two sequential incubations with 0.25% trypsin for 10 minutes at 37°C to ensure that no cells remained on the rough Ti surfaces and counted using an automated cell counter (Z1 Particle counter, Beckman Coulter, Fullerton, CA).

4.2.8 Alkaline Phosphatase Specific Activity

Alkaline phosphatase specific activity (orthophosphoric monoester phosphohydrolase, alkaline; E.C. 3.1.3.1) was measured in the cell lysates as a marker of osteoblastic differentiation. Enzyme activity was determined using a colorimetric assay measuring the release of *p*-nitrophenol from *p*-nitrophenylphosphate at 37°C. Samples were read on a plate reader at 415nm [39].

4.2.9 Osteocalcin

Osteocalcin levels in the conditioned medium of MG63 cells and VEGF-A silenced MG63 cells grown on Ti surfaces were determined as a marker of osteoblast maturation using a commercially available radioimmunoassay (Biomedical Technologies, Inc., Stoughton, MA) following the manufacturer's protocol.

4.2.10 VEGF-A, FGF-2, Ang-1, OPG

Secreted levels of VEGF-A, FGF-2, Ang-1, and OPG by MG63 cells and VEGF-A silenced MG63 cells were determined in the conditioned medium using commercially available ELISA assays (Duoset ELISA Development Systems, R&D Systems, Minneapolis, MN) following the manufacturer's protocols.

4.2.11 Endothelial Cell Differentiation

To determine if the conditioned media were angiogenic, we examined their ability to support endothelial tubule formation using a fibrin gel assay (Millipore, St. Charles, MO). Briefly, each well of a 96-well tissue culture plate were coated with 30 μL of a

fibrinogen solution and 20 μL of a thrombin solution and the mixture was allowed to polymerize for at least 1 hour at 37°C. HAECs were plated in 100 μL of EGM-2 at a density of 5 x 10^3 cells/well and cultured at 37°C for 24h. At 24h, media were removed and a second layer of fibrin was added on top of cells by again mixing 30 μL of fibrinogen and 20 μL of thrombin. The mixture was allowed to polymerize for 5 minutes before 100 μL of conditioned media from either MG63 cell cultures or VEGF-A silenced MG63 cell cultures on TCPS, PT, SLA, or modSLA substrates were added. At 12, 24, and 36 after the addition of conditioned media, images were taken for morphometric analysis to determine total endothelial tube length.

4.2.12 Real-time Reverse Transcriptase Polymerase Chain Reaction

Real-time RT-PCR for human VEGF-A and human glyceraldehyde-3-phosphate dehydrogenase (GAPDH) were run to test for silencing efficiency of VEGF-A in transduced MG63 cell cultures. Briefly, RNA was isolated from confluent cultures of wild-type MG63 cells, H1-H5 transduced MG63 cells, and NT and PLK0.1 transduced MG63 cells using Trizol (Invitrogen). RNA was quantified using a Nanodrop spectrophotometer (Thermo Scientific, Waltham, MA). mRNA quantities were assessed for both VEGF-A and GAPDH using the primers outlined below.

VEGF-A Forward - CTTGCCTTGCTGCTCTACC
VEGF-A Reverse – TTCTGCCCTCCTCCTTCTG

GAPDH Forward - GCTCTCCAGAACATCATCC
GAPDH Reverse – TGCTTCACCACCTTCTTG

To create a cDNA template, 1 μg of RNA was reverse transcribed using random primers (Promega, Madison, WI) and Omniscript reverse transcriptase (Qiagen, Valencia, CA). Quantification of VEGF-A and GAPDH genes was done using real-time qPCR using SYBR Green as a fluorescent marker. Fluorescence values were quantified as starting

quantities using known dilutions of MG63 cell RNA. VEGF-A mRNA levels were normalized to expression of GAPDH for all cell types.

4.2.13 Statistical Analysis

The data presented here are from one of at least two separate sets of experiments. Both sets of experiments yielded comparable observations. For any given experiment, each data point represents the mean ± standard error of six individual cultures. Data were analyzed by ANOVA and when statistical differences were detected, Student's *t*-test for multiple comparisons using Bonferroni's modification was used. p-values < 0.05 were considered significant.

4.3 Results

4.3.1 Flk-1 antibody treatment

We have previously shown that MG63 osteoblast-like cells secrete higher levels of VEGF-A on SLA and modSLA Ti substrates compared to TCPS and smooth PT Ti substrates[22]. It has also been reported that osteoblasts express the VEGF receptor Flk-1/KDR (VEGFR2)[17, 27]. In order to determine if VEGF-A produced by MG63 cells has an autocrine effect, we added an Flk-1 neutralization antibody to MG63 cell cultures on TCPS and Ti substrates. Consistent with previous results, total cell number in MG63 cell cultures were reduced on microrough SLA substrates, and microrough, hydrophilic modSLA surfaces compared to TCPS. Addition of either Flk-1 neutralization antibody or nonspecific IgG antibody had no effect on cell number (Figure 4-1A). Alkaline phosphatase specific activity in MG63 cells were unchanged amongst any of the surfaces examined and addition of either Flk-1 neutralization antibody or IgG control antibody had no effect on alkaline phosphatase specific activity (Figure 4-1B). Secreted levels of osteocalcin, a late marker of osteoblast differentiation, were significantly increased ($p<0.05$) in MG63 cells cultured on SLA and modSLA surfaces compared to

TCPS substrates while the addition of either antibody had no effect on osteocalcin levels compared to MG63 cells (Figure 4-1C). Osteoprotegerin (OPG) secretion by MG63 cells were similar on TCPS and smooth PT Ti substrates. Addition of a rough surface microarchitecture observed on SLA substrates had no effect on secreted levels of OPG by MG63 cells. However, on rough, hydrophilic, modSLA substrates, OPG levels were significantly increased. Addition of either an Flk-1 neutralization antibody or nonspecific IgG antibody had no effect on OPG levels compared to MG63 cells (Figure 4-1D).

Consistent with what we have found previously, production of VEGF-A by MG63 cells was significantly increased on both SLA and modSLA substrates compared to TCPS and smooth PT surfaces. Addition of an Flk-1 neutralization antibody to MG63 cell cultures significantly increased production of VEGF-A on all surfaces compared to MG63 cells with no antibody, with the largest increase occurring on modSLA substrates. A nonspecific IgG antibody had no effect on VEGF-A production versus MG63 cell cultures (Figure 4-2A). FGF-2 production by MG63 cells was not changed in response to treatment with either an Flk-1 neutralization antibody or a nonspecific IgG antibdody, however a surface roughness and energy dependent increase in FGF-2 production was observed in all three treatment groups (Figure 4-2B). Angiopoietin-1 levels were unaffected by treatment with either antibody or by any surface type tested (Figure 4-2C).

4.3.2 VEGF-A silencing

To verify successful silencing of VEGF-A in MG63 cells, we examined both the total secreted protein levels in the conditioned media and VEGF-A gene expression using real-time reverse transcriptase polymerase chain reaction (RT-qPCR) for the five shRNA sequences for human VEGF-A as well as a scrambled shRNA sequence (NT) and an empty vector (PLK0.1). VEGF-A protein levels in MG63 cells, NT, and PLK0.1 cell lines were comparable to each other. VEGF-A shRNA clones H1-H5 secreted

varying levels of VEGF-A into the conditioned media as outlined in table 4-1 below and Figure 4-3A. Notably, clone H4 showed the largest reduction in VEGF-A protein levels, with a 94.1% reduction in VEGF-A compared to MG63 cells.

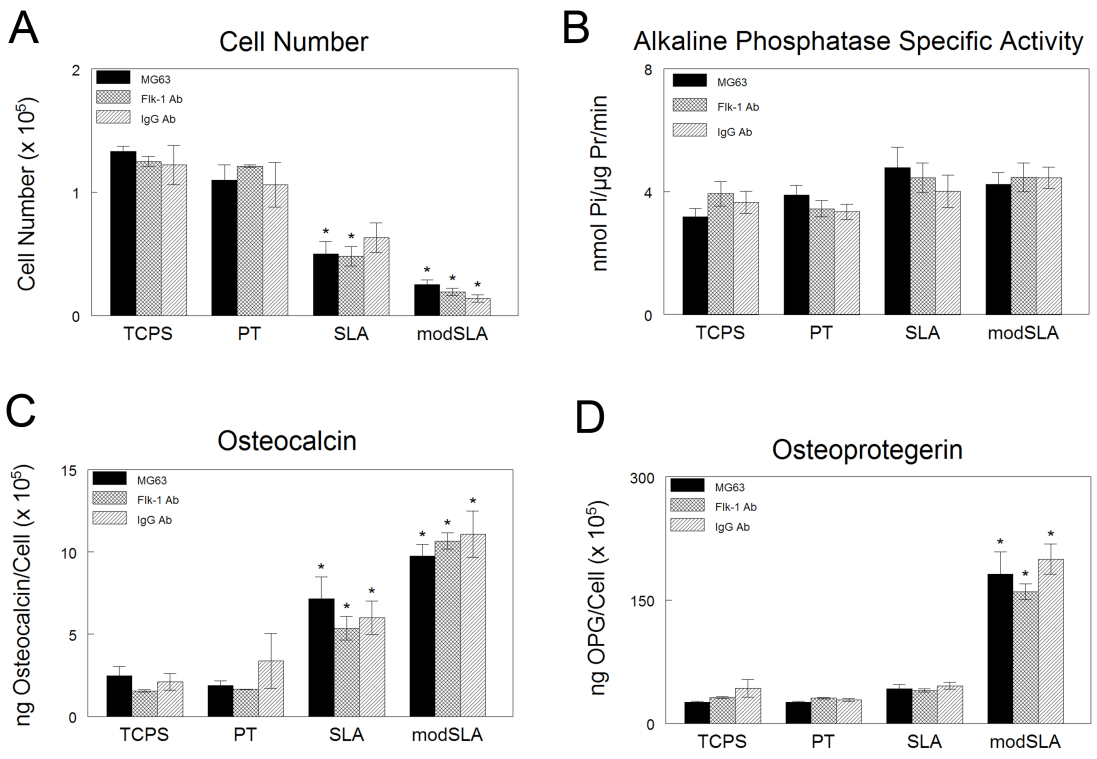

Figure 4-1. Response of MG63 cells cultured on TCPS and Ti surfaces in the presence an Flk-1 neutralizing antibody. (A) Cell Number, (B) Alkaline phosphatase specific activity in the cell lysate, (C) osteocalcin, and (D) osteoprotegerin levels in the conditioned media. Cells were cultured on control (TCPS), PT, SLA, and modSLA Ti surfaces. Values presented are mean ± SEM of six independent cultures. The data presented are from one of two separate experiments with comparable results. Data were analyzed using ANOVA and statistical significance between groups was determined using Bonferroni's modification of Student's t-test. *$p < 0.05$ vs. TCPS.

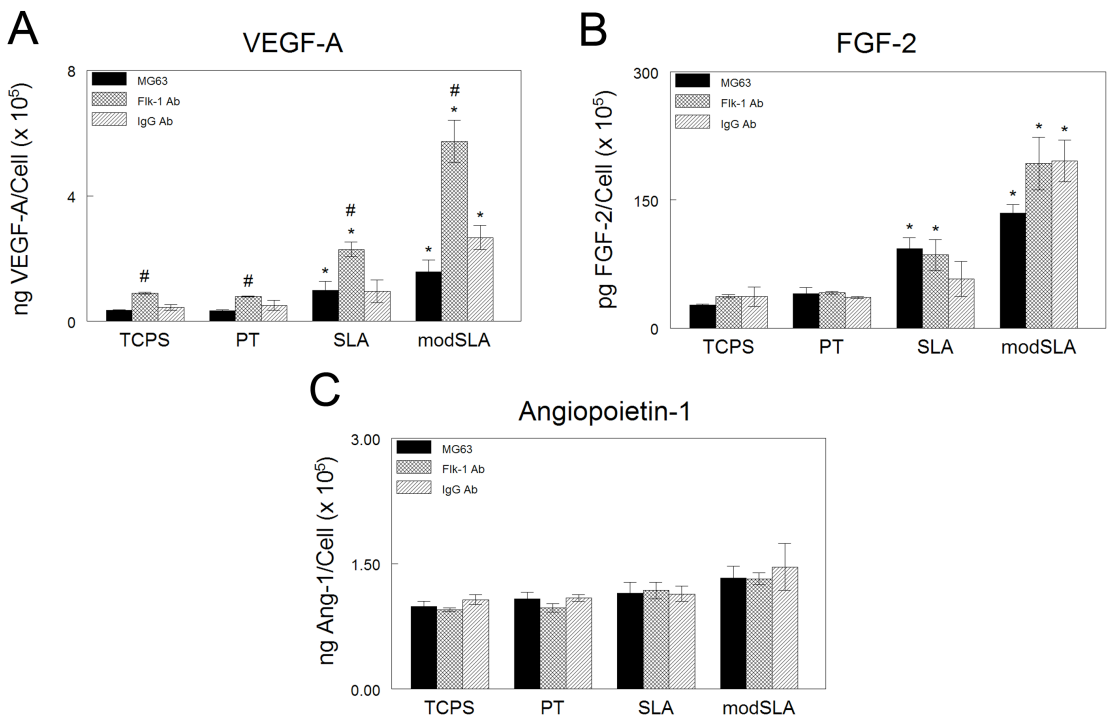

Figure 4-2. Production of angiogenic growth factors by MG63 cells cultured in the presence of an Flk-1 neutralizing antibody. (A) VEGF-A, (B) FGF-2, and (C) angiopoietin-1 levels in the conditioned media. Cells were cultured on control (TCPS), PT, SLA, and modSLA Ti surfaces. Values presented are mean ± SEM of six independent cultures. The data presented are from one of two separate experiments with comparable results. Data were analyzed using ANOVA and statistical significance between groups was determined using Bonferroni's modification of Student's t-test. *$p<0.05$ vs. TCPS ; #$p<0.05$ vs. MG63.

Table 4-1: VEGF-A Protein Levels

shVEGF-A Clone	*% VEGF-A Protein Reduction*
H1	35.2
H2	52.3
H3	91.9
H4	94.1
H5	7.0

To further verify silencing, real-time PCR gene expression for VEGF-A was done. Similar to VEGF-A protein levels, VEGF-A gene expression levels for MG63 cells, NT, and PLK0.1 vectors were similar, while the VEGF-A shRNA clones H1-H5 had varying levels of expression compared to MG63 cells (Table 4-2 and Figure 4-3B).

Table 4-2: VEGF-A Gene Expression

shVEGF-A Clone	*% VEGF-A mRNA Reduction*
H1	N/A
H2	91.0
H3	83.7
H4	92.9
H5	69.5

Based on the results of VEGF-A protein and gene expression levels in shRNA transduced MG63 cells, we selected clone H4 for further experiments. Based on the results observed for VEGF-A at both the gene and protein level where no difference in expression was found in response to transduction with either a scrambled shRNA sequence or an empty vector, it was decided that lentiviral transduction of MG63 cells did not have an adverse effect on cell response and thus in future experiments only wild-type MG63 cells and VEGF-A silenced cells obtained from clone H4 were used to reduce sample size.

To see if the reduced levels of VEGF-A produced in VEGF-A silenced cells had an effect on endothelial cell response, we performed an *in vitro* Matrigel™ endothelial cell tubule formation assay using conditioned media from either MG63 cells or VEGF-A silenced MG63 cells. Total endothelial tubule length was reduced at 4, 8, and 12 hours after the addition of conditioned media from either MG63 cells or VEGF-A silenced MG63 cells (Figure 4-3C).

We next examined the effect of VEGF-A silencing on cell response to Ti substrate microtopography and surface energy. Consistent with previous results, total cell number was reduced on SLA and modSLA Ti surfaces in MG63 cell cultures compared to TCPS and smooth PT Ti surfaces. Cell number in VEGF-A silenced MG63 cells were comparable to that observed in wild-type MG63 cells on all surfaces examined (Figure 4-4A). Alkaline phosphatase specific activity in MG63 cells were unchanged in response to surface microtopography and surface energy. In VEGF-A silenced MG63 cells, levels of alkaline phosphatase specific activity were significantly reduced on TCPS and PT surfaces compared to MG63 cell cultures. Alkaline phosphatase levels were also reduced in VEGF-A silenced cell cultures on SLA and modSLA Ti surfaces compared to MG63 cell cultures, though these reductions were not statistically significant (Figure 4-4B). Secreted levels of both osteocalcin and osteoprotegerin showed surface roughness and energy dependent increases in MG63 cell cultures. Silencing of VEGF-A in MG63 cells significantly reduced secreted levels of both growth factors, though surface roughness and energy dependent increases were still observed (Figure 4-4C,D).

VEGF-A levels were reduced by greater than 80% on all surfaces in VEGF-A silenced MG63 cells (Figure 4-5A). Silencing of VEGF-A in MG63 cells affected the production of FGF-2 and Ang-1. Production of FGF-2 by MG63 cells were increased in response to surface microtopography. Addition of high surface free energy further

increased production of FGF-2, consistent with previous results [Raines]. In VEGF-A silenced cell cultures, FGF-2 levels were only reduced with the combination of surface microtopography and energy seen on modSLA substrates (Figure 4-5B). Angiopoietin-1 levels were unaffected by either surface roughness or energy in both MG63 cells and VEGF-A silenced MG63 cells, though levels in VEGF-A silenced MG63 cells were reduced by at least 50% on all surfaces (Figure 4-5C).

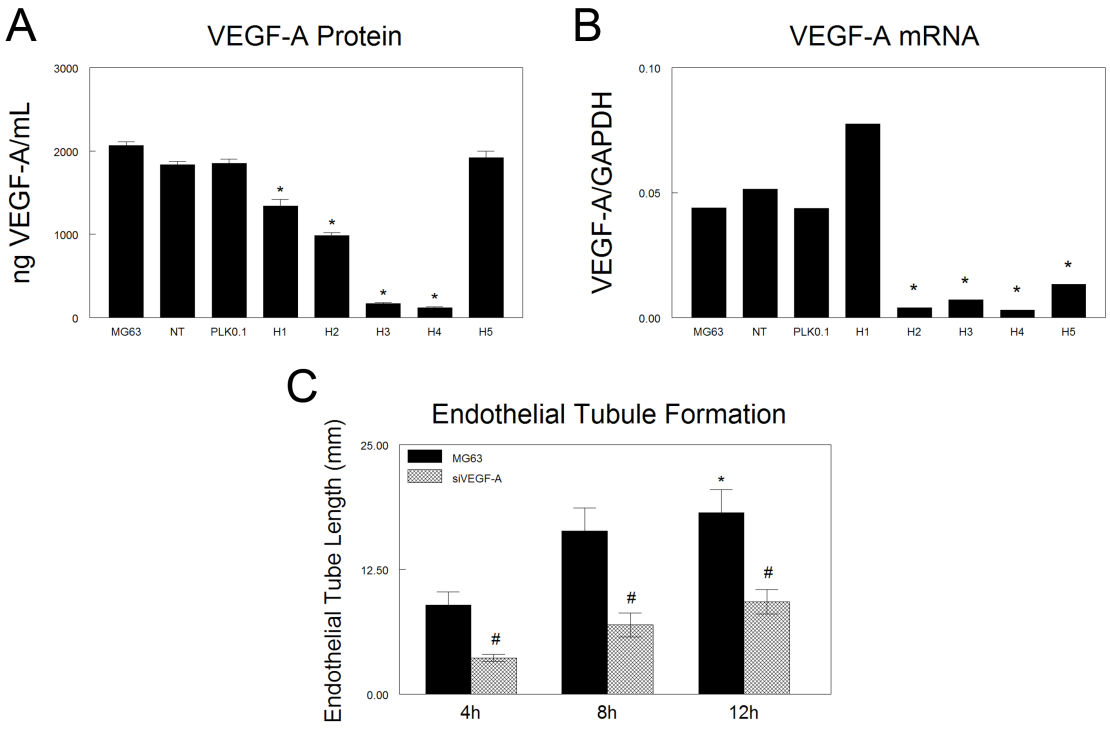

Figure 4-3. Verification of VEGF-A silencing in an MG63 cell line using lentiviral-mediated transduction of shRNA specific for human VEGF-A. (A) VEGF-A protein levels, and (B) VEGF-A mRNA levels were determined in 5 separate MG63 cell lines established using shRNA sequences specific for VEGF-A as well as a scrambled shRNA sequence (NT) and an empty vector control (PLK0.1). *p<0.05 vs. MG63. (C) Total endothelial tube length in the presence of conditioned media from MG63 cells and VEGF-A silenced clone H4 cells. *p<0.05 vs. 4h; #p<0.05 vs. MG63.

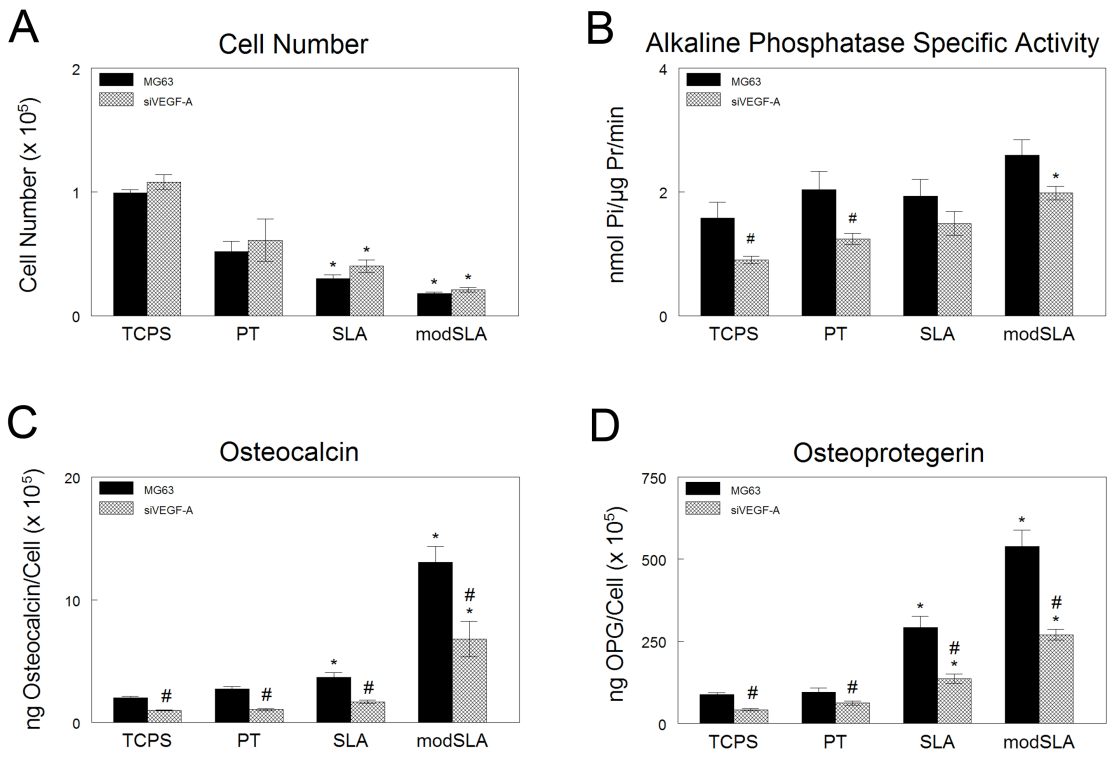

Figure 4-4. Response of MG63 and VEGF-A silenced MG63 cells cultured on TCPS and Ti surfaces. (A) Cell Number, (B) alkaline phosphatase specific activity in the cell lysate, (C) osteocalcin, and (D) osteoprotegerin levels in the conditioned media. Cells were cultured on control (TCPS), PT, SLA, and modSLA Ti surfaces. Values presented are mean ± SEM of six independent cultures. The data presented are from one of two separate experiments with comparable results. Data were analyzed using ANOVA and statistical significance between groups was determined using Bonferroni's modification of Student's t-test. *$p < 0.05$ vs. TCPS ; #$p<0.05$ vs. MG63.

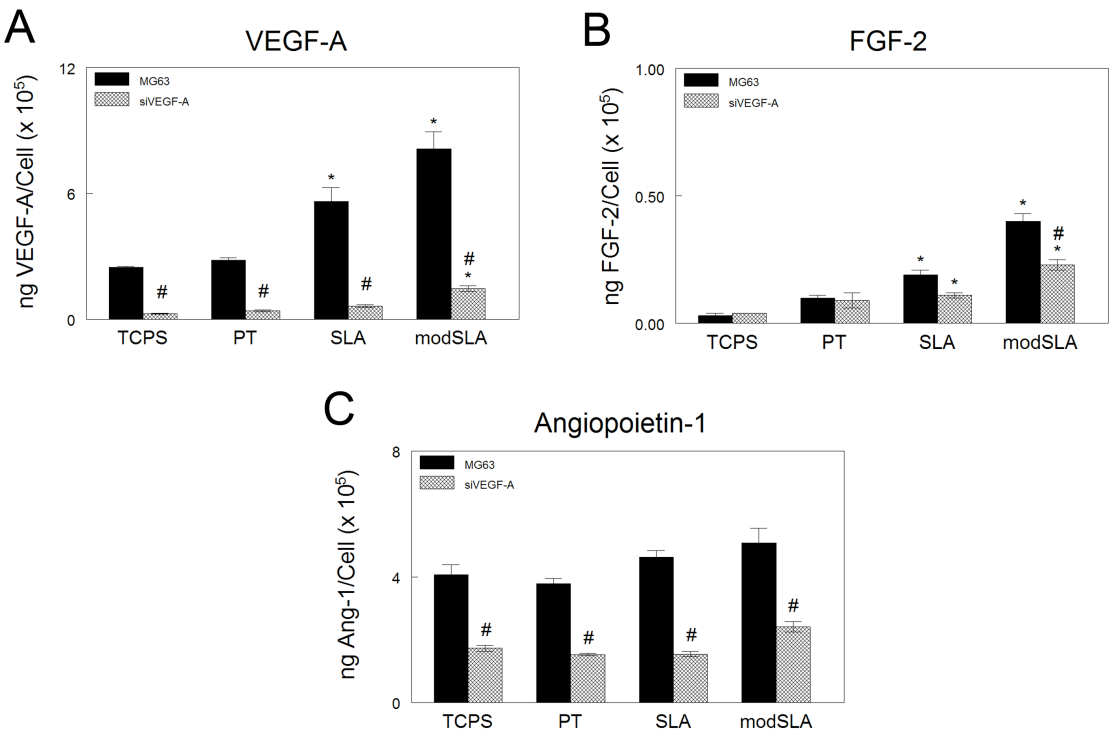

Figure 4-5. Angiogenic response of MG63 cells and VEGF-A silenced MG63 cells cultured on TCPS and Ti substrates. (A) VEGF-A, (B) FGF-2, and (C) angiopoietin-1 levels in the conditioned media. Cells were cultured on control (TCPS), PT, SLA, and modSLA Ti surfaces. Values presented are mean ± SEM of six independent cultures. The data presented are from one of two separate experiments with comparable results. Data were analyzed using ANOVA and statistical significance between groups was determined using Bonferroni's modification of Student's t-test. *$p<0.05$ vs. TCPS ; #$p<0.05$ vs. MG63.

4.3.3 Endothelial cell differentiation

Conditioned media from MG63 cell cultures and VEGF-A silenced MG63 cell cultures were used to assess endothelial cell tubule formation in a fibrin gel assay. At 12, 24, and 36 hours after the addition of conditioned media, total endothelial tube length were increased on SLA and modSLA surfaces compared to TCPS and smooth PT surfaces in MG63 cells. However, in VEGF-A silenced cell cultures, no increase in endothelial tubule formation was observed in response to surface roughness or energy (Figure 4-6A,B). Further, 36 hours after the addition of conditioned media, the total endothelial tubule length in cells treated with media from VEGF-A silenced MG63 cell cultures compared to cells treated with media from MG63 cells were significantly reduced on all surfaces (Figure 4-6C).

4.3.4 rhVEGF-A treatment

To see if the response of VEGF-A silenced MG63 cells to Ti surface microtopography and energy could be restored, we treated MG63 cells and VEGF-A silenced MG63 cells with 20 ng/mL rhVEGF-A_{165}. Total cell number was reduced in response to surface topography and energy for all groups. Treatment with rhVEGF-A_{165} had no effect on cell number in either MG63 cells or VEGF-A silenced MG63 cells compared to untreated controls (Figure 4-7A). Alkaline phosphatase specific activity in MG63 cells were increased only on modSLA surfaces. Treatment of MG63 cells with rhVEGF-A_{165} had no effect on alkaline phosphatase specific activity in response to either surface topography or energy and was unchanged compared to untreated MG63 cells. In VEGF-A silenced MG63 cells and in VEGF-A silenced MG63 cells treated with rhVEGF-A_{165}, alkaline phosphatase specific activity was significantly reduced on all surfaces examined relative to MG63 cell cultures (Figure 4-7B).

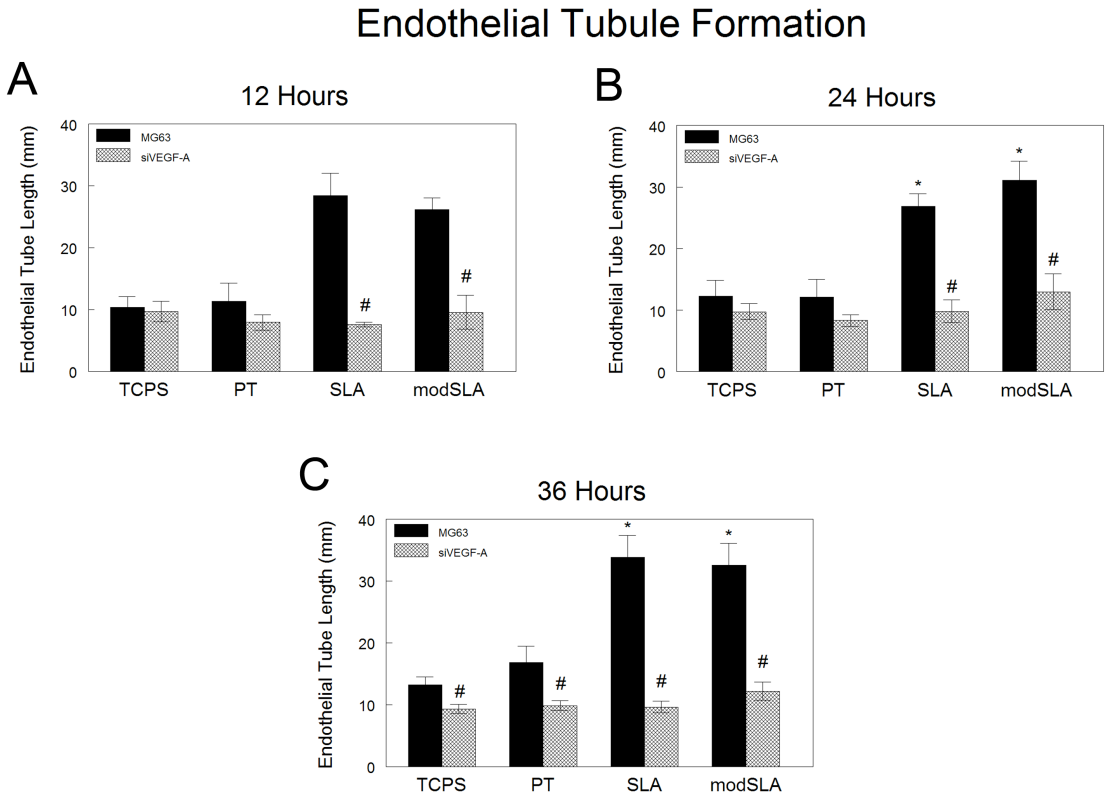

Figure 4-6. Endothelial tubule formation in response to VEGF-A silenced cell cultures. Media from MG63 cell cultures and VEGF-A silenced cell cultures on control (TCPS), PT, SLA, and modSLA Ti substrates were used to assess endothelial cell differentiation using a fibrin gel endothelial tubule formation assay. Total endothelial cell tube length was determined morphometrically at (A) 12 hours, (B) 24 hours, and (C) 36 hours after seeding of endothelial cells onto fibrin gel coated 96-well plates in the presence of conditioned media. *$p<0.05$ vs. TCPS; #$p<0.05$ vs. MG63.

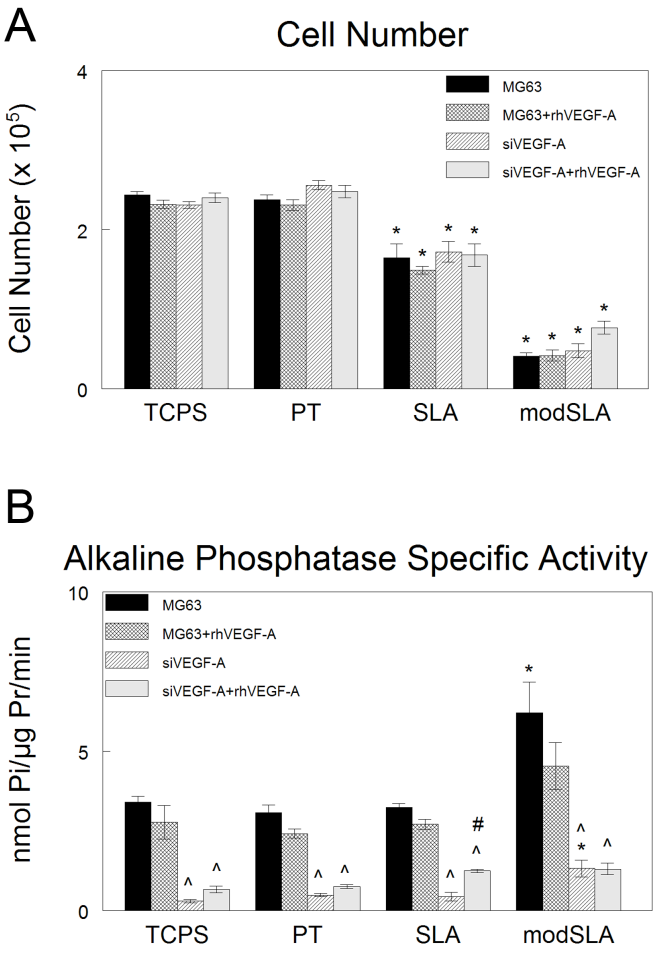

Figure 4-7. MG63 and VEGF-A silenced cell response to treatment with exogenous rhVEGF-A165. (A) Cell number and (B) alkaline phosphatase specific activity in the cell lysate was determined for both MG63 and VEGF-A silenced MG63 cells as well as MG63 and VEGF-A silenced MG63 cells treated with 20 ng/mL of rhVEGF-A165. Values presented are mean ± SEM of six independent cultures. Data were analyzed using ANOVA and statistical significance between groups was determined using Bonferroni's modification of Student's t-test. *$p<0.05$ vs. TCPS; ^$p<0.05$ vs. MG63; #$p<0.05$ vs. no rhVEGF-A treatment.

Osteocalcin and osteoprotegerin levels were similar on control TCPS and smooth PT surfaces in MG63 cells. On microrough SLA and hydrophilic, microrough modSLA surfaces, levels of both osteocalcin and osteprotegerin were significantly increased against control TCPS cultures (Figure 4-8A,B). Similar to our earlier results, levels of osteocalcin and osteoprotegerin in VEGF-A silenced MG63 cell cultures displayed a surface roughness and energy dependent increase but were significantly reduced compared to MG63 cell cultures on all surfaces examined. Treatment of VEGF-A silenced MG63 cells with rhVEGF-A165 increased osteocalcin levels to those comparable to MG63 cell cultures on all substrates. However, levels of osteoprotegerin were only increased in rhVEGF-A165 treated VEGF-A silenced cells on modSLA surfaces (Figure 4-8A,B).

Treatment of MG63 cells and VEGF-A silenced MG63 cells with rhVEGF-A had an effect on the production of angiogenic growth factors in response to surface topography and energy. Secreted levels of FGF-2 were similar amongst all groups on TCPS, PT, and SLA surfaces. The combination of a rough surface microtopgraphy and high surface free energy observed on modSLA surfaces increased FGF-2 production in MG63 cells. Treatment of MG63 cells with rhVEGF-A displayed a further, modest increase in FGF-2 production compared to untreated cells, though this increase was not statistically significant (Figurre 4-9A). In VEGF-A silenced MG63 cells, FGF-2 production was significantly reduced compared to MG63 cells and treatment with rhVEGF-A165 increased FGF-2 production to levels comparable to wild-type MG63 cell cultures (Figure 4-9A). Ang-1 levels were unchanged in response to surface microtopgraphy and surface energy in both MG63 cells and VEGF-A silenced MG63 cells, though levels in VEGF-A silenced MG63 cells were significantly reduced. Treatment with rhVEGF-A165 had no effect on Ang-1 production in response to surface

topography. However, on modSLA surfaces, levels of Ang-1 in both MG63 cells and VEGF-A silenced MG63 cells were significantly increased compared to control TCPS cultures. In addition, levels of Ang-1 in rhVEGF-A165 treated VEGF-A silenced MG63 cells were comparable to those observed in wild-typeMG63 cells (Figure 4-9B).

4.3.5 rhFGF-2 treatment

Since endogenous knockdown of VEGF-A in MG63 cells resulted in a decrease in the production of FGF-2 in response to Ti surface microtopography and energy, we treated VEGF-A silenced MG63 cells with exogenous rhFGF-2 to see if FGF-2 was mediating MG63 cell response to Ti surface properties. In MG63 cells, treatment with 10 ng/mL rhFGF-2 resulted in a significant increase in total cell number at time of harvest against untreated MG63 cells on all surfaces examined (Figure 4-10A). On control TCPS surfaces, VEGF-A silenced MG63 cells treated with rhFGF-2 displayed an increase in cell number compared to untreated VEGF-A silenced MG63 cells. However, treatment with rhFGF-2 did not have any effect on cell number in response to Ti surface topography or energy (Figure 4-10A). In both MG63 cells and VEGF-A silenced MG63 cells, alkaline phosphatase specific activity were increased compared to untreated control cells on control TCPS, smooth PT and SLA Ti surfaces. Further, an increase in alkaline phosphatase specific activity in response to rhFGF-2 treatment was seen on microrough, hydrophilic modSLA Ti surfaces in MG63 cell cultures but not in VEGF-A silenced MG63 cell cultures. In all cell types examined, surface topography and energy had no effect on alkaline phosphatase specific activity (Figure 4-10B).

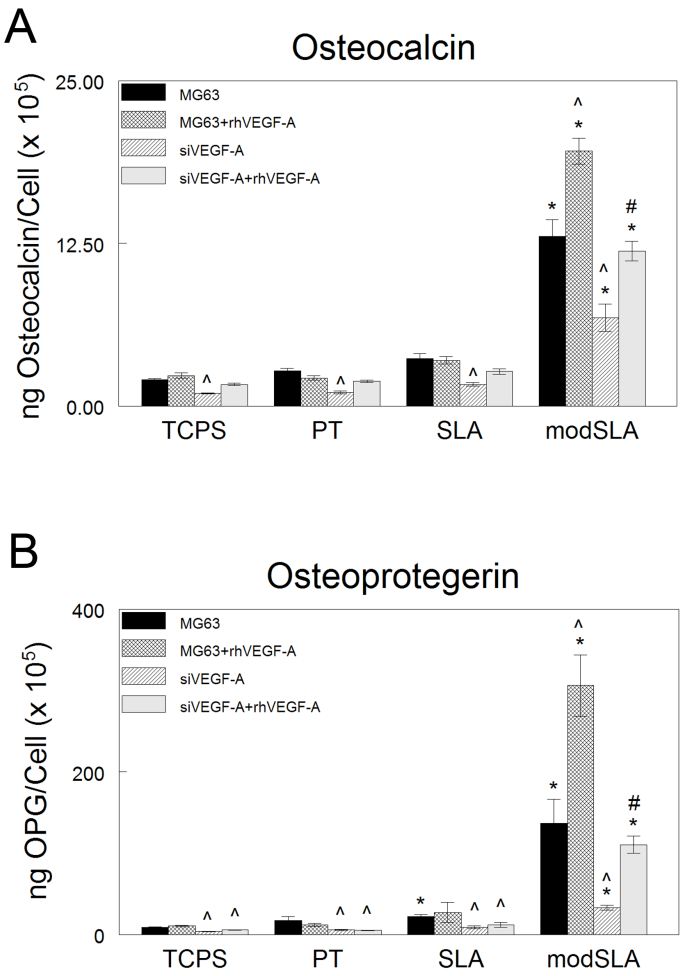

Figure 4-8. MG63 and VEGF-A silenced cell response to treatment with exogenous rhVEGF-A 165. (A) Osteocalcin and (B) osteoprotegerin levels in the conditioned media were determined for both MG63 and VEGF-A silenced MG63 cells as well as MG63 and VEGF-A silenced MG63 cells treated with 20 ng/mL of rhVEGF-A165. Values presented are mean ± SEM of six independent cultures. Data were analyzed using ANOVA and statistical significance between groups was determined using Bonferroni's modification of Student's t-test. *$p<0.05$ vs. TCPS; ^$p<0.05$ vs. MG63; #$p<0.05$ vs. no rhVEGF-A treatment.

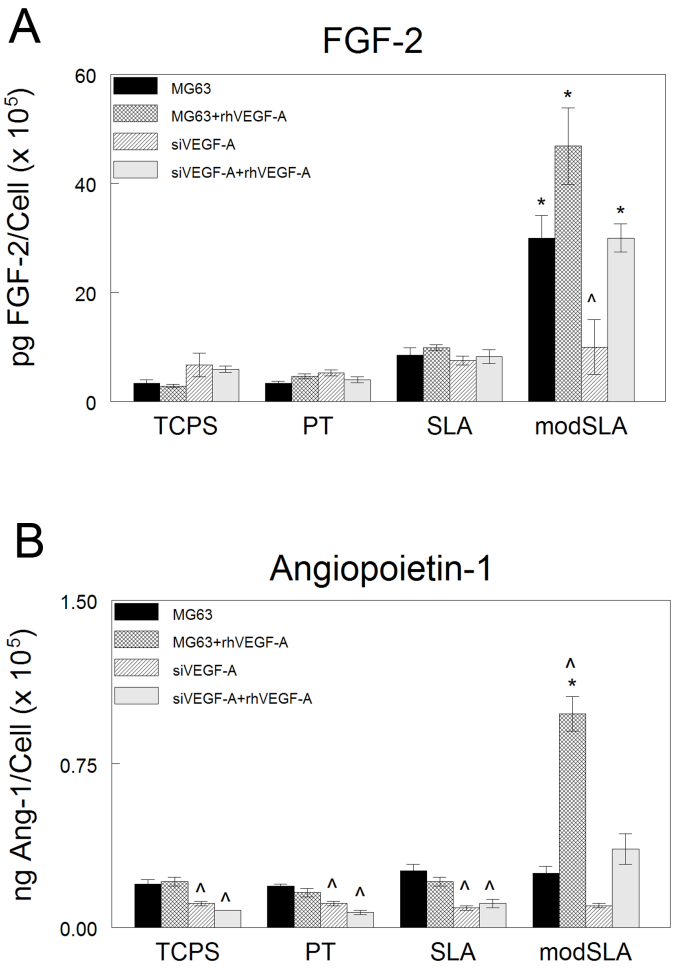

Figure 4-9. MG63 and VEGF-A silenced cell response to treatment with exogenous rhVEGF-A 165. (A) FGF-2 and (B) angiopoietin-1 levels in the conditioned media were determined for both MG63 and VEGF-A silenced MG63 cells as well as MG63 and VEGF-A silenced MG63 cells treated with 20 ng/mL of rhVEGF-A165. Values presented are mean $\pm$ SEM of six independent cultures. Data were analyzed using ANOVA and statistical significance between groups was determined using Bonferroni's modification of Student's t-test. *$p<0.05$ vs. TCPS; ^$p<0.05$ vs. MG63; #$p<0.05$ vs. no rhVEGF-A treatment.

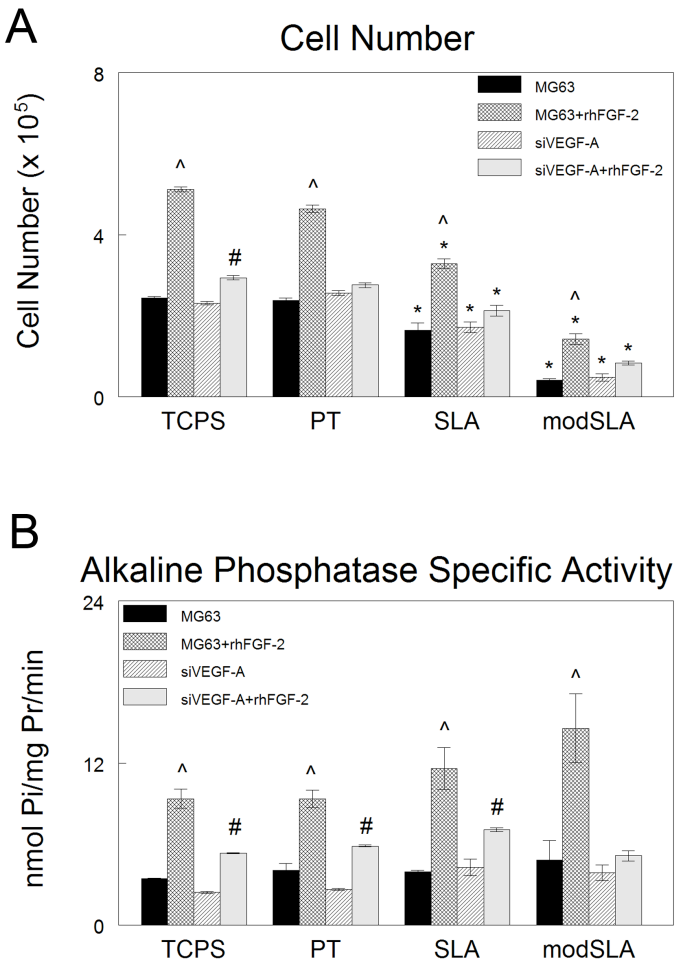

Figure 4-10. MG63 and VEGF-A silenced cell response to treatment with exogenous rhFGF-2. (A) Cell number and (B) alkaline phosphatase specific activity in the cell lysate was determined for both MG63 and VEGF-A silenced cells treated with or without 10 ng/mL rhFGF-2. Values presented are mean ± SEM of six independent cultures. Data were analyzed using ANOVA and statistical significance between groups was determined using Bonferroni's modification of Student's t-test. *$p<0.05$ vs. TCPS; ^$p<0.05$ vs. MG63; #$p<0.05$ vs. no rhFGF-2 treatment.

We next examined whether treatment with rhFGF-2 had an effect on osteoblast phenotype in response to Ti surface topography and energy. Similar to our earlier results, both MG63 cells and VEGF-A silenced MG63 cells displayed a surface roughness and energy dependent increase in osteocalcin and osteoprotegerin production, though production of these growth factors were reduced by at least 50% in VEGF-A silenced MG63 cell cultures on all surfaces (Figure 4-11A,B). Treatment with rhFGF-2 had no effect on the production of either osteocalcin or osteoprotegerin in either cell type on any surface examined (Figure 4-11A,B).

VEGF-A levels in MG63 cells were increased in a surface roughness and energy dependent manner and treatment with 10 ng/mL rhFGF-2 did not have any effect on production of VEGF-A in these cells. In VEGF-A silenced cells, secreted levels of VEGF-A were reduced by at least 60% compared to MG63 wild-type cells on all surfaces and rhFGF-2 treatment did not effect secretion of this growth factor (Figure 4-12A). For both cell types, Ang-1 production was unaffected by either surface roughness or energy, though levels in VEGF-A silenced MG63 cells were significantly reduced compared to MG63 cells and rhFGF-2 treatment also had no effect on secretion of this growth factor (Figure 4-12B).

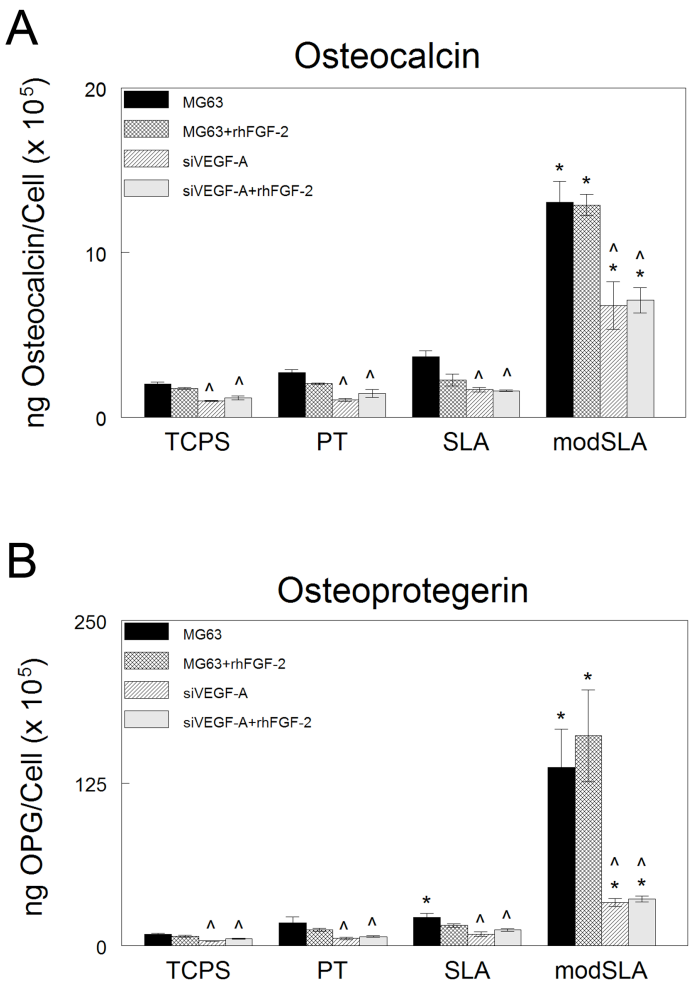

Figure 4-11. MG63 and VEGF-A silenced cell response to treatment with exogenous rhFGF-2. (A) Osteocalcin and (B) osteoprotegerin levels in the conditioned media were determined for both MG63 and VEGF-A silenced MG63 cells as well as MG63 and VEGF-A silenced MG63 cells treated with 10 ng/mL of rhFGF-2. Values presented are mean $\pm$ SEM of six independent cultures. Data were analyzed using ANOVA and statistical significance between groups was determined using Bonferroni's modification of Student's t-test. *$p<0.05$ vs. TCPS; ^$p<0.05$ vs. MG63; #$p<0.05$ vs. no rhFGF-2 treatment.

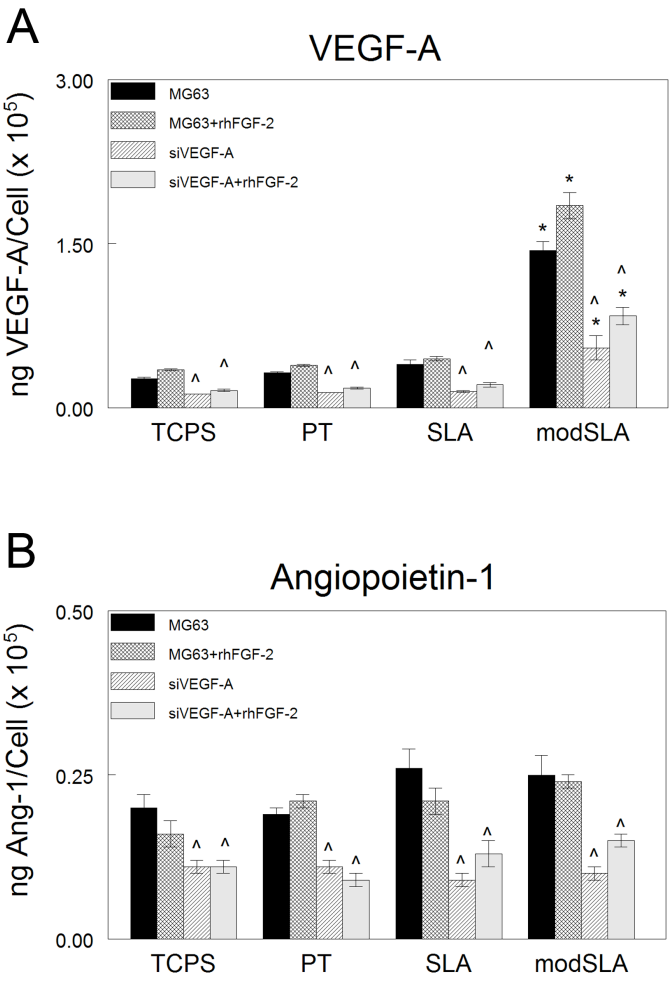

Figure 4-12. MG63 and VEGF-A silenced cell response to treatment with exogenous rhVEGF-A 165. (A) FGF-2 and (B) angiopoietin-1 levels in the conditioned media were determined for both MG63 and VEGF-A silenced MG63 cells as well as MG63 and VEGF-A silenced MG63 cells treated with 10 ng/mL of rhFGF-2. Values presented are mean $\pm$ SEM of six independent cultures. Data were analyzed using ANOVA and statistical significance between groups was determined using Bonferroni's modification of Student's t-test. *$p<0.05$ vs. TCPS; ^$p<0.05$ vs. MG63; #$p<0.05$ vs. no rhFGF-2 treatment.

4.4 Discussion

Osseointegration of orthopaedic and dental implants is dependent not only on direct apposition of bone to the implant surface, but also on the formation of a patent vasculature in the peri-implant space to allow delivery of oxygen, nutrients, and cells. Osteoblasts are known to secrete VEGF-A, a potent endothelial cell mitogen, in response to a number of different stimuli, including hypoxia and several growth factors and hormones [31-34]. VEGF-A has also been found to have a direct role in osteoblast differentiation and maturation [19, 26, 27]. In the present study we show that VEGF-A also has a direct effect on osteoblast-like cell differentiation in response to Ti surface roughness and energy.

Secreted levels of osteocalcin and osteoprotegerin, later markers of osteoblast differentiation, as well as levels of VEGF-A and FGF-2, two pro-angiogenic growth factors were increased by MG63 cells on microrough SLA and microrough, high surface energy modSLA Ti substrates compared to TCPS and smooth PT Ti substrates, while levels of Ang-1 were unaffected by either Ti substrate roughness or energy, consistent with earlier findings [22, 23, 35]. However, in VEGF-A silenced MG63 cell cultures, secretion of these growth factors were reduced compared to wild-type cells. These data suggest that VEGF-A has an autocrine role in mediating osteoblast-like cell differentiation on Ti substrates *in vitro*.

Addition of VEGF to fetal bovine osteoblasts increased migration and alkaline phosphatase expression, but had no effect on proliferation [36], while exogenous VEGF-A_{165} treatment of primary human osteoblasts increased alkaline phosphatase activity and mineralized nodule formation [27]. Our results here show that VEGF-A can enhance osteoblast differentiation in response to Ti surface microtopography and energy. Addition of 20 ng/mL rhVEGF-A_{165} to MG63 cells increased levels of osteocalcin and

osteoprotegerin as well as levels of Ang-1 and FGF-2 on microrough, high surface energy modSLA surfaces, but had no effect on either cell number or alkaline phosphatase specific activity. Further, in MG63 cells that have been permanently silenced for expression of VEGF-A, addition of exogenous VEGF-A increased secreted levels of osteocalcin, osteoprotegerin, FGF-2, and Ang-1 to those observed in wild-type MG63 cell cultures on modSLA Ti surfaces, further supporting the hypothesis that interaction of VEGF-A with its receptors is necessary for osteoblast maturation.

VEGF-A exerts its effects through binding to two receptor tyrosine kinases, VEGFR1 (Flt1) and VEGFR2 (Flk1/KDR) that are expressed by not only endothelial cells, but also chondrocytes, osteoblasts, and osteoclasts [37, 38]. In endothelial cells, VEGFR2 is recognized as the primary mediator of the mitogenic effects of VEGF-A during neo-vascularization. Upon binding, VEGFR2 dimerizes and undergoes strong autophosphorylation, inducing the downstream phosphorylation of multiple proteins in endothelial cells, including phospholipase C-γ, PI-3 kinase, Ras, and members of the Src family [39, 40]. However, a possible role for both VEGFR1 and VEGFR2 has been implicated in bone growth and development.

In Flt1 (VEGFR1) null mice, trabecular bone volume and bone formation rate were reduced *in vivo* and bone marrow stromal cell cultures from Flt1 null mice exhibited decreased mineralization *in vitro* compared to wild-type animals [41]. Interaction of VEGF-A with Flk1 (VEGFR2) has been demonstrated in primary human osteoblasts, and prostanoid mediated upregulation of VEGF-A by these cells is inhibited by treatment with a VEGFR tyrosine kinase inhibitor [28]. It has also been found that VEGF-A increases bone mass through an Flk1 and PI-3 kinase mediated pathway [26].

In our study, we found that addition of a neutralizing antibody specific for Flk1 (VEGFR2) did not have any effect on the production of osteocalcin, osteoprotegerin,

FGF-2 or Ang-1 in MG63 cells in response to Ti substrate features. However, VEGF-A production in response to treatment with an Flk1 antibody was significantly increased. It may be possible that VEGF-A interaction with Flk1 in MG63 cells is necessary for maturation of these cells and to overcome the effect of the neutralization antibody, production of VEGF-A was increased.

FGF-2 has also been reported to be a modulator of bone formation *in vitro* and *in vivo* [42, 43]. In our study, we found that treatment of MG63 cells with 10 ng/mL rhFGF-2 increased cell number and alkaline phosphatase specific activity but had no effect on the production of either osteogenic or angiogenic markers. FGF-2 has also been found to induce proliferation of human mesenchymal progenitor cells and MC3T3-E1 cells [44, 45]. Moreover, treatment of mineralized MC3T3-E1 cultures with FGF-2 reduced the expression of collagen I, BMP-2, and osteocalcin [44]. In VEGF-A silenced cells, addition of rhFGF-2 did not increase cell number to the same extent as seen in MG63 wild-type cell cultures, but did increase alkaline phosphatase specific activity compared to untreated VEGF-A silenced cells. However, no increase in the production of osteogenic or angiogenic markers by VEGF-A silenced cells were observed in response to FGF-2 treatment. Taken together, these results indicate that VEGF-A, but not FGF-2 is necessary for osteoblast differentiation.

Alkaline phosphatase activity in osteoblast-like cells is highly dependent on the state of maturation of the cells at the time of assay. In early osteoblast differentiation, alkaline phosophatase activity increases until the onset of mineralization, at which time its activity decreases, and osteocalcin production is increased [46]. This biphasic curve for alkaline phosphatase acitivity during osteoblast maturation may explain observed differences in alkaline phosphatase specific activity in response to Ti substrate features seen in this study compared to other studies.

In conclusion, we show here that VEGF-A produced by osteoblast-like cells in response to Ti substrate features has an autocrine effect on the differentiation of these cells. shRNA targeted knockdown of VEGF-A resulted in a reduction in secreted levels of osteocalcin, osteoprotegerin, FGF-2, and Ang-1, while treatment with exogenous VEGF-A increased secreted levels of these markers. FGF-2 increased cell number and alkaline phosphatase, but had no effect on the production of osteogenic or angiogenic markers. Taken together, these results indicate that VEGF-A, but not FGF-2 plays an important role in the differentiation of osteoblasts on Ti substrates.

4.5 References

1. Howlett CR, Evans MD, Walsh WR, Johnson G, Steele JG. Mechanism of initial attachment of cells derived from human bone to commonly used prosthetic materials during cell culture. Biomaterials 1994 Feb;15(3):213-222.

2. Meyer AE, Baier RE, Natiella JR, Meenaghan MA. Investigation of tissue/implant interactions during the first two hours of implantation. J Oral Implantol 1988;14(3): 363-379.

3. Pankowsky DA, Ziats NP, Topham NS, Ratnoff OD, Anderson JM. Morphologic characteristics of adsorbed human plasma proteins on vascular grafts and biomaterials. J Vasc Surg 1990 Apr;11(4):599-606.

4. Pearson BS, Klebe RJ, Boyan BD, Moskowicz D. Comments on the clinical application of fibronectin in dentistry. J Dent Res 1988 Feb;67(2):515-517.

5. Terranova VP, Aumailley M, Sultan LH, Martin GR, Kleinman HK. Regulation of cell attachment and cell number by fibronectin and laminin. J Cell Physiol 1986 Jun;127 (3):473-479.

6. Goto T, Yoshinari M, Kobayashi S, Tanaka T. The initial attachment and subsequent behavior of osteoblastic cells and oral epithelial cells on titanium. Biomed Mater Eng 2004;14(4):537-544.

7. Boyan BD, Lossdorfer S, Wang L, Zhao G, Lohmann CH, Cochran DL, et al. Osteoblasts generate an osteogenic microenvironment when grown on surfaces with rough microtopographies. Eur Cell Mater 2003 Oct 24;6:22-27.

8. Zhao G, Schwartz Z, Wieland M, Rupp F, Geis-Gerstorfer J, Cochran DL, et al. High surface energy enhances cell response to titanium substrate microstructure. J Biomed Mater Res A 2005 Jul 1;74(1):49-58.

9. Schwartz Z, Nasazky E, Boyan BD. Surface microtopography regulates osteointegration: the role of implant surface microtopography in osteointegration. Alpha Omegan 2005 Jul;98(2):9-19.

10. Schwartz Z, Raz P, Zhao G, Barak Y, Tauber M, Yao H, et al. Effect of micrometer-scale roughness of the surface of Ti6Al4V pedicle screws in vitro and in vivo. J Bone Joint Surg Am 2008 Nov;90(11):2485-2498.

11. Collin-Osdoby P. Role of vascular endothelial cells in bone biology. J Cell Biochem 1994 Jul;55(3):304-309.

12. Brown RA, Rees JA, McFarland CD, Lewinson D, Ali SY. Microvascular invasion of rabbit growth plate cartilage and the influence of dexamethasone. Bone Miner 1990 Apr;9(1):35-47.

13. Gerber HP, Ferrara N. Angiogenesis and bone growth. Trends Cardiovasc Med 2000 Jul;10(5):223-228.

14. Shapiro IM, Boyde A. Mineralization of normal and rachitic chick growth cartilage: vascular canals, cartilage calcification and osteogenesis. Scanning Microsc 1987 Jun;1 (2):599-606.

15. Abshagen K, Schrodi I, Gerber T, Vollmar B. In vivo analysis of biocompatibility and vascularization of the synthetic bone grafting substitute NanoBone(R). J Biomed Mater Res A 2008 Nov 4.

16. Brandi ML, Collin-Osdoby P. Vascular biology and the skeleton. J Bone Miner Res 2006 Feb;21(2):183-192.

17. Deckers MM, Karperien M, van der Bent C, Yamashita T, Papapoulos SE, Lowik CW. Expression of vascular endothelial growth factors and their receptors during osteoblast differentiation. Endocrinology 2000 May;141(5):1667-1674.

18. Kasama T, Isozaki T, Odai T, Matsunawa M, Wakabayashi K, Takeuchi HT, et al. Expression of angiopoietin-1 in osteoblasts and its inhibition by tumor necrosis factor-alpha and interferon-gamma. Transl Res 2007 May;149(5):265-273.

19. Mayer H, Bertram H, Lindenmaier W, Korff T, Weber H, Weich H. Vascular endothelial growth factor (VEGF-A) expression in human mesenchymal stem cells: autocrine and paracrine role on osteoblastic and endothelial differentiation. J Cell Biochem 2005 Jul 1;95(4):827-839.

20. Sabbieti MG, Agas D, Xiao L, Marchetti L, Coffin JD, Doetschman T, et al. Endogenous FGF-2 is critically important in PTH anabolic effects on bone. J Cell Physiol 2009 Apr;219(1):143-151.

21. Olivares-Navarrete R, Hyzy SL, Hutton DL, Erdman CP, Wieland M, Boyan BD, et al. Direct and indirect effects of microstructured titanium substrates on the induction of mesenchymal stem cell differentiation towards the osteoblast lineage. Biomaterials Apr; 31(10):2728-2735.

22. Raines AL, Olivares-Navarrete R, Wieland M, Cochran DL, Schwartz Z, Boyan BD. Regulation of angiogenesis during osseointegration by titanium surface microstructure and energy. Biomaterials Jun;31(18):4909-4917.

23. Rausch-fan X, Qu Z, Wieland M, Matejka M, Schedle A. Differentiation and cytokine synthesis of human alveolar osteoblasts compared to osteoblast-like cells (MG63) in response to titanium surfaces. Dent Mater 2008 Jan;24(1):102-110.

24. Ferrara N, Gerber HP, LeCouter J. The biology of VEGF and its receptors. Nat Med 2003 Jun;9(6):669-676.

25. Neufeld G, Cohen T, Gengrinovitch S, Poltorak Z. Vascular endothelial growth factor (VEGF) and its receptors. FASEB J 1999 Jan;13(1):9-22.

26. Maes C, Goossens S, Bartunkova S, Drogat B, Coenegrachts L, Stockmans I, et al. Increased skeletal VEGF enhances beta-catenin activity and results in excessively ossified bones. EMBO J Jan 20;29(2):424-441.

27. Street J, Lenehan B. Vascular endothelial growth factor regulates osteoblast survival - evidence for an autocrine feedback mechanism. J Orthop Surg Res 2009;4:19.

28. Clarkin CE, Emery RJ, Pitsillides AA, Wheeler-Jones CP. Evaluation of VEGF-mediated signaling in primary human cells reveals a paracrine action for VEGF in osteoblast-mediated crosstalk to endothelial cells. J Cell Physiol 2008 Feb;214(2): 537-544.

29. Uchida S, Sakai A, Kudo H, Otomo H, Watanuki M, Tanaka M, et al. Vascular endothelial growth factor is expressed along with its receptors during the healing

process of bone and bone marrow after drill-hole injury in rats. Bone 2003 May;32(5): 491-501.

30. Rupp F, Scheideler L, Olshanska N, de Wild M, Wieland M, Geis-Gerstorfer J. Enhancing surface free energy and hydrophilicity through chemical modification of microstructured titanium implant surfaces. J Biomed Mater Res A 2006 Feb;76(2): 323-334.

31. Goad DL, Rubin J, Wang H, Tashjian AH, Jr., Patterson C. Enhanced expression of vascular endothelial growth factor in human SaOS-2 osteoblast-like cells and murine osteoblasts induced by insulin-like growth factor I. Endocrinology 1996 Jun;137(6): 2262-2268.

32. Harada S, Nagy JA, Sullivan KA, Thomas KA, Endo N, Rodan GA, et al. Induction of vascular endothelial growth factor expression by prostaglandin E2 and E1 in osteoblasts. J Clin Invest 1994 Jun;93(6):2490-2496.

33. Schlaeppi JM, Gutzwiller S, Finkenzeller G, Fournier B. 1,25-Dihydroxyvitamin D3 induces the expression of vascular endothelial growth factor in osteoblastic cells. Endocr Res 1997 Aug;23(3):213-229.

34. Steinbrech DS, Mehrara BJ, Saadeh PB, Greenwald JA, Spector JA, Gittes GK, et al. VEGF expression in an osteoblast-like cell line is regulated by a hypoxia response mechanism. Am J Physiol Cell Physiol 2000 Apr;278(4):C853-860.

35. Gittens RA, McLachlan T, Olivares-Navarrete R, Cai Y, Berner S, Tannenbaum R, et al. The effects of combined micron-/submicron-scale surface roughness and nanoscale features on cell proliferation and differentiation. Biomaterials May;32(13): 3395-3403.

36. Midy V, Plouet J. Vasculotropin/vascular endothelial growth factor induces differentiation in cultured osteoblasts. Biochem Biophys Res Commun 1994 Feb 28;199 (1):380-386.

37. Dai J, Rabie AB. VEGF: an essential mediator of both angiogenesis and endochondral ossification. J Dent Res 2007 Oct;86(10):937-950.

38. Maes C, Carmeliet G. Vascular and nonvascular roles of VEGF in bone development. In: Ruhrberg C, editor. VEGF in Development. Austin: Springer, 2008. p. 79-90.

39. Eliceiri BP, Paul R, Schwartzberg PL, Hood JD, Leng J, Cheresh DA. Selective requirement for Src kinases during VEGF-induced angiogenesis and vascular permeability. Mol Cell 1999 Dec;4(6):915-924.

40. Guo D, Jia Q, Song HY, Warren RS, Donner DB. Vascular endothelial cell growth factor promotes tyrosine phosphorylation of mediators of signal transduction that contain SH2 domains. Association with endothelial cell proliferation. J Biol Chem 1995 Mar 24;270(12):6729-6733.

41. Otomo H, Sakai A, Uchida S, Tanaka S, Watanuki M, Moriwaki S, et al. Flt-1 tyrosine kinase-deficient homozygous mice result in decreased trabecular bone volume with reduced osteogenic potential. Bone 2007 Jun;40(6):1494-1501.

42. Canalis E, McCarthy TL, Centrella M. Growth factors and cytokines in bone cell metabolism. Annu Rev Med 1991;42:17-24.

43. Montero A, Okada Y, Tomita M, Ito M, Tsurukami H, Nakamura T, et al. Disruption of the fibroblast growth factor-2 gene results in decreased bone mass and bone formation. J Clin Invest 2000 Apr;105(8):1085-1093.

44. Hughes-Fulford M, Li CF. The role of FGF-2 and BMP-2 in regulation of gene induction, cell proliferation and mineralization. J Orthop Surg Res;6(1):8.

45. Ou G, Charles L, Matton S, Rodner C, Hurley M, Kuhn L, et al. Fibroblast growth factor-2 stimulates the proliferation of mesenchyme-derived progenitor cells from aging mouse and human bone. J Gerontol A Biol Sci Med Sci Oct;65(10):1051-1059.

46. Lian JB, Stein GS. Concepts of osteoblast growth and differentiation: basis for modulation of bone cell development and tissue formation. Crit Rev Oral Biol Med 1992;3(3):269-305.

Chapter 5: Hyaluronic Acid Stimulates Neovascularization During the Regeneration of Bone Marrow After Ablation

5.1 Introduction

A common objective when using biomedical implants, particularly in musculoskeletal tissues, is rapid apposition of host tissue to the implant surface. Currently, several regenerative medicine therapies exist for the restoration and augmentation of bone in orthopaedic and dental applications, including autologous and allogeneic bone grafts as well as synthetic bone graft substitutes. While autologous bone is still the "gold standard" within the field due to its biocompatibility as well as its source of stem cells and growth factors[1, 2], allografts and synthetic bone substitutes also provide an osteoconductive surface to promote bone growth. A critical requirement for the survival of any bone graft is the rapid ingrowth of blood vessels from the surrounding tissue[3].

Hyaluronic acid is a high molecular weight (10^4 – 10^7 Da), negatively charged, non-sulfated glycosaminoglycan consisting of repeating units of *N*-acetylglucosamine and D-glucuronic acid[4]. It is a component of the extracellular matrix (ECM) expressed in nearly all tissue types[4] and plays an important role in tissue morphogenesis and healing[5, 6]. During wound healing, native hyaluronic acid serves as an anti-angiogenic molecule, inhibiting endothelial cell proliferation and migration[7]. These observations have lead to the use of the sodium salt of hyaluronic acid (NaHY) in a number of wound healing applications[8]. Although NaHY inhibits capillary formation in a three dimensional collagen gel[7, 9], low molecular weight degradation products of NaHY have

been demonstrated to stimulate vascular endothelial cell proliferation[10-14], migration [15], collagen synthesis[16], sprout formation[17], and new blood vessel formation[18].

Allogeneic bone graft substitutes like demineralized bone matrix (DBM) are used as filler materials to enhance the healing of fractures and to help regenerate bone in osseous defects[19]. Because the particulate, powdery nature of DBM results in poor handling qualities, it is often combined with materials to improve its handling characteristics for surgical procedures[19, 20]. Commonly used materials for this process include NaHY, calcium sulfate, glycerol, and gelatin[19]. The combination of DBM with these materials creates a more gelatinous substance, allowing for easier insertion and molding into osseous defect sites. DBM is known to promote bone formation by virtue of its osteoinductive and osteoconductive properties, but whether NaHY can also stimulate bone formation when used as a cofactor with DBM is not known. NaHY has also been reported to accelerate bone healing[21]. The exact mechanism by which NaHY promotes bone healing is unknown, but one possibility is that it increases neovascularization in the newly forming bone. NaHY has already been shown to promote neovascularization in non-bony sites[22] and is being investigated for use as a scaffold material for angiogenic tissue engineering[23], supporting this hypothesis.

The purpose of the present study was to determine if NaHY stimulates neovascularization during bone formation induced by DBM. The study took advantage of the rapid endosteal bone formation that occurs following injury to the marrow cavity of rat tibial bone[24]. The rat bone marrow ablation model is an established model for examining bone formation and remodeling[25]. It has been well characterized in a number of academic laboratories and it is used by industry to assess osteogenic properties of biomaterials as well as pharmaceuticals[26, 27]. The model is also

applicable for assessing endosteal bone formation and remodeling in orthopaedics following placement of intramedullary rods and joint prostheses[28]. In this model, the bone marrows of rat tibias are flushed of cells. A blood clot and granulation tissue fill the marrow space over the first three days of healing. Primary bone begins to form on the endosteal surface by day 6 and eventually fills the marrow cavity. Remodeling of the newly formed bone occurs between days 12 and 25, resulting in resorption of the primary bone. By day 35 post-ablation, replacement of the primary bone with bone marrow is complete, resulting in the regeneration of normal tissue phenotype[29]. This process follows a well-documented time table[25, 30], which makes it a very useful model for the study of normal bone repair and for the evaluation of extrinsic and intrinsic factors that may influence it. The enclosed environment of the marrow space restricts the distribution of test materials and localizes their effects, thus allowing the model to be useful for the study of the effects of biomaterials that have been designed for bone augmentation.

In this study, neovascularization occurring within the ablated marrow cavity was assessed over time by perfusing the vasculature of rats with a radio-opaque silicone contrast agent and imaging the vasculature using micro-computed tomography (μCT). To determine the role of NaHY in stimulating neovascularization during endosteal bone formation, we placed various formulations of NaHY with and without DBM in the ablated marrow space of rats. Vascular morphology of the ablated limbs was assessed 14 days post-ablation using both μCT analysis as well as histology.

5.2 Materials & Methods

5.2.1 Materials

Implant materials were prepared by the Musculoskeletal Transplant Foundation (MTF, Edison, NJ) and packaged in sterile syringes. Materials were able to be extruded through an 18-gauge needle, which is the largest size able to fit into the hole created for the marrow ablation. The DBM used for the study was from a single donor and was shown to be osteoinductive in the mouse gastrocnemius muscle pouch assay. DBM particulates ranged in size from 212 to 500 μm in diameter.

5.2.2 Marrow Ablation

The Institutional Animal Care and Use Committee (IACUC) at the Georgia Institute of Technology approved all animal procedures. Either eight-week or 9-month old, male immunocompromised (rNu/rNu) rats were purchased from Harlan Laboratories (Harlan, Indianapolis, IN). Rats were anesthetized with isoflurane gas inhalation, laid on their backs and covered with a sterile surgical drape. The surgical area was shaved and disinfected with providone iodine. An incision was made over the diaphysis of the tibia and the surrounding muscles were moved aside using blunt dissection to expose the bone. A round perforation was made in the mid-diaphysis through the cortical bone using a 0.9mm round dental bur. Marrow was excavated with an inverted cone dental bur and the marrow space was then flushed with sterile, physiological saline.

A time course study was first performed to determine the time at which neovascularization was greatest. The marrow space was left empty, and the covering muscles were returned to their normal positions and the skin incision was closed with wound clips. Immediately after recovery from anesthesia, rats were injected with buprenorphine to relieve pain. Animals had access to food and water *ad libitum* for the duration of the study. At days 3, 6, 14, 21, and 28 post-ablation, animals (n = 3) were perfused-fixed and imaged as described below. Based on the results of the time course study, 14 days post-ablation was selected as the endpoint for the DBM + NaHY study.

To examine the role of NaHY in promoting neovascularization during endosteal bone formation, we ablated the marrow of eight-week old rat tibias and injected test compounds (v ~ 125 μL) corresponding to the groups outlined in Table 1. The left hind tibias of n = 9 animals were ablated for each group.

5.2.3 Vascular Perfusion

Following anesthetization, the abdominal cavity of rats was opened and the internal organs were moved aside. A 22-gauge 1" catheter was inserted into the descending aorta and the caudal vena cava was severed to allow for the vasculature to be flushed. 250μL of heparin (1000 units/mL) was injected into the catheter to prevent clotting of the blood. The vasculature was flushed with 0.9% normal saline using a peristaltic pump set to a flow rate of 15 mL/min. Specimens were subsequently pressure fixed with 10% neutral buffered formalin. Formalin was flushed from the vessels with 0.9% normal saline, and the vasculature was injected with a radio-opaque silicone rubber compound containing lead chromate (Microfil MV-122, Flow Tech, Inc., Carver, MA), according to the manufacturer's protocol. Animals were stored at 4^{o} C overnight to allow for contrast agent polymerization. Rat hind limbs were dissected from the specimens and soaked for 4 days in 10% neutral buffered formalin to ensure complete tissue fixation prior to μCT imaging.

5.2.4 μCT Image Analysis

Tissue samples were imaged using a high-resolution desktop micro-CT imaging system (vivaCT, Scanco Medical, Bassersdorf, Switzerland) as described by Duvall et al [31]. Briefly, samples were imaged using a 36 μm voxel size with a voltage of 55 kV and a current of 109 μA. Serial image sections were created in a 1024 x 1024 pixel image matrix. Serial tomograms were reconstructed from raw data using a cone beam filtered back-projection algorithm[32]. Noise was reduced using a low pass Gaussian filter

(sigma = 1.2, support = 2). The serial tomograms were globally thresholded based on x-ray attenuation and used to render binarized three dimensional (3D) volume images of the repair gap vascular network. The paramaters for three dimensional vascular morphology (vessel volume, number, connectivity, thickness, and spacing) were determined using the method by described in detail by Duvall et al[31] and were quantified with histomorphometric analysis based on direct distance transform methods [33, 34].

5.2.5 Histology

Following decalcification and μCT imaging, samples were embedded in paraffin, and sectioned along the sagittal plane. 5μm sections were stained with haematoxylin and eosin (H&E) to assess vascular structures. The number of blood vessels within the ablated marrow space was counted in four serial sections from each sample and the values were averaged to obtain the mean blood vessel number for each treatment group.

5.2.6 Statistical Analysis

Both μCT and histology data from each group were analyzed by ANOVA and when statistical differences were detected, Student's t-test for multiple comparisons using Bonferroni's modification was used. p-values < 0.05 were considered statistically significant.

Table 5-1. Demineralized bone matrix and hyaluronic acid experimental group formulations

Group #	Carrier	DBM	Comments
A	No Carrier	No DBM	Empty Defect
B	**Carrier I**: 3.8-4.0% solution of 700-800kD NaHY in PBS buffer pH 7.4	31%	Heat denatured DBM Negative control for test system
C	0.9% Saline	31%	No NaHY carrier, DBM baseline
D	**Carrier I**: 3.8-4.0% solution of 700-800kD NaHY in PBS buffer pH 7.4	31%	Represents commercial DBX® putty
E	**Carrier II**: 3.8-4.0% solution of 35kD NaHY in PBS buffer pH 7.4	31%	Low MW NaHY carrier with 31% DBM
F	**Carrier I** 50:50 **Carrier II** mixture	31%	Equal mixture of the two carriers with 31% DBM
G	**Carrier I**: 3.8-4.0% solution of 700-800kD NaHY in PBS buffer pH 7.4	0%	Carrier for commercial DBX putty, no DBM
H	**Carrier II**: 3.8-4.0% solution of 35kD NaHY in PBS buffer pH 7.4	0%	Low MW NaHY carrier only, no DBM
I	**Carrier I** 50:50 **Carrier II** mixture	0%	50:50 mixture of the two carriers only, no DBM

5.3 Results

Ablated, perfused tibias were imaged using μCT to examine the bone (Figure 1A) and surrounding vasculature (Figure 1B). Samples were subsequently incubated for 72 hours at 22°C in formic acid (CalEx II, Fisher Scientific, Pittsburgh, PA) to decalcify the bone and facilitate image segmentation of the vasculature both surrounding (Figure 1C) and within (Figure 1D) the ablated tibias. The region of interest (ROI) in 2-D serial sections for vascular morphology analysis was determined by using the 2-D sections of calcified images as a template for the selection of the appropriate area for the ablated marrow space. Assessment of the 3-D vascular morphology for both the time course study and the NaHY + DBM study was done using the results based on the images like the one shown in figure 1D.

Neovascularization within the marrow cavity of 8-week old, male athymic rats varied as a function of time post-ablation. Peak blood vessel volume within the marrow cavity was observed on day 14 (Figure 2A) and was significantly higher at this time than at all other time points examined ($p<0.05$). Similarly, blood vessel connectivity also reached its maximum at day 14 (Figure 2B). μCT analyses of blood vessel number (Figure 2C), vessel thickness (Figure 2D), and vessel spacing (Figure 2E) did not reveal any significant differences amongst any of the time points examined. However, it should be noted that on day 14 post-ablation, a moderate increase in blood vessel number and a corresponding in decrease in blood vessel spacing was observed. The average diameter of blood vessels in the marrow remained constant at all time points. Based on these data, it was determined that at 14 days post-ablation, neovascularization occurring within the ablated marrow cavity is at its peak and this time point was selected as the endpoint for the NaHY + DBM study.

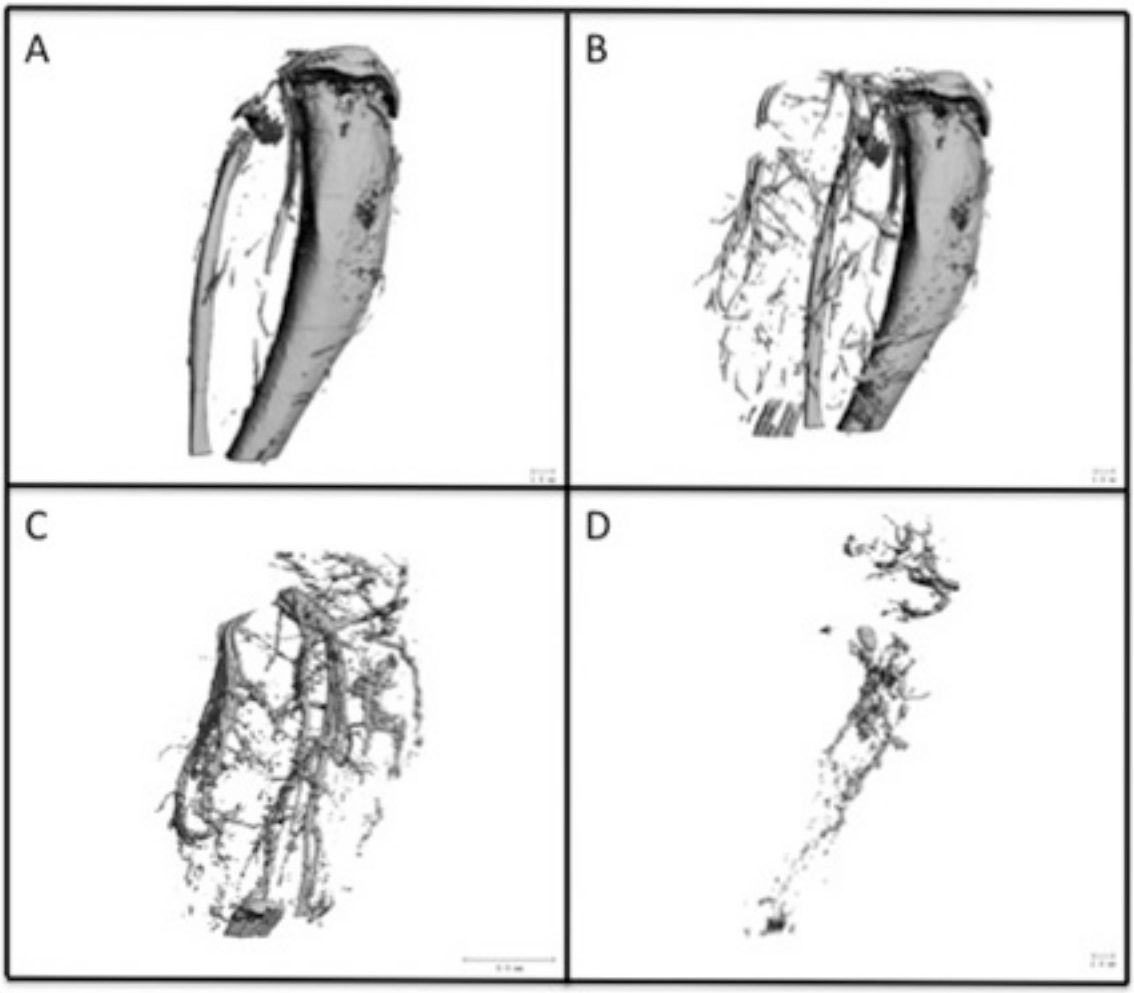

Figure 5-1. To demonstrate feasibility of the procedure, at the time of harvest, rat vasculature was perfused-fixed using 10% formalin and a radio-opaque silicone based contrast agent (Microfil, Carver, MA). Ablated, perfused tibias were imaged using μCT to examine the bone (Figure 1A) and surrounding vasculature (Figure 1B). Tissues were subsequently decalcified and imaged with μCT a second time to isolate the vasculature both surrounding (Figure 1C) and within (Figure 1D) the ablated tibias.

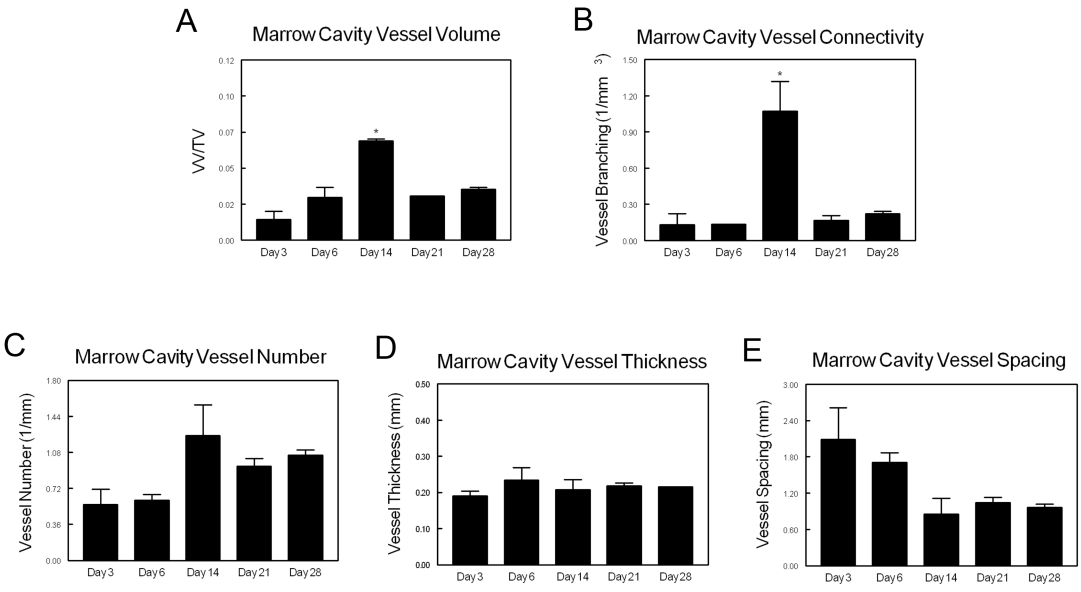

Figure 5-2: Time course of neo-vascularization following tibial marrow ablation. At days 3, 6, 14, 21, and 28 post-ablation, rats were perfused-fixed with Microfil (Flow-Tech Inc, Carver, MA) and imaged using μCT. (A) Marrow cavity vessel volume fraction, (B) vessel connectivity, (C) vessel number, (D) vessel thickness, and (E) vessel spacing were quantitatively assessed. Data are presented as the mean $\pm$ SEM of three animals for each time point. *$p < 0.05$ vs. all other time points.

μCT analysis showed that neovascularization within the marrow cavity at 14 days post-ablation was sensitive to the formulations of NaHY and NaHY + DBM that were injected into the marrow space. DBM alone increased the total blood vessel volume fraction in the ablated marrow space compared to heat inactivated DBM ($p<0.05$) and empty defects (not significant). Addition of low MW NaHY to DBM further enhanced blood vessel volume within ablated marrows compared to empty defects, heat inactivated DBM and DBM alone. High MW NaHY, low MW NaHY, and high + low MW NaHY by themselves displayed moderate increases in total vessel volume compared to empty defects, although none of these were significant (Figure 3A). Similar to total blood vessel volume, the combination of low MW NaHY with DBM increased blood vessel connectivity compared to empty defects, DBM alone and NaHY alone. High and low MW NaHY decreased blood vessel connectivity compared to DBM alone (Figure 3B).

Three dimensional μCT analysis of vessel number showed that all three formulations of NaHY administered either alone or in combination with DBM as well as DBM alone increased the total number of blood vessels in ablated marrows compared to empty defects and heat inactivated DBM (Figure 3C). The average vessel diameter in the ablated marrow space was found to decrease in low MW NaHY and high + low MW NaHY groups compared to empty defects. High MW NaHY + DBM showed the lowest average vessel diameter amongst all treatment groups (Figure 3D).

When combined with DBM, NaHY also increased the total volume fraction of radio-opaque tissue within the marrow cavity as observed by μCT. 31% DBM by itself did not promote greater bone formation compared to empty defects, however the addition of low MW NaHY to 31% DBM significantly increased the volume of radio-opaque tissue within the marrow space compared to DBM alone. In addition, both high

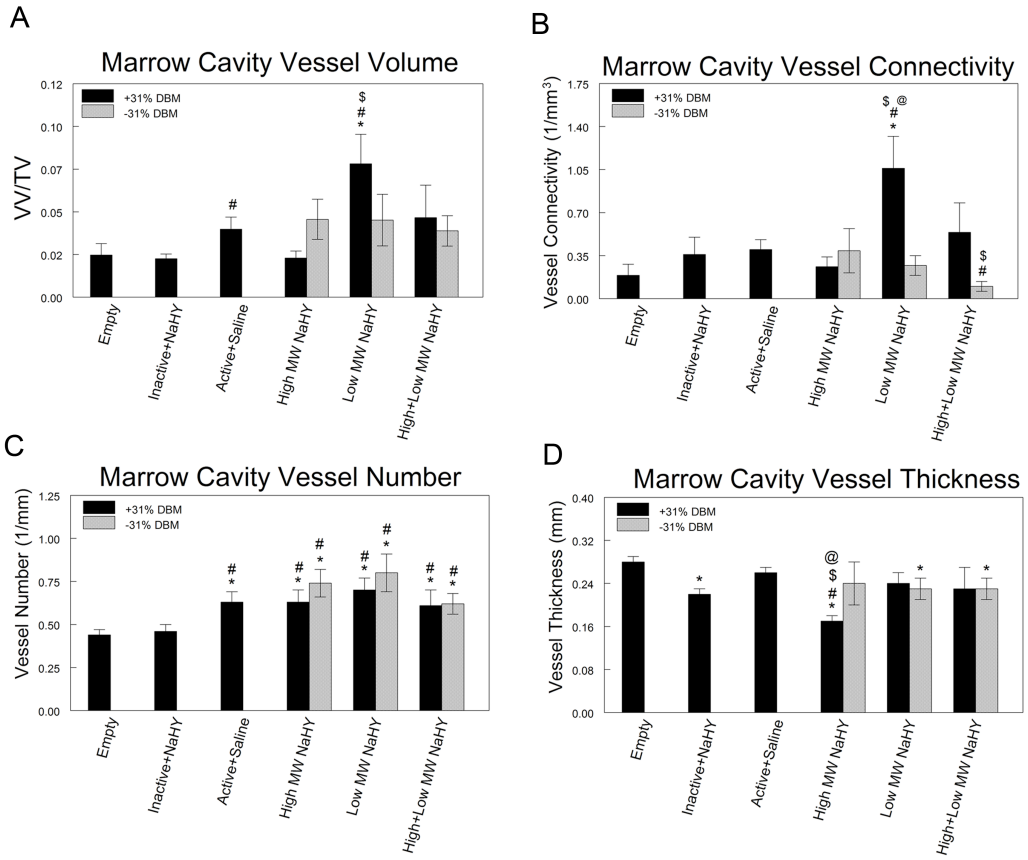

Figure 5-3: Influence of DBM and NaHY on neo-vascularization after tibial marrow ablation. 14 days after marrow ablation and injection of test compounds, rats were perfused-fixed with Microfil and imaged with μCT. (A) Marrow cavity vessel volume fraction, (B) vessel connectivity, (C) vessel number, and (D) average vessel diameter (vessel thickness). Data are presented as the mean ± SEM of nine animals per group. *p< 0.05 vs. Empty Defect; #p< 0.05 vs. Inactive + NaHY; $p< 0.05 vs. Active + Saline; @p< 0.05 vs. no DBM.

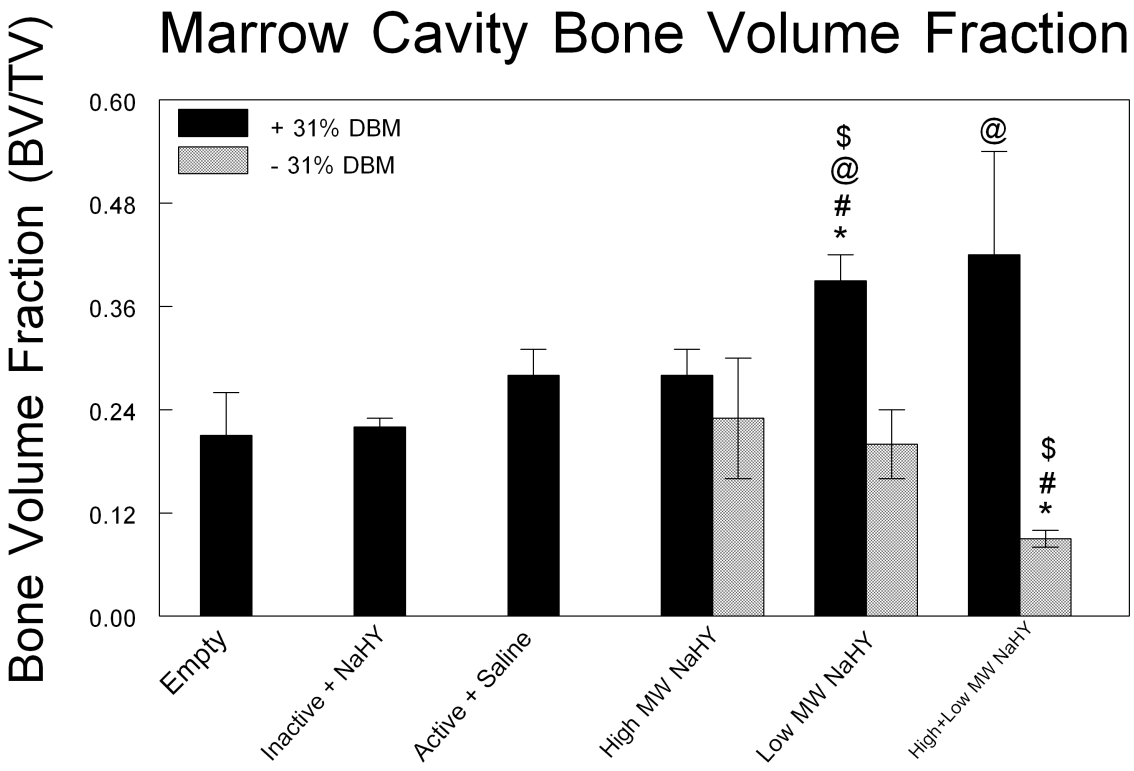

Figure 5-4: Marrow cavity new bone volume. μCT was used to assess the volume of new bone within marrow cavities 14 days after ablation. *p< 0.05 vs. Empty; #p< 0.05 vs. Inactive + NaHY; @p< 0.05 vs. no DBM.

MW NaHY and low MW NaHY promoted new bone formation to a similar extent as DBM alone. The combination of high + low MW NaHY significantly reduced the formation of new bone compared to empty defects and DBM alone (Figure 4).

To account for the volume occupied by the DBM within the ablated marrow cavities on reducing the volume available for neovascularization, we corrected the total blood vessel volume fraction in all experimental groups containing DBM. Based on observations from μCT scans, we estimated that DBM occupied approximately 60% of the ablated marrow space. Figure 4 shows the total blood vessel volume fraction adjusted to subtract the volume occupied by DBM. The results demonstrate that in both the low MW NaHY + DBM and the high + low MW NaHY + DBM groups that when the volume occupied by DBM in the ablated marrows is removed, the blood vessel volume fraction is significantly increased compared to the treatment groups containing either low MW NaHY or high + low MW NaHY alone, respectively (Figure 5).

Haematoxylin and eosin stained sagittal sections of the treated tibias showed the presence of new bone. Blood vessel structures containing Microfil were visible in cuts from all treatment groups (Figure 6). Histomorphometric analysis of total marrow cavity blood vessel number showed that addition of low MW NaHY significantly increased the number of blood vessels compared to empty defects, heat inactivated DBM, active DBM, and a combination of low MW NaHY + 31% DBM (Figure 7). Addition of both high MW NaHY and a combination of high + low MW NaHY increased the number of blood vessels in the marrow cavity compared to heat inactivated DBM.

To determine the influence of patient age on the normal healing process, we ablated the marrows of 9-month old, male athymic rats and at days 3, 6, 14, 21, and 28 post-ablation, perfused-fixed the animals and used μCT imaging to assess the three dimensional parameters of the vascular network similar to the method used in Figure 2.

Assessment of the total vessel volume fraction (Figure 8A), vessel connectivity (Figure 8B), vessel number (Figure 8C), vessel thickness (Figure 8D), and vessel spacing (Figure 8E) did not reveal any statistically significant differences amongst any of the time points examined. However, similar to the results found for 8 week-old animals, there was a moderate increase in the total vessel volume fraction and vessel connectivity, with a corresponding decrease in the mean vessel spacing distance observed at 14 days post-ablation. The total number of blood vessels and mean vessel thickness did not change amongst any of the time points examined.

We also examined new bone formation within the ablated marrows of 9-month old rats (Figure 9). Peak bone volume fraction was observed at 14 days post-ablation, although there was no statistically significant difference in the bone volume fraction observed at 14 days post-ablation versus all other time points examined.

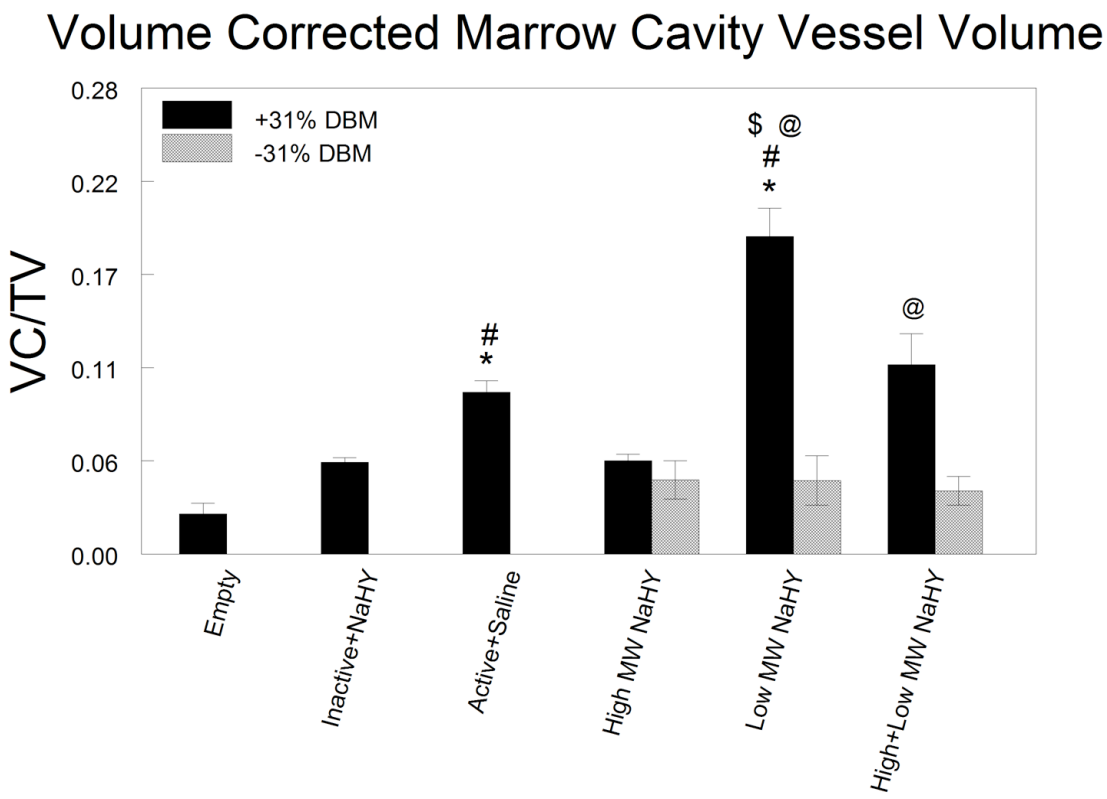

Figure 5-5: Corrected total blood vessel volume fraction. μCT total blood vessel volume fractions were adjusted to account for the volume occupied by the DBM within the ablated marrow space. Data are presented as the mean ± SEM of nine animals per group. *p< 0.05 vs. Empty Defect; #p< 0.05 vs. Inactive + NaHY; $p< 0.05 vs. Active + Saline; @p< 0.05 vs. no DBM.

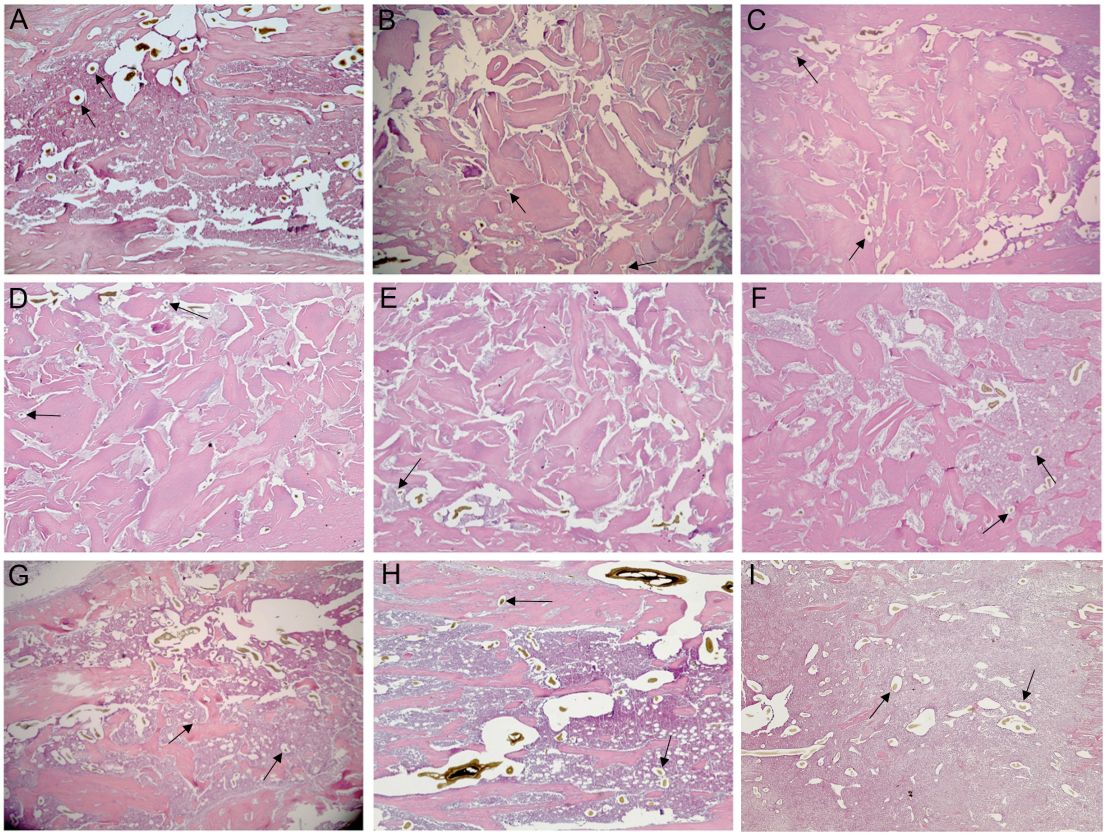

Figure 5-6: Representative histological sections of ablated tibias. Following μCT imaging, ablated tibias were embedded in paraffin and processed for histology. Sections were stained with haematoxylin and eosin. Arrows indicate the presence of vascular structures containing Microfil. Groups analyzed were (A) empty defect, (B) Inactive + NaHY, (C) Active + Saline, (D) High MW NaHY + 31% DBM, (E) Low MW NaHY + 31% DBM, (F) High + Low MW NaHY + 31% DBM, (G) High MW NaHY, (H) Low MW NaHY, and (I) High + Low MW NaHY.

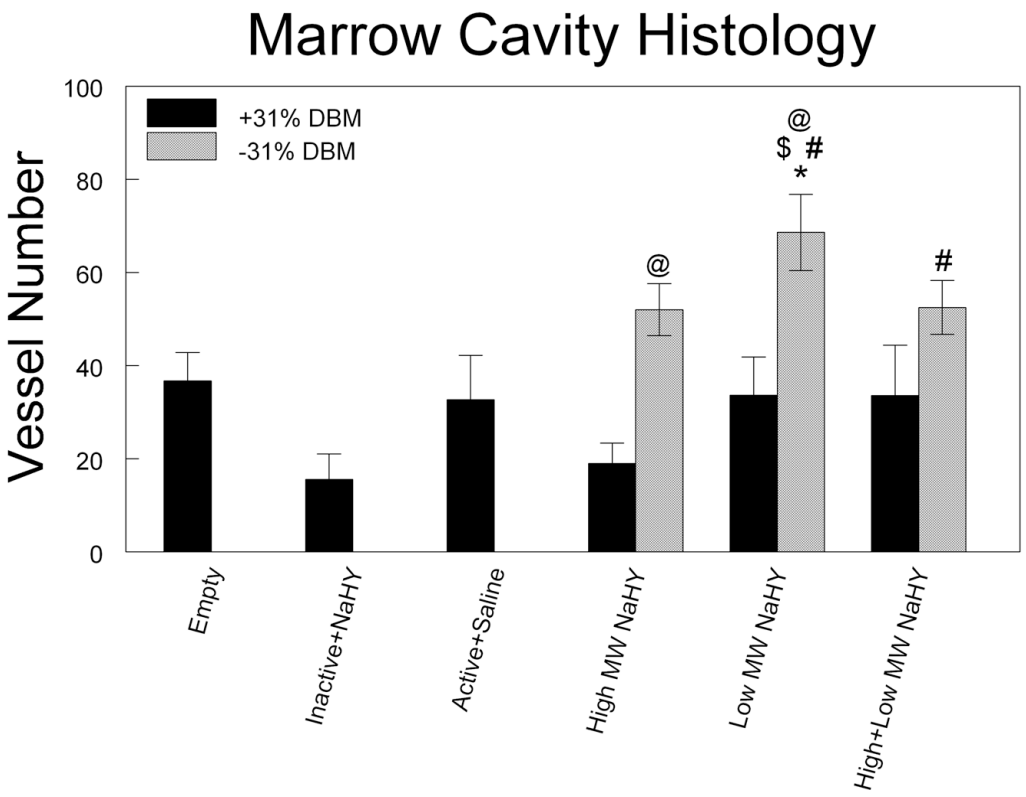

Figure 5-7: Effect of tibial marrow ablation on average vessel number within the marrow cavity 14-days post-ablation, determined by histomorphometry. *p< 0.05 vs. Empty Defect; #p< 0.05 vs. Inactive + NaHY; $p< 0.05 vs. Active + Saline; @p< 0.05 vs. no DBM.

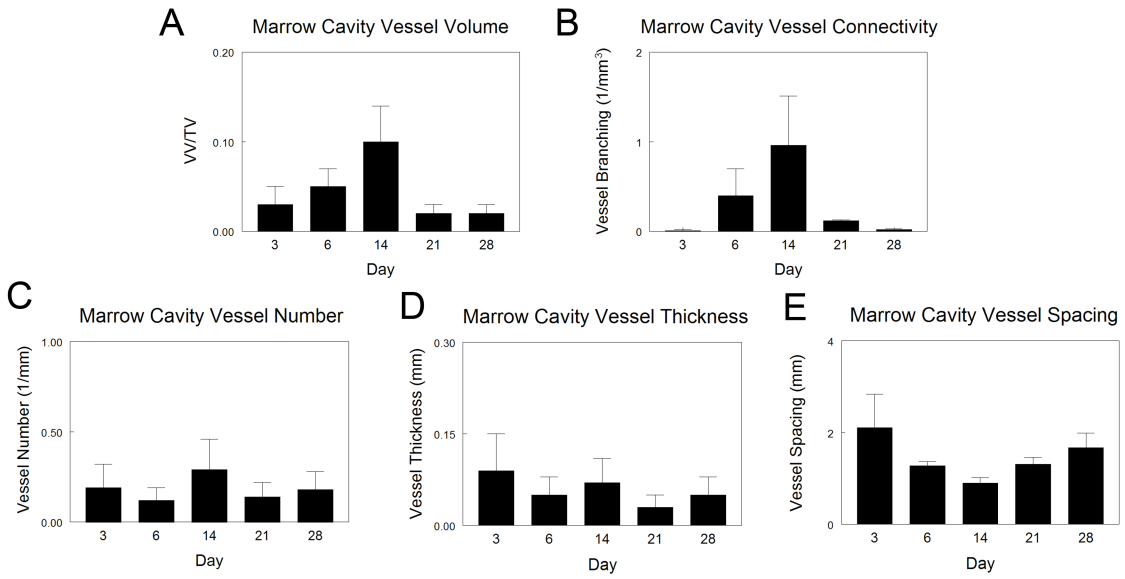

Figure 5-8: Time course of neo-vascularization following tibial marrow ablation in 9-month old male athymic rats. At days 3, 6, 14, 21, and 28 post-ablation, rats were perfused-fixed with Microfil (Flow-Tech Inc, Carver, MA) and imaged using μCT. (A) Marrow cavity vessel volume fraction, (B) vessel connectivity, (C) vessel number, (D) vessel thickness, and (E) vessel spacing were quantitatively assessed. Data are presented as the mean ± SEM of three animals for each time point.

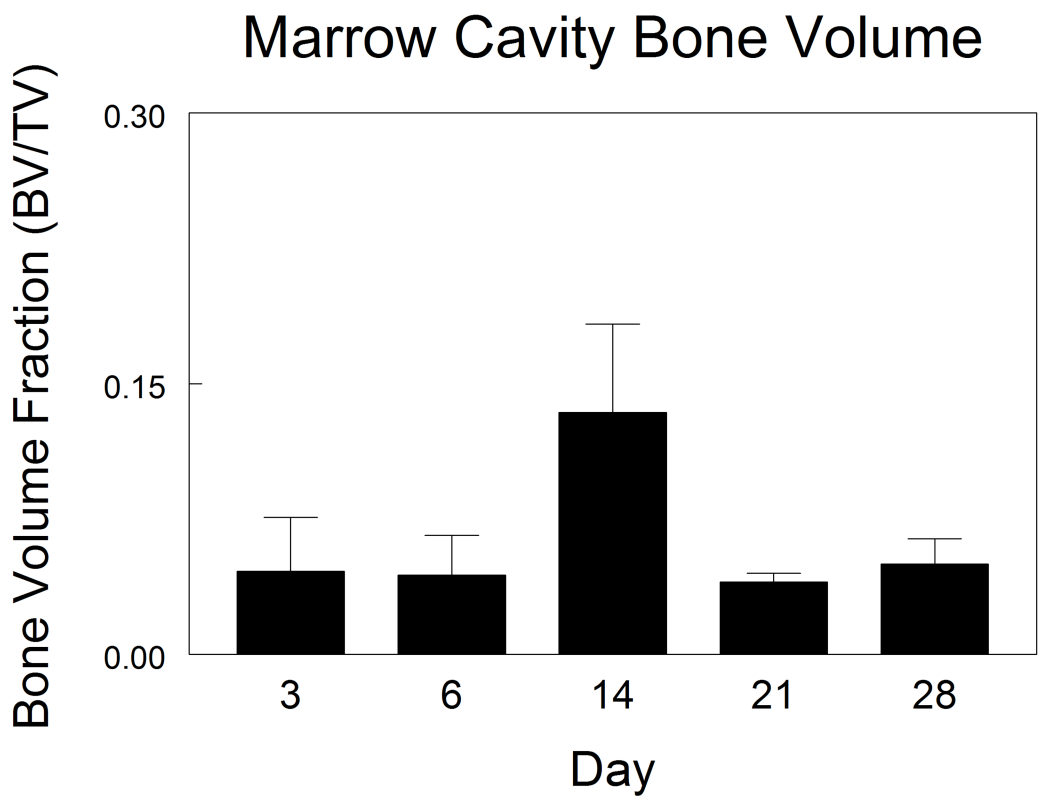

Figure 5-9: Marrow cavity new bone volume. μCT was used to assess new bone formation within the ablated marrows of 9-month old male athymic rats at days 3, 6, 14, 21, and 28 post-ablation.

5.4 Discussion

Successful bone formation surrounding implants is dependent on the establishment of a patent vasculature at the bone-implant interface. This study demonstrates that NaHY increases the number of new blood vessels in the ablated marrow cavity and suggests that it is also helps to promote osteogenesis. Both high and low MW NaHY increased the total vessel number compared to empty defects, with a corresponding decrease in average vessel diameter. Determination of the number of vascular structures of mid-sagittal sections supported the μCT observations. Overall, addition of low MW NaHY to DBM resulted in an increase in the total vessel volume fraction and vessel connectivity within ablated marrows. In addition, a combination of low MW NaHY + DBM resulted in an increase in bone volume fraction compared to empty defects, DBM alone, and NaHY alone. This suggests that low MW NaHY may enhance osteogenesis when combined with DBM via increased vascularity as confirmed by greater numbers of smaller vessels.

Bone is a highly vascularized tissue, and the link between bone formation and vascular invasion is well established[35]. Vascularization of cartilage is a prerequisite for bone formation during growth and development[36] and the development of a vascular bed is necessary during fracture healing and bone repair and regeneration to allow for the migration of osteoprogenitor cells to the healing site as well as to supply oxygen and nutrients and allow for removal of waste[37].

DBM is a commonly used bone graft substitute, due to its osteoconductive and osteoinductive properties. However, VEGF expression and micro-vessel density (MVD) are low during bone healing with DBM compared to autologous bone and synthetic bone graft substitutes[3, 38]. When DBM was used in a rat craniotomy defect together with a pro-angiogenic compound, both new bone formation and MVD were increased[39]. In a

similar manner, hyaluronic acid may serve to stimulate neovascularization when combined with DBM during bone regeneration within ablated marrows of immunocompromised rats.

Effects of NaHY on cells have been previously shown to be dependent on the chain length of the polymer. High molecular weight hyaluronic acid serves as a structural polymer, sequestering growth factors and other signaling molecules[23]. In addition, high molecular weight forms of NaHY inhibit endothelial cell proliferation and disrupt endothelial cell monolayers[14]. On the other hand, short, oligomeric fragments of NaHY (less than 20 monomers) have been found to be produced at sites of injury and within tumors[13]. The short NaHY fragments bind to cell-surface hyaluronic acid receptor proteins such as CD-44, receptor for hyaluronan-mediated motility (RHAMM), and toll-like-receptor-4 (TLR-4)[23]. Activation of these receptors on endothelial cells promotes their proliferation and migration, resulting in sprout formation and neovascularization[40]. The ability of NaHY to promote neovascularization has been demonstrated both subcutaneously[41] and in a murine epigastric skin flap model[42].

High molecular weight hyaluronic acid is broken down *in vivo* by a class of enzymes called hyaluronidases[43]. In particular, hyaluronidase-1 (HYAL-1) is responsible for the generation of short, pro-angiogenic hyaluronic acid oligomers[18]. The generation of these hyaluronic acid oligomers is significantly increased at sites of injury and inflammation[43, 44]. While no examination of hyaluronidase expression was performed in this study, it is possible that following injection of NaHY within the ablated marrow, expression of HYAL-1 is increased, resulting in the breakdown of NaHY into smaller fragments, which bind to CD-44 receptors present on endothelial cells, promoting neovascularization during bone formation.

In our model of tibial marrow ablation, we observed that after 14 days, DBM particulates were still present within the ablated marrow cavities. Based on μCT as well as histology observations, we estimated that DBM occupied approximately 60% of the total marrow cavity. This results in a decrease in the total volume available for blood vessel invasion. We have demonstrated in this study that the enhanced neovascularization observed in ablated marrows treated with low MW NaHY + DBM is further increased when we account for the volume occupied by the DBM, indicating that the neovascularization induced by NaHY is further stimulated by the presence of DBM.

μCT imaging has been shown to be a good model for the three dimensional analysis of vascular structures *in vivo*. The ability of μCT to detect smaller vessels and capillaries is dependent on the resolution of the imaging system and has been investigated previously[45, 46]. In the present study, three dimensional reconstructions of the vasculature were generated using a voxel size of 36 μm. It is possible in our model of vascular perfusion that the resolution of the μCT imaging system was unable to detect all of the capillaries present in the marrow space, however, a 36 μm voxel size has been demonstrated to provide a good analysis of the three dimensional vascular network[31].

This study was designed to limit the number of animals required to meet the experimental objectives. By using μCT and H&E of decalcified tissues to quantify blood vessel number and volume, all measurements could be made on a single set of animals. For this reason, only static histomorphometry was performed. We did not do dynamic measurements requiring undecalcified sections and fluorochrome labeling. H&E and Microfil were sufficient to identify vascular structures, and for this reason we did not perform immunohistochemistry for endothelial markers like PCAM-1 or von Willebrand's

factor. Importantly, the histologic analysis supported the μCT data with regards to blood vessel number.

In conclusion, we have shown here that normal bone healing after tibial marrow ablation is accompanied by an increase in neovascularization within the marrow space, peaking at 14 days post ablation. We also show that NaHY stimulates new blood vessel formation during new bone formation during healing when used as a carrier for DBM. In particular, low molecular weight (35kDa) NaHY + DBM resulted in increases in total blood vessel volume and total bone volume in ablated limbs. The contribution of the vascularization to remodeling isn't known. In an orthotopic site, low molecular weight NaHY might contribute to bone formation by both supporting MSC and progenitor cell migration in early phases of healing and vascular ingrowth as the NaHY is degraded to smaller fragments. However, as a whole, the data suggest that the increase in neovascularization due to the NaHY may enhance overall bone formation when used as a carrier.

5.5 References

1. Degidi M, Artese L, Rubini C, Perrotti V, Iezzi G, Piattelli A. Microvessel density in sinus augmentation procedures using anorganic bovine bone and autologous bone: 3 months results. Implant Dent 2007 Sep;16(3):317-325.

2. Hallman M, Cederlund A, Lindskog S, Lundgren S, Sennerby L. A clinical histologic study of bovine hydroxyapatite in combination with autogenous bone and fibrin glue for maxillary sinus floor augmentation. Results after 6 to 8 months of healing. Clin Oral Implants Res 2001 Apr;12(2):135-143.

3. Abshagen K, Schrodi I, Gerber T, Vollmar B. In vivo analysis of biocompatibility and vascularization of the synthetic bone grafting substitute NanoBone. J Biomed Mater Res A 2009 Nov;91(2):557-566.

4. Slevin M, Krupinski J, Gaffney J, Matou S, West D, Delisser H, et al. Hyaluronan-mediated angiogenesis in vascular disease: uncovering RHAMM and CD44 receptor signaling pathways. Matrix Biol 2007 Jan;26(1):58-68.

5. Aslan M, Simsek G, Dayi E. The effect of hyaluronic acid-supplemented bone graft in bone healing: experimental study in rabbits. J Biomater Appl 2006 Jan;20(3): 209-220.

6. Jung M, Tuischer JS, Sergi C, Gotterbarm T, Pohl J, Richter W, et al. Local application of a collagen type I/hyaluronate matrix and growth and differentiation factor 5 influences the closure of osteochondral defects in a minipig model by enchondral ossification. Growth Factors 2006 Dec;24(4):225-232.

7. Rooney P, Kumar S, Ponting J, Wang M. The role of hyaluronan in tumour neovascularization (review). Int J Cancer 1995 Mar 3;60(5):632-636.

8. Jiang D, Liang J, Noble PW. Hyaluronan in tissue injury and repair. Annu Rev Cell Dev Biol 2007;23:435-461.

9. West DC, Kumar S. Tumour-associated hyaluronan: a potential regulator of tumour angiogenesis. Int J Radiat Biol 1991 Jul-Aug;60(1-2):55-60.

10. Deed R, Rooney P, Kumar P, Norton JD, Smith J, Freemont AJ, et al. Early-response gene signalling is induced by angiogenic oligosaccharides of hyaluronan in endothelial cells. Inhibition by non-angiogenic, high-molecular-weight hyaluronan. Int J Cancer 1997 Apr 10;71(2):251-256.

11. Slevin M, Krupinski J, Kumar S, Gaffney J. Angiogenic oligosaccharides of hyaluronan induce protein tyrosine kinase activity in endothelial cells and activate a cytoplasmic signal transduction pathway resulting in proliferation. Lab Invest 1998 Aug; 78(8):987-1003.

12. Slevin M, Kumar S, Gaffney J. Angiogenic oligosaccharides of hyaluronan induce multiple signaling pathways affecting vascular endothelial cell mitogenic and wound healing responses. J Biol Chem 2002 Oct 25;277(43):41046-41059.

13. Slevin M, West D, Kumar P, Rooney P, Kumar S. Hyaluronan, angiogenesis and malignant disease. Int J Cancer 2004 May 1;109(5):793-794; author reply 795-796.

14. West DC, Kumar S. The effect of hyaluronate and its oligosaccharides on endothelial cell proliferation and monolayer integrity. Exp Cell Res 1989 Jul;183(1): 179-196.

15. Sattar A, Rooney P, Kumar S, Pye D, West DC, Scott I, et al. Application of angiogenic oligosaccharides of hyaluronan increases blood vessel numbers in rat skin. J Invest Dermatol 1994 Oct;103(4):576-579.

16. Rooney P, Wang M, Kumar P, Kumar S. Angiogenic oligosaccharides of hyaluronan enhance the production of collagens by endothelial cells. J Cell Sci 1993 May;105 (Pt 1):213-218.

17. Montesano R, Kumar S, Orci L, Pepper MS. Synergistic effect of hyaluronan oligosaccharides and vascular endothelial growth factor on angiogenesis in vitro. Lab Invest 1996 Aug;75(2):249-262.

18. West DC, Hampson IN, Arnold F, Kumar S. Angiogenesis induced by degradation products of hyaluronic acid. Science 1985 Jun 14;228(4705):1324-1326.

19. Acarturk TO, Hollinger JO. Commercially available demineralized bone matrix compositions to regenerate calvarial critical-sized bone defects. Plast Reconstr Surg 2006 Sep 15;118(4):862-873.

20. Kohles SS, Vernino AR, Clagett JA, Yang JC, Severson S, Holt RA. A morphometric evaluation of allograft matrix combinations in the treatment of osseous defects in a baboon model. Calcif Tissue Int 2000 Aug;67(2):156-162.

21. Mendes RM, Silva GA, Lima MF, Calliari MV, Almeida AP, Alves JB, et al. Sodium hyaluronate accelerates the healing process in tooth sockets of rats. Arch Oral Biol 2008 Dec;53(12):1155-1162.

22. Gao F, Liu Y, He Y, Yang C, Wang Y, Shi X, et al. Hyaluronan oligosaccharides promote excisional wound healing through enhanced angiogenesis. Matrix Biol 2009 Nov 12.

23. Pardue EL, Ibrahim S, Ramamurthi A. Role of hyaluronan in angiogenesis and its utility to angiogenic tissue engineering. Organogenesis 2008 Oct;4(4):203-214.

24. Sasaki T, Watanabe C. Stimulation of osteoinduction in bone wound healing by high-molecular hyaluronic acid. Bone 1995 Jan;16(1):9-15.

25. Bab IA. Postablation bone marrow regeneration: an in vivo model to study differential regulation of bone formation and resorption. Bone 1995 Oct;17(4 Suppl): 437S-441S.

26. Kondo N, Tokunaga K, Ito T, Arai K, Amizuka N, Minqi L, et al. High dose glucocorticoid hampers bone formation and resorption after bone marrow ablation in rat. Microsc Res Tech 2006 Oct;69(10):839-846.

27. Kuroda S, Virdi AS, Dai Y, Shott S, Sumner DR. Patterns and localization of gene expression during intramembranous bone regeneration in the rat femoral marrow ablation model. Calcif Tissue Int 2005 Oct;77(4):212-225.

28. Braun G, Kohavi D, Amir D, Luna M, Caloss R, Sela J, et al. Markers of primary mineralization are correlated with bone-bonding ability of titanium or stainless steel in vivo. Clin Oral Implants Res 1995 Mar;6(1):1-13.

29. Schwartz Z, Doukarsky-Marx T, Nasatzky E, Goultschin J, Ranly DM, Greenspan DC, et al. Differential effects of bone graft substitutes on regeneration of bone marrow. Clin Oral Implants Res 2008 Dec;19(12):1233-1245.

30. Schwartz Z, Sela J, Ramirez V, Amir D, Boyan BD. Changes in extracellular matrix vesicles during healing of rat tibial bone: a morphometric and biochemical study. Bone 1989;10(1):53-60.

31. Duvall CL, Taylor WR, Weiss D, Guldberg RE. Quantitative microcomputed tomography analysis of collateral vessel development after ischemic injury. Am J Physiol Heart Circ Physiol 2004 Jul;287(1):H302-310.

32. Feldkamp LA, Davis LC, Kress JW. Practical cone-beam algorithm. J Opt Soc Am A 1984;1(6):612-619.

33. Hildebrand T, Laib A, Muller R, Dequeker J, Ruegsegger P. Direct three-dimensional morphometric analysis of human cancellous bone: microstructural data from spine, femur, iliac crest, and calcaneus. J Bone Miner Res 1999 Jul;14(7):1167-1174.

34. Hildebrand T, Ruegsegger P. A new method for the model-independent assessment of thickness in three-dimensional images. J Microsc 1997;185(1):67-75.

35. Kanczler JM, Oreffo RO. Osteogenesis and angiogenesis: the potential for engineering bone. Eur Cell Mater 2008;15:100-114.

36. Deckers MM, Karperien M, van der Bent C, Yamashita T, Papapoulos SE, Lowik CW. Expression of vascular endothelial growth factors and their receptors during osteoblast differentiation. Endocrinology 2000 May;141(5):1667-1674.

37. Carano RA, Filvaroff EH. Angiogenesis and bone repair. Drug Discov Today 2003 Nov 1;8(21):980-989.

38. Boeck-Neto RJ, Artese L, Piattelli A, Shibli JA, Perrotti V, Piccirilli M, et al. VEGF and MVD expression in sinus augmentation with autologous bone and several graft materials. Oral Dis 2009 Mar;15(2):148-154.

39. Hansen A, Pruss A, Gollnick K, Bochentin B, Denner K, Von Versen R. Demineralized Bone Matrix-stimulated Bone Regeneration in Rats Enhanced by an Angiogenic Dipeptide Derivate. Cell Tissue Bank 2001;2(2):69-75.

40. Cao G, Savani RC, Fehrenbach M, Lyons C, Zhang L, Coukos G, et al. Involvement of endothelial CD44 during in vivo angiogenesis. Am J Pathol 2006 Jul;169 (1):325-336.

41. Baier Leach J, Bivens KA, Patrick CW, Jr., Schmidt CE. Photocrosslinked hyaluronic acid hydrogels: natural, biodegradable tissue engineering scaffolds. Biotechnol Bioeng 2003 Jun 5;82(5):578-589.

42. Perng CK, Wang YJ, Tsi CH, Ma H. In Vivo Angiogenesis Effect of Porous Collagen Scaffold with Hyaluronic Acid Oligosaccharides. J Surg Res 2009 Oct 23.

43. Stern R. Hyaluronan catabolism: a new metabolic pathway. Eur J Cell Biol 2004 Aug;83(7):317-325.

44. Noble PW. Hyaluronan and its catabolic products in tissue injury and repair. Matrix Biol 2002 Jan;21(1):25-29.

45. Guldberg RE, Ballock RT, Boyan BD, Duvall CL, Lin AS, Nagaraja S, et al. Analyzing bone, blood vessels, and biomaterials with microcomputed tomography. IEEE Eng Med Biol Mag 2003 Sep-Oct;22(5):77-83.

46. Young S, Kretlow JD, Nguyen C, Bashoura AG, Baggett LS, Jansen JA, et al. Microcomputed tomography characterization of neovascularization in bone tissue engineering applications. Tissue Eng Part B Rev 2008 Sep;14(3):295-306.

CHAPTER 6. Discussion

The results presented in this thesis demonstrate the important role that biomaterial properties have in regulating the angiogenic response of cells *in vitro* and host tissue *in vivo*. In particular, the results presented herein show that titanium (Ti) surface topography and surface free energy can affect not only osteoblastic differentiation of cells as has been demonstrated in earlier work, but can also affect the production and secretion of pro-angiogenic growth factors that serve both an autocrine and paracrine role in osteoblast maturation. Further, this thesis has demonstrated that by combining osteogenic and angiogenic biomaterials, neovascularization and new bone formation can be enhanced during healing. While these studies have provided insight into the role that biomaterial properties have in regulating peri-implant neovascularization, there are still several questions to be answered regarding the mechanism by which this process occurs. Obtaining a greater understanding of how biomaterials regulate host cellular and tissue response will allow for the design of implants to better promote osseointegration, improving implant success rates and implant lifetimes.

6.1 Role of Ti surface features in promoting neovascularization

The results presented in Chapter 2 of this thesis show that both Ti surface roughness and surface free energy mediate the production of pro-angiogenic growth factors by cells. Increasing Ti surface roughness resulted in an increase in the production of VEGF-A, FGF-2, and EGF by an MG63 osteoblast-like cell line and an increase in the production of VEGF-A by primary human osteoblasts (HOB). By combining surface roughness with a high surface free energy, the production of these

pro-angiogenic growth factors by both MG63 cells and HOBs were further increased. In addition, conditioned media from MG63 cell cultures on SLA and modSLA Ti substrates promoted the differentiation of human aortic endothelial cells (HAEC) using an *in vitro* Matrigel® and fibrin gel tubule formation assay to a greater extent than did conditioned media from control TCPS and smooth PT Ti substrates, suggesting that the increase in pro-angiogenic growth factor production observed in response to Ti surface microtopography and surface free energy has a paracrine role in the activation and differentiation of endothelial cells.

It should be noted that MG63 cells are a transformed cell line, originally isolated from a 14-year-old Caucasian male with osteosarcoma, and represent an immature osteoblast-like phenotype. It is well established in the literature that cancer cells express higher levels of multiple pro-angiogenic growth factors, including VEGF-A, FGF-2, and EGF. This may explain why secreted levels of FGF-2 and EGF by HOBs were undetectable in our ELISA assay systems. In order to more definitively show that Ti surface features can promote the production of pro-angiogenic growth factors, further characterization using HOBs and other primary bone cell lines should be done. Techniques such as real-time polymerase chain reaction (qPCR) to check for expression of pro-angiogenic growth factors or more sensitive ELISA systems could be used to achieve this. Using conditioned media from HOB cell cultures in the *in vitro* Matrigel® and fibrin gel assays, as well as *in vivo* angiogenesis assays like the chick chorioallantoic membrane (CAM) assay or Matrigel® plug assay could be done to further verify the paracrine effect that the pro-angiogenic growth factors produced by these cells have on endothelial cell response.

In vivo, it is likely that the first cells to come into contact with the implant surface are mesenchymal progenitor cells that differentiate down an osteoblast lineage. Earlier

studies from our laboratory have found that Ti surface features have the ability to induce osteoblastic differentiation of human MSCs without the addition of exogenous growth factors or chemicals. The effect that Ti surface properties have on the ability to regulate the production of pro-angiogenic growth factors in MSCs during osteoblastic differentiation should be more fully characterized.

Our results from Chapter 2 of this thesis also established that Ti implant surface characteristics have an effect on both bone formation and new blood vessel formation *in vivo*. Using a novel, murine intramedullary femoral press-fit model, we observed an increase in both bone-to-implant-contact and new blood vessel formation in aged mice, though in young, healthy mice, no differences in bone-to-implant contact were observed. In this thesis, we harvested implants after either 28 or 35 days for analysis. It would be useful to perform a time course study in mice to look at the development of new vasculature and new bone over time. Additional techniques, such as μCT analysis of the three dimensional vascular network and mechanical testing could be also be done to provide a more in depth analysis of the effect that Ti surface features have on bone formation *in vivo*. Taking advantage of the numerous transgenic mice that have been developed, this model could be used to look at the roles of specific growth factors involved in osteogenesis and angiogenesis *in vivo*.

6.2 Integrin signaling in angiogenic growth factor production

Integrins are a family of heterodimeric cell adhesion molecules that play an important role in cellular processes in multiple tissue types in the body. Signaling through integrin receptor complexes is known to initiate intracellular signaling cascades that control cellular proliferation and differentiation. The results presented in Chapter 3 of this thesis found that the production of pro-angiogenic growth factors by osteoblast-like cells is at least partially regulated through specific integrin receptor signaling. Using

shRNA techniques, we stably silenced MG63 human osteoblast-like cells for integrin subunits α_1, α_2, α_5, and β_1. Our results found that the production of the pro-angiogenic growth factors VEGF-A, FGF-2, and Ang-1 were affected by knockdown of these integrin subunits. In particular, secreted levels of VEGF-A were increased in cells silenced for integrins α_2, α_5, and β_1 whereas silencing of integrin α_1 resulted in a decrease in VEGF-A production in response to Ti surface topography and energy. Levels of FGF-2 were only affected in response to knockdown of either α_1 or α_2, and were decreased on modSLA Ti surfaces in these cells. In contrast, secretion of Ang-1 was increased on modSLA Ti surfaces in α_1, α_2, and β_1 silenced cells compared to wild-type MG63 cells. Taken together, these results suggest that signaling events through integrin adhesion receptors may regulate the production of pro-angiogenic growth factors to induce endothelial cell migration and subsequent vascular formation during peri-implant healing.

Earlier studies showed that the α_2 and β_1 integrin subunits are particularly important in mediating the differentiation of osteoblasts in response to Ti surface features. Knockdown of either the α_2 or β_1 integrin subunits in MG63 cells blocks surface roughness dependent differentiation of those cells. In these studies as well as our results presented here, only one integrin α or β subunit is examined. *In vivo*, multiple integrin receptors are expressed and involved in cell interaction with the extracellular matrix. Thus, it is possible that other integrin receptor pairs may be involved in the angiogenic response cells to the implant surface, including $\alpha_v\beta_3$, $\alpha_3\beta_1$, $\alpha_v\beta_5$, or others. In order to more fully elucidate the role that integrin signaling has in cell response to implant surfaces, knockdown of other α and β subunits should be done.

It is also possible that other mechanisms are involved in the production of angiogenic growth factors by these cells. Tissue hypoxia is one of the most well known

initiators of neovascularization within the body. The hypoxia inducible factor pathway is activated in response to hypoxia. Under conditions of normal oxygen tension, HIF-1α subunits are hydroxylated and marked for degradation by the proteosome by the von Hippel-Lindau (VHL) tumor suppressor protein. However, when oxygen concentrations drop below approximately 5%, HIF-1α accumulates in the cytoplasm and translocates to the nucleus, where it interacts with the constitutively expressed HIF-1β subunit to activate gene transcription. Several genes associated with angiogenesis are either directly or indirectly affected in response to hypoxia, including vascular endothelial growth factor and its receptors, fibroblast growth factors, and angiopoietins. When implants are inserted into the body *in vivo*, it is likely that hypoxia plays a major role in the angiogenic response. In our studies *in vitro* however, the hypoxia inducible factor pathway is not likely to be activated, indicating that other mechanisms, such as integrin receptor signaling or growth factor signaling may be regulating the production of pro-angiogenic growth factors.

6.3 Role of VEGF-A

VEGF-A is widely recognized as the most potent endothelial cell mitogen and is one of the primary growth factors involved in the initiation of angiogenesis. Bone is a highly vascularized tissue and osteoblasts and osteoblast progenitor cells are known to produce and secrete VEGF-A and express the VEGF receptors, VEGFR1 (Flt1) and VEGFR2 (Flk1/KDR). In Chapter 4, we found that VEGF-A has both an autocrine and paracrine role in osteoblast-like cell differentiation in response to Ti surface microtopography and surface free energy. shRNA silencing of the VEGF-A gene in human MG63 cells resulted in a decrease in the production of osteocalcin, osteoprotegerin, VEGF-A, FGF-2, and Ang-1 by these cells in response to Ti surface features, suggesting that interaction of VEGF-A with its receptors present on these cells

at least partially mediates MG63 cell differentiation. Additionally, conditioned media from VEGF-A silenced cell cultures failed to stimulate endothelial cell tubule formation to the same extent as media from wild-type cell cultures, indicating that VEGF-A produced by these cells has a paracrine role in mediating endothelial cell differentation.

While inhibition of endogenous VEGF-A by MG63 cells inhibited the differentiation of these cells, blocking VEGF-A interaction with the Flk1 receptor did not effect MG63 cell differentiation, though production of VEGF-A was significantly increased, possibly as a response to overcome the effect of the Flk1 neutralization antibody. Further, addition of exogenous VEGF-A to MG63 cell cultures increased the production of osteocalcin, osteprotegerin, FGF-2, and Ang-1 by these cells in response to Ti substrate roughness and surface free energy.

While the results presented in this thesis illustrate the important role that VEGF-A has in osteoblast-like cell differentiation, it raises further questions about the interaction of growth factors with their receptors during osteoblast differentiation. It is possible that VEGF-A is acting through VEGFR1, neuropilins, or another receptor in our system and further studies should be done to determine what receptor for VEGF-A is the primary mediator of osteoblast cell response. The effect of VEGF-A on osteoblast differentiation in response to Ti surface features should also been done using HOBs since the expression of VEGF-A and its receptors may be dysregulated in MG63 cells. Also, what effect VEGF-A has on the differentiation of MSCs in response to Ti surfaces would also be interesting to examine.

The interaction between VEGF-A and other growth factors during osteoblast differentiation should also be examined. Osteoblasts express receptors for numerous growth factors, including BMP-2, TGFβ, FGFs, and Ang-1. The spatio-temporal expression of these growth factors and their receptors during osteoblast differentiation in

response to Ti surface features would aid in our general understanding of osteoblast interaction with implant surfaces.

6.4 Neovascularization *in vivo*

In Chapter 5 of this thesis, we found that a combination of demineralized bone matrix (DBM) with low molecular weight sodium hyaluronate (NaHY) improved both new bone formation and neovascularization *in vivo* using the marrow ablation model. Three dimensional micro-computed tomography (μCT) analysis showed that the total bone volume fraction as well as several vascular network parameters, including vessel volume fraction, vessel number, and vessel connectivity within ablated limbs were increased over empty defect controls at 14-days post-ablation. These results suggest that by combining an osteogenic stimulus with an angiogenic stimulus, new bone formation may be enhanced via increased vascularity. This data represents a good first step in designing combination materials for use in bone regeneration.

In the marrow ablation model, the marrow space is filled with new bone that is subsequently remodeled to restore normal tissue phenotype. This process is well documented and occurs during normal healing without any intervention. In order to more fully determine if a combination of NaHY and DBM can lead to greater bone formation at a faster rate, it would be useful to use an injury model such as a segmental or critical sized defect, where complete healing will not occur without intervention. It would also be interesting to see how NaHY and DBM are exerting their effects on cells *in vivo* through examination of receptors present on osteoblast and endothelial cells as well as their progenitors, and the expression of different growth factors in the regenerating tissue.

Our results presented in Chapter 5 also found that there appeared to be no difference in the normal healing response after marrow ablation between young (8 week)

and old (9 month) rats. Data in the literature suggests that healing ability after injury in older populations is reduced and that the healing process occurs over a longer period of time after injury. In our study, we examined both neovascularization and new bone formation at 3, 6, 14, 21, and 28 days post-ablation. In both young and old animals, we observed peak neovascularization and peak new bone at 14 days post ablation. It is possible that in young animals, neovascularization and bone formation peak somewhere between 6 and 14 days post-ablation and that the results we observed for neovascularization and bone formation were declining at the 14 day time point. A more detailed anlaysis should be done that incorporates more time points between 6 and 14 days to confirm this.

6.5 Conclusions

This thesis has demonstrated that biomaterial properties are important in determining host cellular and tissue response with regards to the production of pro-angiogenic growth factors during osseointegration. However, more work remains to fully understand the mechanism of interaction between cells and a biomaterial surface. A more detailed examination using the studies outlined in the above sections of this chapter will help in understanding this process. In addition to the role that biomaterial properties have in promoting osteogenesis and angiogenesis at the bone/implant interface, two other cell types that play an important role in the early healing events after implant implantation are inflammatory cells and nerve cells. Other work in our lab has shown that modSLA Ti substrates may reduce the inflammatory response. In addition to mineralized tissue and blood vessels, bone is a highly innervated tissue and the ability of implant materials to promote not only osteogenesis and angiogenesis but new nerve growth is essential for the design of next generation biomaterials. The results presented

here provide more fundamental insight into the interaction between cells and biomaterials and will ultimately aid in the better design and evaluation of biomaterials.

APPENDIX

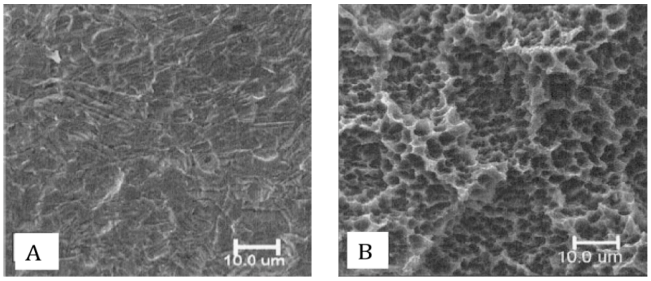

Figure A-1. Scanning electron micrographs of (A) PT and (B) SLA Ti surfaces.

Ti Surface Characterization

Table A-1: Characterization of surface roughness. S_a, arithmetic mean deviation of the surface; S_q, root-mean-square deviation of the surface; S_t, maximum peak-to-valley height of the surface; S_k, amplitude distribution skew. Values are means + SEM of 10 independent cultures. *p<0.05, v. SLA and modSLA.

Roughness Parameter (μm)	SLA	ModSLA	PT
S_a	1.2 ± 0.04	1.2 ± 0.03	0.6 ± 0.1*
S_q	1.5 ± 0.05	1.5 ± 0.03	0.7 ± 0.1*
S_t	7.9 ± 0.5	7.8 ± 0.3	3.9 ± 0.6*
S_k	4.5 ± 2.3	4.6 ± 2.2	1.8 ± 0.5

Table A-2: Characterization of surface chemical composition. Surface chemical composition was measured by X-ray photoelectron spectroscopy. Values are means + SEM of 10 independent cultures. *p<0.05, v. SLA and modSLA; †p<0.05, v. SLA; ‡p<0.05 v. mod SLA.

Chemistry Composition (%)	SLA	modSLA	PT
O	50.2 ± 2.6	60.1 ± 0.7†	47.6 ± 1.2‡
Ti	14.3 ± 1.4	23.0 ± 1.1†	17.9 ± 1.0*
N	1.3 ± 0.3	0.7 ± 0.2†	1.2 ± 0.4
C	34.2 ± 2.0	14.9 ± 0.9†	29.2 ± 1.5*

Total Vessel Volume Fraction for Ablated and Contralateral Control Limbs

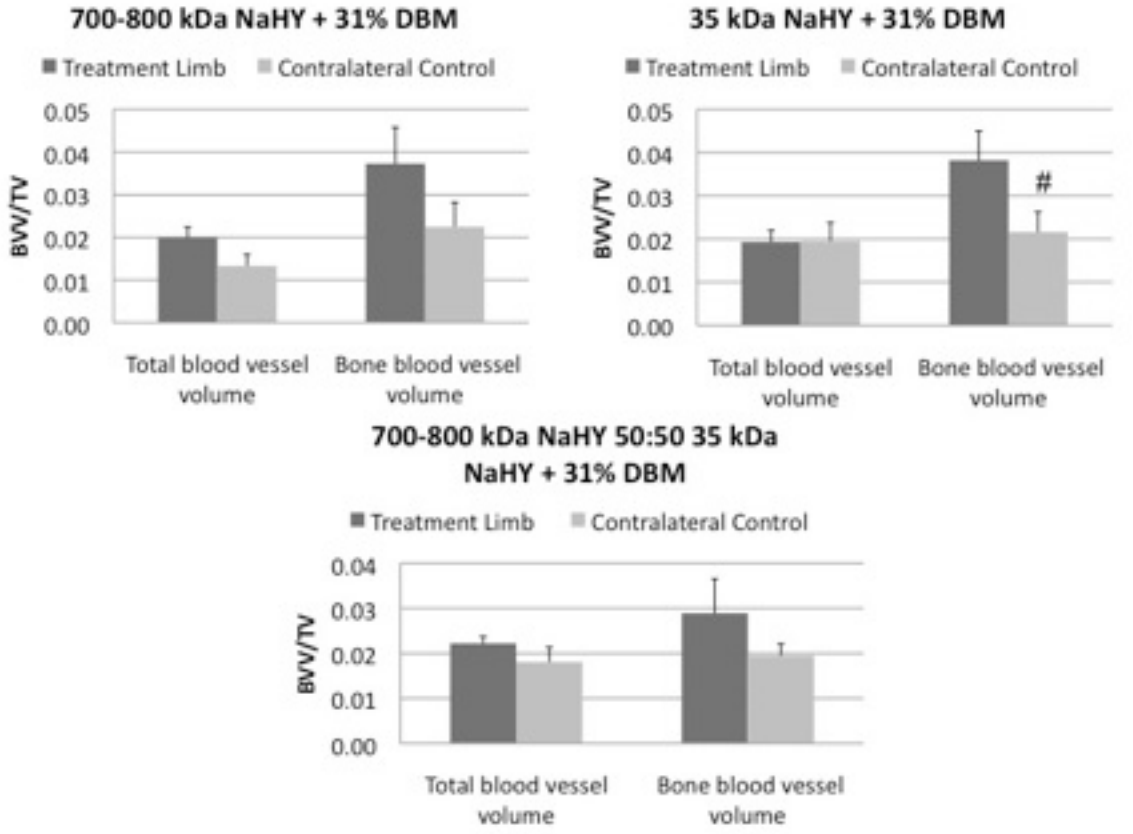

Figure A-2. Vessel volume fraction for ablated and contralateral control limbs. μCT analysis was used to quantify both the total and bone marrow blood vessel volume fractions for ablated and contralateral control limbs for the following treatment groups: 700-800 kDA NaHY + 31% DBM, 35 kDa NaHY + 31% DBM and 700-800 kDa NaHY 50:50 35 kDa NaHY + 31% DBM. Results show that ablation and subsequent treatment did not elicit a systemic effect on neovascularization.

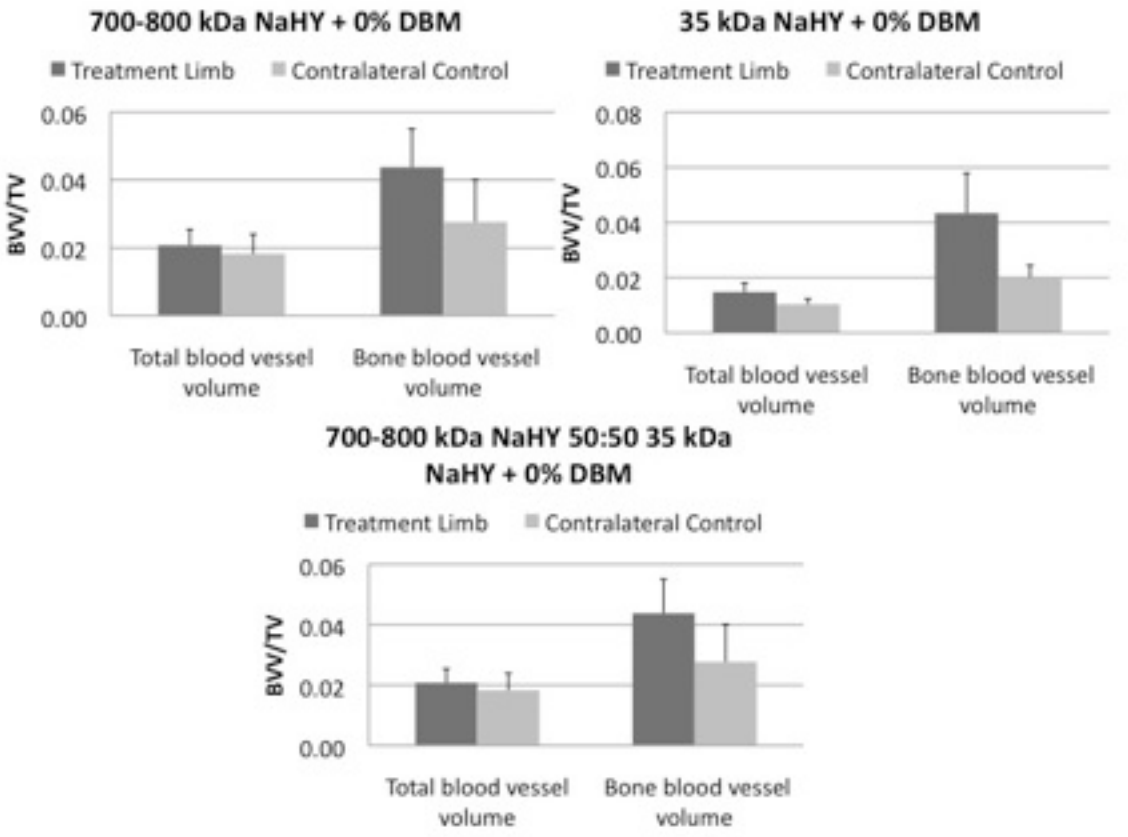

Figure A-3. Vessel volume fraction for ablated and contralateral control limbs. μCT analysis was used to quantify both the total and bone marrow blood vessel volume fractions for ablated and contralateral control limbs for the following treatment groups: 700-800 kDA NaHY + 0% DBM, 35 kDa NaHY + 0% DBM and 700-800 kDa NaHY 50:50 35 kDa NaHY + 0% DBM. Results show that ablation and subsequent treatment did not elicit a systemic effect on neovascularization.

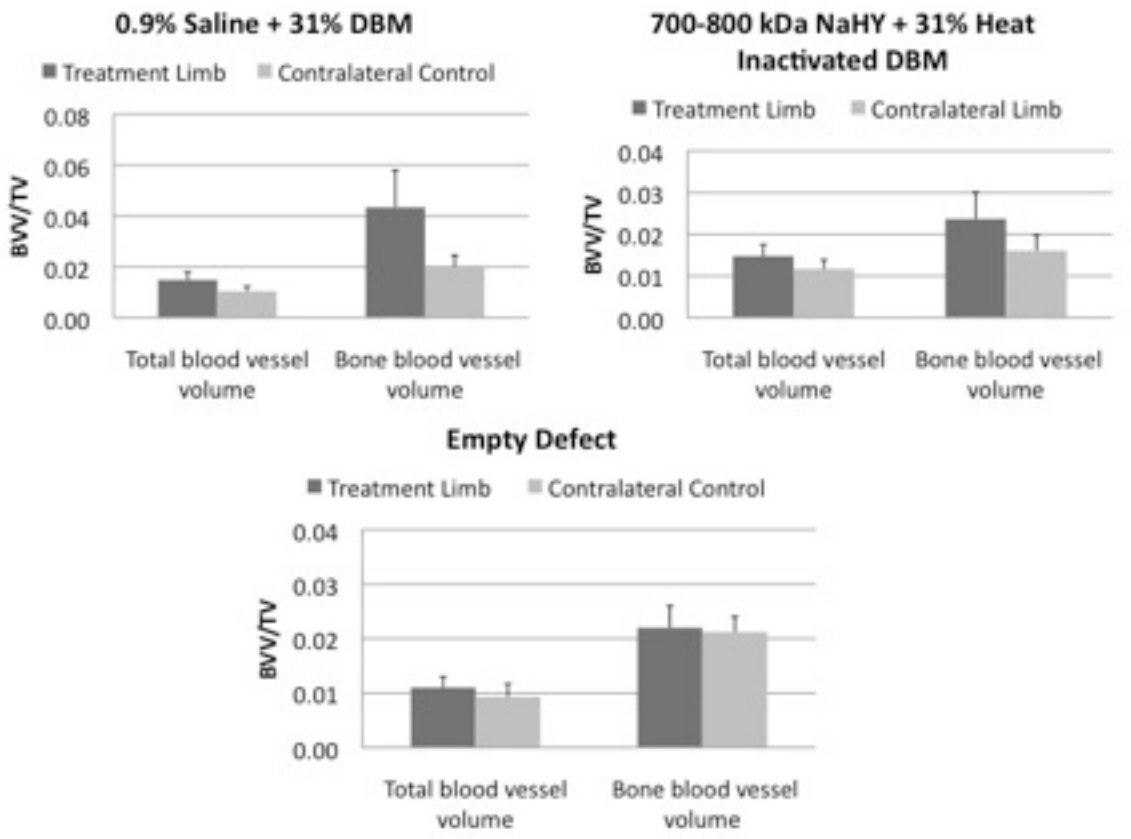

Figure A-4. Vessel volume fraction for ablated and contralateral control limbs. μCT analysis was used to quantify both the total and bone marrow blood vessel volume fractions for ablated and contralateral control limbs for the following treatment groups: 0.9% Saline + 31% DBM, 700-800 kDa NaHY + 31% Heat Inactivated DBM and Empty Defect. Results show that ablation and subsequent treatment did not elicit a systemic effect on neovascularization.